# EVALUATION OF PLAIN AND FIBER REINFORCED CONCRETE PROPERTIES FOR THE PAVEMENT STRUCTURAL DESIGN APPLICATIONS

by

Onur Öztürk

B.S., Civil Engineering, Istanbul Technical University, 2016

M.S., Civil Engineering, lstanbul Technical University, 2018

Submitted to the Institute for Graduate Studies in
Science and Engineering in partial fulfillment of
the requirements for the degree of
Doctor of Philosophy

Graduate Program in Civil Engineering
Boğaziçi University
2023

# ACKNOWLEDGEMENTS

I would like to express my sincere appreciation to my advisor, Prof. Nilüfer Özyurt Zihnioğlu, for her invaluable support and guidance throughout my thesis study. I would also like to thank Prof. Hakan Nuri Atahan, Prof. Kutay Orakçal, Assoc. Prof. Zeynep Başaran Bundur, and Assist. Prof. Esat Selim Kocaman for serving on my thesis committee and providing invaluable feedback. Additionally, I want to acknowledge Prof. Turan Özturan for sharing his valuable experiences with me during my time at Boğaziçi University.

I anı deeply grateful to my colleagues and friends, Dr. Abdullah Huzeyfe Akca, Dr. Ahmet Onur Pehlivan, Dr. Anıl Niş, Dr. Semih Gönen, Hasan Yıldırım, Ahmet Alperen Koç, Arda Sepetci, Elifsu Balcı, Mert Güner, Olcay Gürabi Aydoğan, and Uğur Can Erginağ, for their invaluable contributions and for making my time in the Construction Materials Laboratory a rewarding experience.

I dedicate this thesis to my mother, Emine Öztürk, who has supported and inspired me throughout my life. I also want to thank my father, Sedat Öztürk, and my sisters, Şennur Öztürk and Şeyma Öztürk, for their endless support. I anı glad to have them.

I would like to acknowledge the assistance of Construction Materials Laboratory technician, Ümit Melep, during the experimental part of my thesis. Furthermore, I would like to express my gratitude to the technicians of Boğaziçi University Structural and Geotechnical Laboratories for their kind assistance during my time spent in their facilities for experiments.

I also would like to state my special thanks to Boğaziçi University undergraduate students for their support during both casting and testing parts of the experiments, without them it was impossible to do this much work.

I would like to acknowledge TUBITAK - Turkish Technological and Scientific Research Institute for the financial support given during my PhD study. I anı also grateful Boğaziçi University Research Fund [Grant Number: 22AD5] for the financial support given for this dissertation.

Lastly, I express my sincere appreciation to Akcansa Cement Industry and Trade Incorporated Company, Istanbul Environmental Protection and Waste Processing Corporation (ISTAC), Bogazici Concrete Industry and Trade Incorporated Company, and Sika Construction Chemicals Incorporated Company for the material support.

# ABSTRACT

## EVALUATION OF PLAIN AND FiBER REINFORCED CONCRETE PROPERTIES FOR THE PAVEMENT STRUCTURAL DESIGN APPLICATIONS

As one of the important infrastructure facilities, concrete pavements are commonly used due to their several benefits, and they have a considerable impact on the environment during their construction and use phases. The properties of construction materials and the design approach used greatly affect the overall performance of concrete pavements.

This study aimed to improve the current practices in concrete pavement engineering by improving the efficiencies of materials, as well as the design and evaluation approaches in use. To achieve this goal, performance of various concrete mixtures measured under different loading scenarios and numerical analyses were conducted.

In the scope of this dissertation, new testing methodologies have been developed to measure the cyclic loading performance of concrete mixtures with reduced variation and to measure the effect of reversed cyclic bending loading on the fatigue performance of concrete. Additionally, two-stage mixing approach employed for the first time to improve the performance of fiber reinforced concrete by enhancing fiber-matrix interface. Moreover, the effects of using of discrete structural fibers and recycled aggregates for concrete pavement applications extensively studied through experiments and numerical analyses. Based on the results obtained, recommendations for the future research and design works were provided.

# ÖZET

## YOL KAPLAMASI YAPISAL TASARIM UYGULAMALARI İÇİN YALIN VE LİF DONATILI BETON ÖZELLİKLERİNİN DEĞERLENDİRİLMESİ

Önemli altyapı tesislerinden biri olan beton yollar çeşitli faydaları dolayısıyla sıklıkla kullanılmaktadır ve beton yollar hem kullanım hem de yapım aşamalarında çevre üzerinde büyük etkiye sahiptir. Kullanılan malzemelerin özellikleri ve kullanılan tasarım yaklaşımı beton yolların toplam performansı üzerinde büyük etkiye sahiptir.

Bu çalışmada beton yollarda kullanılan malzemelerin etkinliği ile tasarım ve değerlendirme yaklaşımları üzerine yapılan çalışmalar ile beton yol mühendisliğinde kullanılan güncel yaklaşımların geliştirilmesi hedeflenmiştir. Bu amaca ulaşmak için, çeşitli beton karışımların performansı değişen yükleme senaryoları için ölçülmüş ve nümerik analizler yapılmıştır.

Bu tez kapsamında, betonların yorulma performansların düşük varyasyonla tespit edilebilmesi ve tersinir tekrarlı eğilme yüklemesi durumunun betonun yorulma performansı üzerindeki etkilerinin değerlendirlmesi için yeni deney yöntemleri geliştirilmiştir. Ayrıca, lif-matris arayüzünün geliştirilmesi yoluyla lif donatılı beton karışımlarının performanısının artırılmasını sağlamak amacıyla iki aşamalı karıştırma yöntemi bu çalışma kapsamında ilk kez kullanılmıştır. Ek olarak, çalışma kapsamında yapısal liflerin ve geri dönüşüm agregalarının beton yol uygulamalarında kullanımının etkilerin deneysel ve nümerik çalışmalarla detaylı olarak incelenmiştir. Elde edilen sonuçlara dayanılarak gelecekte yapılacak araştırma ve tasarım çalışmaları için çeşitli öneriler verilmiştir.

# TABLE OF CONTENTS

# LIST OF FIGURES

# LIST OF TABLES

# LIST OF SYMBOLS

| | |
|---|---|
| $C$ | Cement amount by weight |
| $C_1$ | Adjustment factor for base |
| $C_2$ | Adjustment factor for shoulder |
| $CO_2$ | Carbon dioxide |
| $CW$ | Crack width |
| $D_1$ | Calculated value of Kolmogorov - Smirnov test |
| $D_e$ | Critical value of Kolmogorov - Smirnov test |
| $h$ | Slab thickness |
| $k$ | Support modulus |
| $l$ | Radius of relative stiffness |
| $L$ | Span length |
| $N_e$ | Number of allowable load repetition for erosion |
| $N_f$ | Number of allowable load repetition for fatigue |
| $p$ | Power |
| $p(BUC)$ | Failure probability for bottom-up cracking |
| $p(TDC)$ | Failure probability for top-down cracking |
| $R_{150}$ | Residual flexural strength ratio at of 'span length /150' |
| $t_{eff}$ | Effective depth |
| $W$ | Water amount by weight |
| $\alpha$ | Scale parameter of Weibull distribution function |
| $\beta$ | Shape parameter of Weibull distribution function |
| $\delta$ | Corner deflection |
| $\delta_{peak,e}$ | Estimated peak differential displacement |

# LIST OF ACRONYMS/ABBREVIATIONS

| | |
|---|---|
| 3D | 3-Dimensional |
| 4PBT | 4-Point Bending Test |
| AASHTO | American Association of State Highway and Transportation Officials |
| ACI | American Concrete Institute |
| ACPA | American Concrete Pavement Assocoiation |
| AGG | Joint Stiffness |
| ASTM | American Society for Testing and Materials |
| ATS | Aggregate Top Size Terms |
| BUC | Bottom-Up Cracking |
| CE | Carbon Emission |
| COV | Coefficient of Variation |
| CS | Crushed Sand |
| CSt | Crushed Stone |
| CStC | Crushed Stone Concrete |
| CW | Crack Width |
| DPT | Double-Punch Test |
| EDX | Energy-Dispersive X-Ray Spectroscopy |
| EN | Euro Norm |
| FRC | Fiber Reinforced Concrete |
| HSC | High Strength Concrete |
| IRC | lndian Road Congress |
| ITZ | Interfacial Tranzition Zone |
| JCI | Japan Concrete Institute |
| JPCP | Jointed Plain Concrete Pavements |
| LA | Los Angeles Abrasion |
| LTE | Load Transfer Efficiency |
| LVDT | Linear Variable Displacement Transducer |

| | |
|---|---|
| MEPDG | Mechanistic-Emprical Pavement Design Guide |
| MOE | Modulus of Elasiticity |
| MOR | Modulus of Rupture |
| MOR' | Effective Modulus of Rupture |
| MS | Microsilica |
| N | Cycle Number |
| NAC | Natural Aggregate Concrete |
| NS | Natural Sand |
| NSC | Normal Strength Concrete |
| p | Power |
| PC | Plain Concrete |
| PCA | Portland Cement Association |
| pp | Polypropylene |
| PPF | Polypropylene Fiber |
| PPFR | Volume ratio of polypropylene fibers to the total volume of concrete in percent |
| RBA | Recycled Brick Aggregate |
| RBAC | Recycled Brick Aggregate Concrete |
| RCA | Recycled Concrete Aggregate |
| RCAC | Recycled Concrete Aggregate Concrete |
| RCC | Roller Compacted Concrete |
| RFS | Residual Flexural Strength |
| RFSR | Residual Flexural Strength Ratio |
| RILEM | The International Union of Laboratories and Experts in Construction Materials, Systems and Structures |
| S | Stress Ratio |
| SA | Single Axle |
| SCM | Supplementary Cementitious Material |
| SD | Standard Deviation |
| SEM | Environmental Scanning Electron Microscopy |
| SF | Steel Fiber |

| | |
|---|---|
| SP | Superplasticizer |
| SR | Stress Ratio |
| TDC | Top-Down Cracking |
| TRBAC | Treated Recycled Brick Aggregate Concrete |
| TRCAC | Treated Recycled Concrete Aggregate Concrete |
| TA | Tandem Axle |
| TS | Turkish Standard |
| TSMA | Two-Stage Mixing Approach |
| US | United States |
| W45 | Concrete Mixture with 0.45 Water-to-Cement Ratio |
| W60 | Concrete Mixture with 0.60 Water-to-Cement Ratio |

# 1. INTRODUCTION

Conerete pavements, as one of the important infrastrueture faeilities, are widely used all around the world due to several benefits obtained from them, sueh as high strength, high stiffness, and high durability. Conerete pavements have a eonsiderable impaet on the environment and governments' budgets in both eonstruetion (due to the materials used, eonstruetion aetivities, ete.) and use (due to the vehicle road inter-aetion, traffie delay, ete.) phases. Therefore, sustainability of the eonerete pavements has a erueial importanee, and a variety of methods have been implemented up to now to improve their sustainability.

Among the types of eonerete pavements, jointed plain eonerete pavements (JPCP) are the one that eommonly used, due to both low eost and high performanee. Fatigue of pavement slabs and faulting of pavement joints are the two eommon failure modes eonsidered for the design of JPCP, and seleetion of pavement material has a eonsid-erable impaet on both failure modes. Therefore, seleetion of pavement material and proper struetural design of eonerete pavements have a erueial importanee in terms of eonerete pavements' sustainability.

Pavement slab fatigue due to the repeated applieation of axle loads is one of the important failure modes eonsidered for JPCP design, and performanee of eonerete pavement slabs under fatigue loading is dependent on the properties of eonerete mixture used. Therefore, determination of eonerete performanee under fatigue loading is an important issue for design. On the other hand, eonerete fatigue test results usually exhibit eonsiderable seatter whieh make hard to determine the performanee of speeifie eonerete type and eompare the performanee of eonerete mixtures under fatigue loading. In addition, due to the temperature differenee oeeur in the depth of pavement, the slab eurls in downward and upward direetions during the day and night, respeetively. This faet leads to ehange in the part of the eonerete slab that works under tension due to applied axle loads. Though, the bottom part of the pavement slab exposed to tension

during the $d_{a\,y}$ hours, the top part of the pavement slab exposed to tension during the night hours. Thus, measurement of the effect of change in stress state during the day and night hours is an issue to design the concrete pavements correctly.

Use of macro fibers allows to produce concrete pavements with lower thicknesses due to the improved cracking resistance, and they are the type of reinforcement that can be put into concrete easily in its fresh state. Due to these benefits, use of fibers in concrete pavement applications is of great interest of the researchers and authorities, and several studies have been carried out in this topic. According to the project specific requirements, various concrete types (conventional concrete, roller compacted concrete, pervious concrete, ete.) are used in concrete pavement applications, and it is known that the properties of matrix have a considerable impact on the overall contribution of fibers to the performance of fiber reinforced concrete (FRC). Therefore, determination of the performance of fibers in different concrete pavement mixtures and optimization of the matrix properties to obtain the maximum performance from the fibers are crucial to increase the benefit that could be obtained from them.

Faulting of JPCP joints is an another failure mode commonly considered in structural design. Load transfer capability of concrete slab has an important impact on the overall performance of concrete pavement joints, and it depends on several factors, such as maximum aggregate size, aggregate hardness, reinforcements, ete. Based on the relevant literature, though single axle loads mostly critical for fatigue failure mode, tandem and tridem axles have larger impact on the faulting failure mode.

With the increasing interest in the use of FRC in pavement applications various design approaches have been proposed to design concrete pavements with fibers. However, all of the design methods currently available considers the effect of concrete pavements on the fatigue performance of concrete pavements and their effects on the faulting performance was not addressed. On the other hand, limited number previous studies showed that the use of fibers improves the shear load transfer capability of pavement joints. Limitedness of the works in this topic is one of the reasons for

the absence of design method regarding the contribution of fibers to the performance of pavement joints, and this might lead to uneconomical solutions especially for the pavements that will carry heavy tandem and tridem axle loads. Therefore, further studies are needed to clearly / numerically represent the contribution of fibers to the joint performance of concrete pavements.

Since almost all the products of the construction industry have a limited lifespan ranging from years to decades, recycling of the construction products at the end of their lives is a vital issue. Due to the large scale use of materials in concrete pavements, the use of aggregates recovered from demolished concrete structures (recycled aggregates) in them is one of the subjects widely studied. Due to the weakness (in terms of hardness, porosity, ete.) of the recycled aggregates (mainly due to the weak mortar attached to the aggregates) their mechanical and structural performance may vary in considerable amount compared to virgin ones. Therefore, before its widely usage, studies that investigate the overall performance of recycled aggregate concrete mixtures in concrete pavements are needed.

This dissertation has been designed to fill the gaps in the literature related to the important issues for concrete pavement engineering summarized above. To fill the mentioned gaps, an extensive experimental and numerical studies were carried out in the scope of this dissertation and the results were presented under the following headings:

- Variation in concrete fatigue tests.
- Effects of stress reversal on flexural fatigue life.
- Effectiveness of fibers in concrete pavement mixtures.
- Effects of fibers on the joint performance of concrete pavements.
- Two-stage mixing approach to improve fiber-matrix interface.
- Structural behaviour o recycled aggregate concrete pavements.
- Joint performance of recycled aggregate concrete pavements.

For each of the headings given above, first the current literature and the gaps that need to be filled were given clearly. Then, details of methodologies followed for experimental and numerical works carried out in the scope were given. Afterward, results of the experiments were given for each of the topic, and discussions were presented based on the obtained results and available literature. In the end, the results were summarized for each of the topics investigated in the scope of this dissertations, and recommendations were given for the following research and design works on concrete pavements. It is believed that the results, discussions and recommendations presented below will be very beneficial for the following works.

# 2. LITERATURE REVIEW

Due to the limitedness of earth's sources and increase in the number and energy use of humans, social and environmental impacts of the engineering works take a great amount of interest, especially in recent years. Construction industry is one of the largest consumers of earth's resources, and materials used by the industry have a considerable impact on the environment [1, 2], from their production to use phases. Therefore, several strategies have been implemented to reduce the environmental impact of construction works / materials, such as optimization of production process [3,4], optimization of design process [5-7], use of alternative raw materials [8-12], use of alternative binders [13-17], use of waste materials [18-22], reducing waste production [23-25], use of local products [26], production of durable structures [23, 27].

United States (US) has approximately 4.5 million km paved and 2.1 million km unpaved public road (as a sum of urban and rural roads), and in each year an enormous amount of investment is made to produce new roads and maintenance activities of the existing roads [28]. in 2017, approximately 181 billion US dollar was spent on US highways, which was reported to be one of the largest consumers of the US resources [28]. in 2021, over 40% of US public roadways (approximately 43%) are evaluated as poor or mediocre conditions [29], which demonstrates that the investments to the roads will continue in the following years. Due to the materials used and the construction process itself, construction of pavements has a considerable detrimental effect on the environment [19, 30]. in addition to this, interaction between pavement and vehicles, traffic delay and albedo-related impacts of pavements during their service lives also contributes environmental impact of the pavements in considerable amount [31]. When, the huge scales of pavement projects, costs and environmental impacts of pavements considered together, the efficient production of pavements has a great importance in terms of sustainability and cost-effectiveness.

Since pavement material has one of the most prominent effects on the road investments, selection of suitable materials is one of the critical issues for pavement sustainability [32-34]. Concrete pavements are often used around the world, due to their several advantages [35], and a variety of methods has been recommended to improve the sustainability of concrete pavements; development of sustainable design [32, 36-38] and preservation strategies [32], reduction of cementitious content [34], use of supplementary cementitious materials [39-41], use of recyded materials [42-45], use of discrete fibers [32, 40, 46], ete.

The aim of this dissertation is to enhance the sustainability of concrete pavements by improving the current practice in concrete pavement engineering (from material to structural point of views), and a variety of important topics were induded in this work. in the following parts, current literature related to the subjects examined in the scope of this dissertation, as well as the literature gaps and summary of the approach implemented in this study to fill the gaps were given.

## 2.1. Variation in Concrete Fatigue Tests

Fatigue is a progressive growth of cracks or flaws within the materials under cyclic application of load that produces a stress lower than the strength of the material [47, 48]. Various engineering structures are exposed to repeated loadings from automobile traffic, sea waves, machine vibration, ete. [49]. The type of fatigue loading usually defined according to the number of cydic loads applied. Hsu [50] reported the level of cydic load application to various types of concrete structures (reinforced concrete building structures, bridges, pavements, sea structures, ete.), and defined the number of load application approximately between; $1x10^2$ to $1x10^3$ cydes as 'low eyde fatigue', $1x10^3$ to $1x10^7$ cydes as 'high eyde fatigue', and $1x10^7$ to $5x10^8$ cydes as 'super-high eyde fatigue'.

Due to its inherently brittle structure, plain concrete is much vulnerable to tensile stresses, compared to compressive ones, and combination of tensile stresses with cydic

loading can be extremely deteriorative for concrete [48]. Due to the practical reasons, cyclic tensile performance of concrete is rarely measured by direct tests, and indirect testing configurations are used [51]; such as cyclic bending test [52-57], and cyclic splitting test [51, 58].

Results for all the concrete tests exhibit considerable variations from specimen to specimen, due to inherent change in properties of the tested specimens resulting from the change in composition, consistency, applied compaction energy, environmental conditions, alignment, ete. On the other hand, though the amount of variation in quasi-static tests is usually in considerable amount, it is much higher for cyclic tests [49, 59].

Bending test is the most common type of test used to evaluate the performance of concrete under both quasi-static and cyclic tensile stresses. For the quasi-static bending tests, in batch coefficient of variation (COV) values from 4.0% to 20.8% were reported in literature [19,35,60,61]. Besides, considerable batch - to - batch variations were also reported for the quasi-static bending tests (COV between 4.5% to 10.7%) [56,62,63]. On the other hand, the COV values from 28.6% to 161.3% (between 40% and 90%, most of the time) were reported for cyclic bending tests [62-66]). it is worth noting here that the COVs given here were calculated by assuming normal distribution for quasi-static tests, but Weibull distribution is used for cyclic tests, since the normal distribution assumption was not found suitable for the analysis of most of the cyclic test <lata. Since this study includes some statistical analysis, details for the calculations are provided in the following sections.

Schive [67] listed the sources of scatter for laboratory fatigue test results as follows: structure of material, specimen production, surface quality of specimen, type and frequency of fatigue load, test frame accuracy, laboratory environment (temperature and humidity), skill of staff. When the given sources are examined, it could be said that most of the parameters that affect the scatter of fatigue life <lata are the parameters which also affect the strength of material. Therefore, one of the main reason in the variation of cyclic test is the variation in strength of the test specimens.

Double-punch test (DPT) is a method, firstly proposed by Chen [68] to evaluate the tensile strength of plain concrete, then retrieved to evaluate the tensile performance of FRC by Molins et al. [61]. it was indicated in previous studies that the use of DPT to measure the tensile properties of concrete reduces the variation of the results, with respect to both bending and splitting tests [61, 69-71]. Molins et al. [61] attributed the decreased variation for DPT to the large cracking surface and cracking energy, compared to bending test. in another study, Colgrove and Chen [69] emphasized the importance of the load alignment and loading surface smoothness on the variation of DPT results.

### 2.1.1. Literature Gap

As explained above, though the variation in quasi-static concrete test results are in considerable amount, it is much higher for cyclic tests. in terms of structural design against cyclic loading, one of the critical issue is to determine the Wöhler (Stress Ratio (S) - Cycle Number (N)) curve that will be used in design. The design curves usually given for a specific level of reliability (survival probability). However, when higher reliability levels are desired for the design, the large variation of test results leads to significant decrease in the allowable number of load repetition, which may cause to an uneconomic design. Another issue related to the variation of test results is that so many samples need to be tested to obtain representative results for a specific kind of concrete or to compare the performance of different concrete types. On the other hand, even testing of single specimen under fatigue loading requires considerable effort and time (especially for high eyde fatigue).

### 2.1.2. Examination Methodology

Variation in strength measurements is one of the common sources of the variation of fatigue test results (explained above), and lower variations were reported in the literature for DPT compared to bending test commonly used to evaluate the performance of concrete under tensile fatigue loading. in the scope of this thesis cyclic DPT was

applied for the first time, and variation obtained for the results were compared with the variation of cyclic bending test obtained in this study and the literature, by doing statistical analyses. it is believed that the presented results will be very beneficial for the following studies focused on the performance of concrete under cyclic loading.

## 2.2. Effects of Stress Reversal on Flexural Fatigue Life

Fatigue in concrete pavements occurs due to the repeated application of wheel / axle loads throughout their service life and is one of the commonly used failure criteria in design codes [19]. in each day, due to the reversed temperature differential, pavement slab curl in downward and upward directions during the day and night, respectively. Though it was not considered in the early concrete pavement design codes [72, 73], since curling has a considerable impact on the magnitude of maximum tensile stress occurs in the pavement slab [74-80], recently published design codes consider the curling of the slab for the stress calculations, such as Swedish design method [81], lndian Road Congress (IRC) 58 - 3rd revision [82], American Association of State Highway and Transportation Officials (AASHTO) - Mechanistic Empirical Pavement Design Guide (MEPDG) [83] and IRC 58 - 4th revision [84].

For the design, when the pavement slab curled in downward direction (daytime (upper part of the slab hotter than the lower part)) bottom-up cracking (BUC) case is taken into account and the critical loading condition occurs when the wheel loads applied from the midpoint of the curled slab. On the other hand, when the pavement slab curled in upward direction (nighttime (upper part of the slab cooler than the lower part)) top-down cracking (TDC) case is considered, and the critical loading condition occur when the loads applied from both end of the slab (near the transverse joints) [82-84]. Figure 2.1 illustrates the critical loading cases and stress states for the day and night hours (prepared based on [79, 84]), accordingly.

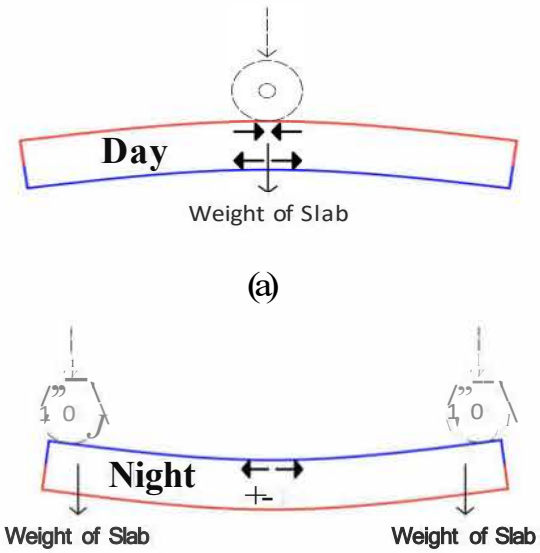


Figure 2.1. Stress states during (a) day and (b) night (dashed lines show the critical locations far the movable wheel loads).

In Swedish [81] design guide, effect of curling on the magnitude of stresses is only considered far positive temperature gradient (top of the slab hotter than the bottom, which increases the stress levels far the BUC case), and in the guides total fatigue damage is calculated far only bottom-up cracking case (TDC mode is not taken into account). However, it was emphasized in a variety of studies that the failure of concrete pavements under cyclic load application might starts from the top and goes through bottom (TDC) [80, 85-87], which is due to combined effect of axle loads and environmental loads (temperature and moisture changes) [80]. Therefare, in addition to BUC, TDC case was alsa addressed in the recent design guides [82-84], and different design approaches are suggested to consider bottom-up and top-down cracking, together.

In the farmer version of IRC concrete pavement design guide (IRC 58 - 3rd revision [82]) fatigue damage due to BUC and TDC cases considered separately far the damage calculations, but in the later version of the guide (IRC 58 - 4th revision [84]) fatigue damage occur in the slab is calculated as a sum of the damage due to TDC and BUC. As in IRC 58 - 3rd revision [82], AASHTO MEPDG [83] accounts the damages

occur due to BUC and TDC, separately. AASHTO MEPDG [83] calculates the total fatigue damage as

$$TFD = (p(BUC) + p(TDC) - p(BUC) \times p(TDC)) \times 100\%, \quad (2.1)$$

where $TFD$ is total fatigue damage, and $p(BUC)$ and $p(TDC)$ are the failure probabilities for BUC and TDC, respectively. in the relevant guide, given formula is explained as the slab may fail under BUC or TDC, but both cannot occur at the same time [83].

To summarize the design approaches; IRC 58- 4th revision [84] reduce the number of allowable stress cycles in one direction considering the cyclic loads applied in the opposite direction, but AASHTO MEPDG [83] and IRC 58 - 3rd revision [82] assume that the cyclic loading capacity of slab in one direction will not be jeopardized by the cyclic loading applied in the opposite direction.

Effect of stress reversal on the fatigue performance of laboratory scale specimens were studied in a number of previous studies, varying reductions in fatigue resistance were reported. in one of the earliest studies, Williams [88] investigated the performance of lightweight aggregate concrete mixtures, produced with burnt shale aggregates, under repeated (one-way) and reversed (two-ways) cyclic bending loading, and he reported notable reduction in fatigue performance for reversed cyclic loading. Moreover, Tepfers [89] studied the effect of stress reversal on the fatigue life of cube and beam specimens. in the mentioned study, he combined the splitting and compressive loads to produce cyclic stress alternating between tension and compression, and slight reduction in the fatigue performance for both cube and beam specimens were reported. Furthermore, Zhang et al. [90] investigated the effect of change in maximum to minimum stress ratio (applied maximum stress / applied minimum stress) (from '+0.5' to '-1.0') on the flexural fatigue performance of concrete mixtures. Based on the cyclic bending test results, decreased fatigue resistance with decreasing maximum to minimum stress ratio were reported in the mentioned study [90], and the amount of change in fatigue resistance due to varying maximum to minimum stress ratio was reported more pronounced for the positive stress ratios. Cornelissen and Reinhardt [91] and Lü et al. [92] investigated the effect of cyclic stress reversal (alternating between uniaxial

tension and compression) on the fatigue performance of dog-bone shaped specimens, and in both studies considerable reductions in fatigue lives were reported.

### 2.2.1. Literature Gap

Due to the change in temperature differential occur in the slab during the day and night, pavement slabs are exposed to different critical loading conditions which creates tensile stresses in different part of the slab. Although, it is a common issue for concrete pavements, different approaches are used in different design guides (explained above). Üne important reason of this difference is the lack of experimental data related with the fatigue life of concrete under stress reversal.

It has been shown in the previous studies [88-92] that fatigue performance of concrete adversely affected when subjected to stress reversal repetitively. However, in the mentioned studies the effect was measured by applying cyclic loadings that produce cyclic stress alternated repetitively between tension and compression in each eyde. On the other hand, this loading protocol does not represent the case in concrete pavements, as stress states of concrete pavements changes from day to night (not changes in each load application as explained above).

### 2.2.2. Examination Methodology

In the scope of this dissertation, a novel cyclic loading protocol (which generates cyclic stresses similar to that occur in pavements) was developed and beam specimens were tested under the developed fatigue testing protocol (two-way cyclic loading) and ordinary one (one-way cyclic loading). Based on the results, change in performance due to the application of two-way loading compared to the one-way loading was determined, and meanings of obtained results in terms of pavement design were discussed, considering the concrete pavement design approaches currently available.

## 2.3. Effectiveness of Fibers in Concrete Pavement Mixtures

The use of discrete fibers is one of the outstanding ways to reduce the environmental impact of concrete pavements, as the fibers allow to reduce pavement thickness and increase joint spacing by increasing flexural capacity, fracture properties, fatigue resistance, and cracking resistance of pavement concrete [60, 93-96]. Additionally, large surface areas of concrete pavements make them susceptible to shrinkage cracks, and popularity of using macro fibers instead of steel mesh reinforcements to restrain the shrinkage cracks increases gradually, due to their advantages in terms of construction time, labor cost, and construction afford [97]. In a previous study [98], doubled construction cost for steel mesh reinforced slab was reported, compared to its FRC alternative. Since production and transportation of steel mesh reinforcements are also energy-intensive processes, elimination of these reinforcements may also be considered as an important advantage of using macro fibers in terms of environmental impact of concrete pavements.

Due to the increasing interest in the use of discrete fibers in pavement applications, several design methodologies have been proposed to determine the thickness requirement of fiber reinforced concrete (FRC) pavements [93, 95, 99-101]. In all of the design approaches mentioned, the post-cracking performance of concrete is taken into account to consider the contribution of fibers to the structural performance of concrete slab, and this performance depends on the properties and amount of fibers used, as well as properties of concrete matrix [60,102,103]. Depending on the project requirements, concrete pavements are produced by using a variety of concrete types (conventional concrete, pervious concrete, roller compacted concrete, ete.), and the effectiveness of fibers may vary in different concrete pavement mixtures.

### 2.3.1. Literature Gap

Since the use of discrete macro fibers increases the structural performance of pavement material and allow to produce pavements with lower thickness and without steel

meshes, use of them might be considered as one of the ways to reduce environmental impact and cost of concrete pavements. However, the number of studies that extensively examine effects of structural fibers on the performance, cost, and environmental impact of concrete pavements are still limited.

### 2.3.2. Examination Methodology

Considering above mentioned things, following aspects of using fibers in concrete pavement mixtures were studied:

- The effect of using macro fibers in varying amounts on the overall performance of concrete pavements (from structural point of view to the economic and environmental aspects).
- The efficiency of fibers in different concrete matrices commonly used for pavement construction.

For the investigations, first, an extensive experimental study was carried out to determine the effects of different types (steel and polypropylene) and amount of fibers on widely used concrete pavement mixtures (normal and high strength conventional concrete, as well as roller compacted concrete). Then, by using the experimentally obtained material parameters, thickness requirements for all mixtures were determined by considering a sample pavement, and the thickness values were used to determine the cost and environmental impact of the mixtures.

## 2.4. Effects of Fibers on the Joint Performance of Concrete Pavements

Jointed concrete pavements (most commonly used concrete pavement type) usually designed by considering two different failure modes: fatigue (failure of concrete slab under repeated axle loadings), and faulting (failure of pavement joints due to repeated axle loadings). Besides, the required pavement thickness is determined based on the critical one [72, 83,104]. it is reported in the literature that single axles are more

deleterious for fatigue failure mode, but tandem and tridem axles are more destructive for faulting failure mode [19, 72,105].

In all the fiber reinforced concrete pavement design methods [93, 95,100,101] developed up to now, contribution of fibers to the fatigue performance of concrete pavements was addressed, and recommendations were given for design of FRC pavements under fatigue loading. However, in addition to fatigue, faulting is an important failure mode (especially critical for the pavements that will carry large number of heavy axle loads) for the structural design of concrete pavements, and it has not been addressed in the FRC design methods proposed up to now.

To improve the faulting performance of concrete pavements, dowel hars are used in most of the time, especially, when heavy weight vehicles are considered. However, in some cases dowel hars are not used due to practical (low pavement thickness, roller compacted concrete pavements) or economic (material, storage, and placement costs) reasons. When, the dowel hars are not used, load transfer between the adjacent joints provided only by the aggregate interlocking effect. Therefore, pure aggregate shear load transfer mechanism has been studied by lots ofresearchers [106-111]. The performance of un-doweled joints depends on various parameters: joint type and opening; distance between the cracks; aggregate size, distribution and angularity; subgrade strength and stiffness; magnitude and number of applied loads, ete. [106,107,109,111]. Contribution of fibers to the joint performance of concrete pavements were emphasized in a limited amount of the previous studies. For example, Nanni and Johari [96] linked the enhanced crack control and micro-dowel effect provided by the fibers with improved load transfer capacity within the joint. Thompson [112] showed that the use of steel fibers both reduce the shear displacement and shear degradation rate. Besides, he emphasized the importance of crack width (considerable reduction in the shear performance with increasing crack widths) on the post-cracking shear performance and concluded that the use of steel fibers might improve the shear performance indirectly by decreasing the crack widths due to the improved tensile performance. In another study, Arnold et al. [113] examined the contribution of steel fibers to the post-cracking shear performance of

concrete beams and reported considerable improvement in the performance by adding steel fibers. They also reported increase in the performance with the increasing amount of fiber usage. in a more recent study, Barınan and Hansen [114] reported improved post-cracking shear performance for synthetic fiber reinforced concrete mixtures, in varying amounts.

### 2.4. 1. Literature Gap

With the increasing interest in the use of discrete fibers for the pavement applications, a variety of methodologies proposed for the structural design of FRC pavements. However, none of the method currently available account the contribution of fibers to the performance of pavement joints which might leads to uneconomic design results, especially for the pavements that will carry large number of heavy axle loads. Üne of the reasons for this issue is the limitedness of the research studies concentrated on the joint performance of fiber reinforced concrete pavements.

### 2.4.2. Examination Methodology

In the scope of this study, contribution of polypropylene fibers to the post-cracking performance of concrete mixtures was examined. For the examinations, first, 3 different concrete mixtures with varying fiber ratios were designed, and basic mechanical properties (compressive strength, modulus of elasticity, flexural performance) of the mixtures were determined according to the relevant standards. Then, post-cracking shear performance of the mixtures were measured by using a small-scale testing methodology, recommended in the literature. Afterward, test results were evaluated, and several discussions / suggestions were provided by considering them and outcomes of previous studies.

## 2.5. Two-Stage Mixing Approach to Improve Fiber-Matrix Interface

Performanee of FRC (both before and after eraeking) depends on a variety of parameters, sueh as fiber type, fiber amount, fiber distribution and orientation, properties of eonerete matrix [60, 115-119]. lmportanee of fiber-matrix interfaeial transition zone (ITZ) properties in terms of FRC performanee was emphasized in numerous studies, whieh depends on both properties of fibers and eonerete matriees [102,103, 119-122]. Due to the dependenee of overall performanee of FRC to the quality of fiber-matrix interfaee, a variety of methods have been developed until now to improve the interfaee, sueh as fiber surfaee modifieation [122], fiber geometry modifieation [123], densifieation of matrix (using supplementary eementitious materials (SCMs), low water/ eement, ete.) [124-127].

Two-stage mixing approaeh (TSMA) firstly proposed by Tam et al. [128] to improve the performanee of eonerete produeed with reeycled aggregate by filling the pores and improving the ITZ around the reeyeled aggregates. in the mentioned study, by modifying the mixing protoeol it was aimed to eover the reeycled aggregates with eement paste that includes low amount of water (low water/eement paste), and up to 21.2% inerease in the eompressive strength was reported, based on the experiments earried out the study. Following this primary study, several studies have been earried out to investigate the effeets of supplementary eementitious materials (fly aslı, slag, siliea fume, ete.), ehanging mixing protoeols and reeycled aggregate replaeement ratios on the benefits obtained from TSMA [129-137]. in addition, it was shown in the previous studies [133,138,139] that the use of TSMA is also give favorable performanees in terms of durability eharaeteristies of eonerete produeed with reeycled aggregates.

### 2.5.1. Literature Gap

it was indieated in several previous studies that the use of diserete fibers might be a way to reduee environmental impaet of eonerete, and amount of eontribution that eould be obtained heavily depends on the overall performanee of FRC. Besides, depen-

dence FRC performance to the fiber-matrix interface quality was emphasized in several studies, together with the parameters that have an impact on that (fiber geometry and surface properties, water to cement ratio of concrete matrix, ete.). Although, varying methods were proposed in literature to improve the fiber-matrix interface up to now, the studies are still going on to obtain further benefits from the fibers.

### 2.5.2. Examination Methodology

TSMA commonly used to improve the performance of recycled aggregate concrete mixtures, was revisited in the scope of this thesis, to enhance the fiber-matrix interface, and to improve the overall FRC performance of FRC. To investigate the contribution that could be obtained from the mixing approach implemented, first mechanical tests (compressive strength, modulus of elasticity, and flexural performance) and micro-structural analyses (environmental scanning electron microscopy and energy-dispersive X-ray spectroscopy) were carried out. Then, the effects of contribution, obtained from the implementation of TSMA on the cost and environmental impact of concrete were examined by doing a case study.

## 2.6. Structural Behavior of Recycled Aggregate Concrete Pavements

Since almost all the products of the construction industry (a large consumer of natural resources) have a limited lifespan ranging from years to decades, recycling of the construction products at the end of their lives is a vital issue. Therefore, a considerable number of studies (e.g. [140-145] have been carried out on this subject. The use of aggregates recovered from demolished concrete structures (recycled concrete aggregates) in concrete pavement applications is one of the subjects drawing researchers' attention intensely. Thus, the effects of recycled concrete aggregates on the properties of concrete pavements were studied in various aspects, such as fresh state properties [146], mechanical properties (e.g., strength, fatigue performance) [147-150], cost [151,152], field performance [153-155], structural performance [19], durability [156, 157], and environmental impact [44, 46,152].

Because of their various advantages, concrete pavements are widely used all around the world [35]. To design the concrete pavements a variety of design methods (e.g. [72, 73, 83, 84]) are used in different countries. In most of the design guides (e.g. [72, 73, 83]), fatigue of concrete slab and erosion of the slab support are two common failure cases considered in design, and the design is done to determine the slab thickness required to resist the repeated application of axle loads during the life of the pavement. Besides, flexural strength, modulus of elasticity and density are the important properties of concrete used to determine the required thickness of the pavement. Since the properties of the aggregates used to prepare the concrete mixtures have an important impact on the concrete properties used in design, required thickness values may significantly alter based on the type of aggregate used.

As previously explained, recycled aggregate concrete mixtures are usually known for their low strength, elastic modulus and densities, compared to the mixtures produced with virgin aggregates [145,158]. However, performance that could be obtained from the recycled aggregates depends on both the types and amount of recycled aggregate used.

### 2.6.1. Literature Gap

Though the effects of recycled aggregate usage on the performance of concrete has been widely-studied in the literature, there is a lack of data for the effect of obtained performance on the structural behaviors / requirements of concrete pavements.

### 2.6.2. Examination Methodology

To fill the above mentioned gap in literature, 3-dimensional (3D) finite element analyses were carried out in the scope of this dissertation for various concrete mixtures that includes virgin and recycled aggregates, by using the mechanical properties of the mixtures measured experimentally. It should be emphasized here that the 3D finite element analyses have been done by following a novel methodology which considers the

well-known previous works. According to obtained results, several recommendations have been given for the future research and design works, which are believed to be very beneficial for the future studies and design applications that include the use of recycled aggregates.

## 2.7. Joint Performance of Recycled Aggregate Concrete Pavements

Joint faulting is an important mode of failure for concrete pavements [159-161] which is considered to be one of the main design criteria in concrete pavement design guides [72, 83]. Faulting performance of concrete pavements is affected by a variety of sources, such as strength and stiffness of road layers, joint spacing, dowel bars (if any), traffic loads, edge support, and base-subbase characteristics [83, 162-164]. Relative deflection of neighbor slabs (usually represented as 'Load Transfer Efficiency (LTE) (%) = deflection of unloaded slab / deflection of loaded slab x 100') under the applied load is one of the crucial indicators that shows the performance of concrete pavement joints in terms of faulting [109, 163,165]. For pavement joints, total LTE is provided by the following contributors: aggregate interlock, dowel bars (if they exist), and base/subbase [164].

Ioannides and Corovesis [106] defined the aggregate interlock as a natural mechanism that transfers the loads within the pavement discontinuities (cracks, joints). The load transfer provided by the aggregate interlock mechanism is significant for the joints without load transfer devices (dowel bars). Properties of aggregates (e.g., stiffness of aggregates, the shape of aggregates, largest aggregate size, aggregate size distribution) used in the concrete mixture, as well as joint crack width, have a great impact on the load transfer provided by aggregate interlocking [109, 166-172].

Joint performance for concrete pavement mixtures produced with recycled aggregates was studied in a limited number of previous studies. Volz et al. [155] reported similar joint performance in field for doweled pavement joints produced with virgin and recycled aggregate concrete mixtures. Cross et al. [173] investigated the field

performance of non-dowelled jointed concrete pavements produced with recycled and virgin aggregates, and they reported higher joint faulting values for recycled aggregate concrete pavement. in a study, Vandenbossche [167] attributed the reduced joint performance obtained for the recycled aggregate concretes to the two-phase (natural aggregate + old mortar) structure of recycled aggregates which yields lower roughness in fracture (crack) surfaces (due to the smaller size of natural aggregates inside the recycled aggregates). in another study, Ozturk et al. [19] reported lower faulting performance for RCA, and they attributed the performance to the increased shrinkage (which leads to higher joint crack widths) and lower abrasion resistances obtained for recycled aggregates.

### 2.7.1. Literature Gap

Use of recycled aggregates in concrete pavement mixtures is a popular topic studied in its various aspects in detail. On the other hand, the number of studies concentrated on the effects of recycled aggregates on the faulting performance of concrete pavements, which is considered as one of the major failure modes in design, is very limited.

### 2.7.2. Examination Methodology

in this study, 3 different concrete mixtures were designed, as a mixture with full of virgin aggregates, two mixtures containing 50% and 100% recycled coarse aggregates. Then, basic mechanical (compressive strength, modulus of elasticity, Poisson's ratio, and flexural strength) and physical properties (density, absorption, and porosity), as well as abrasion resistance and post-cracking shear performance of concrete mixtures were measured. Based on the results obtained experimentally, a variety of discussions were presented in the paper, and recommendations were given accordingly.

# 3. EXPERIMENTAL AND NUMERICAL STUDIES

## 3.1. Materials

For the experimental studies carried out in the scope of this dissertation, two different Euro Norm (EN) 197-1 [174] CEM I 42.5 R type Portland cement, as well as ground granulated blast furnace slag and microsilica (MS) were used as binding materials, and their properties were given in Table 3.1. Various concrete mixtures (various plain, fiber reinforced, and recycled aggregate concrete mixtures) were produced in the scope of this thesis, and aggregates obtained from various sources (with various sizes and properties) were used to produce the mixtures. Properties of all the aggregates used were given in Table 3.2. For all the mixtures, tap water was used as mixing water. in addition, to adjust the workability of mixtures two different type of superplasticiser (SP) (modified polycarboxylate ether and naphthalene sulfonated formaldehyde). Moreover, one type of polypropylene and one type of steel fibers were used to produce FRC mixtures. Properties and photos of the fibers used were given in Table 3.3 and Figure 3.1, respectively.

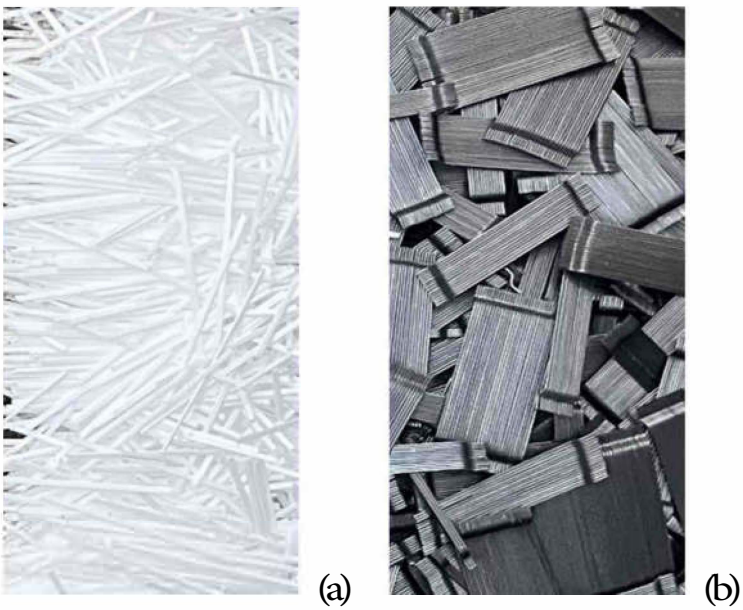


Figure 3.1. Photos of (a) polypropylene and (b) steel fibers.

Table 3.1. Ingredients / properties of binders.

| Ingredient / Property | Cement | Cement_A | Slag | MS |
|---|---|---|---|---|
| CaO (%) | 63.23 | 63.70 | 36.63 | 0.03 |
| Si02(%) | 18.71 | 19.80 | 40.95 | 90.21 |
| $Al2O_3$ (%) | 4.26 | 5.58 | 12.10 | - |
| $Fe2O_3$ (%) | 3.29 | 3.42 | 1.28 | - |
| MgO (%) | 1.06 | 1.22 | 5.48 | - |
| $SO_3$ (%) | 3.21 | 3.34 | 0.16 | 0.35 |
| Na20(%) | 0.24 | 0.24 | 0.56 | 0.45 |
| K20(%) | 0.68 | 0.66 | 0.36 | 0.85 |
| cı-(%) | 0.04 | 0.04 | 0.02 | - |
| Loss oflngition (%) | 3.37 | 1.85 | 0.11 | 2.87 |
| Insoluble Residue (%) | 0.70 | 0.29 | - | - |
| Unknown (%) | 1.91 | 0.15 | - | - |
| Free Lime (%) | 1.47 | 2.20 | - | - |
| Specific Gravity ($g/cm^3$) | 3.14 | 3.14 | 2.95 | 2.26 |
| Specific Surface ($cm^2/g$) | 3800 | 3490 | 5253 | 257000 |
| $C_3S$ (%) | 66.69 | 47.92 | - | - |
| C2S(%) | 3.42 | 20.70 | - | - |
| $C_3A$(%) | 5.73 | 9.01 | - | - |
| C4AF(%) | 10.01 | 10.41 | - | - |

## 3.2. Mixtures, Mix Design and Specimen Production

### 3.2.1. Mixtures

Conventional concrete mixtures with virgin and recycled aggregates, as well as conventional and roller compacted fiber reinforced concrete mixtures were designed and tested in the scope of this dissertation. Since several investigations were made in the scope of this dissertation independently from each other, properties and ingredients of the concrete mixtures used were given in the relevant part of the 'Results and Discussion' chapter, to make clear them for the readers. On the other hand, basics of the methodologies followed to design the concrete mixtures were given in the next part.

Table 3.2. Properties of aggregates.

| Aggregate Type | Partide Size (mm) | Oven-Dried Partide Density (g/cm$^3$) | Saturated&Surface Dried Partide Density (g/cm$^3$) | Water Absorption (%) |
|---|---|---|---|---|
| CSt: No I | 5 - 12 | 2.70 | 2.72 | 0.8 |
| CSt: No II | 12 - 24 | 2.69 | 2.71 | 0.6 |
| e s | O - 5 | 2.65 | 2.68 | 1.1 |
| NS | O - 5 | 2.60 | 2.62 | 0.8 |
| CSt: No LA | 4 - 8 | 2.68 | 2.70 | 0.65 |
| CSt: No ILA | 8 - 16 | 2.69 | 2.70 | 0.54 |
| RCA:Nol | 4 - 8 | 2.24 | 2.40 | 6.65 |
| RCA: No II | 8 - 16 | 2.36 | 2.43 | 3.04 |
| RBA:Nol | 4 - 8 | 1.80 | 2.08 | 13.50 |
| RBA: No II | 8 - 16 | 1.86 | 2.10 | 11.54 |
| cs_A | O - 4 | 2.67 | 2.70 | 1.2 |
| NS_A | O - 4 | 2.63 | 2.65 | 0.8 |
| Free Lime (%) | 1.47 | 2.20 | - | - |
| Specific Gravity (g/cm$^3$) | 3.14 | 3.14 | 2.95 | 2.26 |
| Specific Surface (cm$^2$/g) | 3800 | 3490 | 5253 | 257000 |
| $C_3S$ (%) | 66.69 | 47.92 | - | - |
| $C_2S$ (%) | 3.42 | 20.70 | - | - |
| $C_3A$ (%) | 5.73 | 9.01 | - | - |
| *C4AF(%)* | 10.01 | 10.41 | - | - |

### 3.2.2. Mix Design

Conventional concrete mixtures were designed by using the concrete technology method. For all the investigation cases, first the binder, fiber and water amount was selected and fixed, by considering the expected concrete performance (strength, ductility, ete.). Then, aggregates were proportioned for the relevant mixture considering the suggestions given in Turkish Standard (TS) 802 [175]. in the end, trial mixtures were prepared to determine the amount of SP required to achieve desired concrete consistency. Amount of concrete ingredients for 1 m$^3$ concrete mixtures were given for all the conventional concrete mixtures in the relevant part of 'Results and Discussions' chapter.

On the other hand, roller compacted concrete mixtures were designed by using the soil compaction method [176]. For all plain and fiber reinforced concrete mix-

tures, first, cement dosage and fiber amount was selected and fixed considering the expected concrete performance (strength, ductility, ete.). Afterward, aggregates were proportioned based on the suggestions given in American Concrete Institute (ACI) guide [176]. Then, amount of water required to achieve maximum dry density was determined for both plain and fiber reinforced concrete mixtures via modified proctor tests, as suggested in ACI 327R [176]. it is worth noting here that the RCC mixtures were designed without SP.

### 3.2.3. Specimen Production and Curing

3.2.3.1. Mixing Method. Two different pan mixers with 55 L and 90 L capacities were used to mix the concrete mixtures. First, dry materials (aggregates and cement) put into mixer and mixed for 2 minutes. Second, water and SP (if any) were added gradually in 1 minute while the mixer was still running, and the wet mix was mixed for additional 1 minute. in the final step, wet mixtures were mixed for 2 minutes to achieve uniformity. it should be noted here that for fiber reinforced concrete mixtures, fibers were added in 1 minute gradually in the first part of the final 2 minutes mixing (while the mixer is running). After completion of mixing protocol, slump values of mixtures were measured according to American Society for Testing and Materials (ASTM) C143 [177], to check if the final mix satisfies the requirements of aimed concrete. However, since RCC is a zero-slump concrete, the measurement was not done for the RCC mixtures.

Table 3.3. Properties of polypropylene (PPF) and steel (SF) fibers.

| Fiber | Surface | Shape | Length (mm) | Diameter (mm) | Aspect Ratio | Elastic Modulus (GPa) | Tensile Strength (MPa) |
|---|---|---|---|---|---|---|---|
| PPF | Embossed | Straight | 40 | 0.72 | 56 | 8.5 | 550 |
| SF | Smooth | Hooked-end | 36 | 0.55 | 65 | 200 | 1345 |

3.2.3.2. Specimen Production. Following the mixing protocol, for the physical and mechanical test specimens (cylindrical (10x20 cm) and prismatic (10xlüx35 cm)) were produced for all the mixtures. Conventional concrete mixtures produced in the scope of the dissertation were compacted by using a vibrating table in two layers. On the other hand, a vibratory hammer was used to compact the RCC mixtures, and the specimens were compacted in two layers with approximately similar thickness, according to ASTM C1435 [178].

3.2.3.3. Cracking Operation for Cyclic Shear Test Specimens. Following the demolding process (at approximately 24 hours), prismatic specimens (10xlüx35 cm) produced for shear tests were cracked with the cracking protocol suggested in literature [112, 113] and explained below.

First, to weaken the sections, two '10 mm' thick notches were sawn all around the specimen perimeters, where both notches were away from the middle of the specimen by '5 cm'. Then, reference points were mounted to both sides of the induced cracks to measure the crack widths. Afterward, the specimens were uniformly cracked from the weakened sections to a predefined crack width (0.2 mm) in 4 steps as follows:

In the first step, one of the weakened sections (by cutting the notches) of the specimen was loaded under the three-point bending test configuration until cracking as shown in Figure 3.2, and the specimen is unloaded. Then, specimen was shifted to induce a crack in the other weakened section and loaded again until cracking. Following this, the specimen was rotated upside down, and loaded from the first and second cracks, respectively, until the crack width in the middle of the section reaches '0.2 mm'. The four stages of cracking protocol were also shown in Figure 3.3. An MTS closed-loop servo-hydraulic testing machine was used for cracking operations and for all the crack width measurements done in this study a caliper with 'O.Ol mm' sensitivity was used. Following the cracking operation, cracked specimens were carefully put into the water tank (with 23 ±2 ℃ temperature), and cured for 28 days.

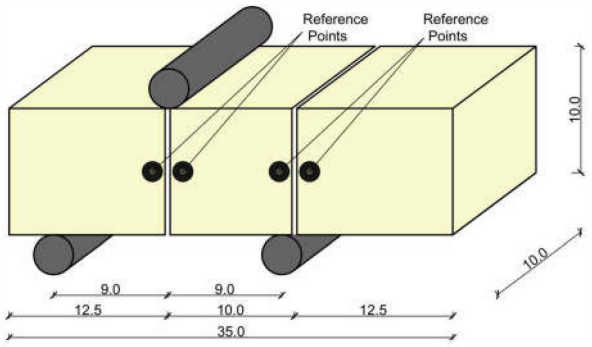


Figure 3.2. Three-point loading configuration for the cracking of shear specimens (units are given in 'cm').

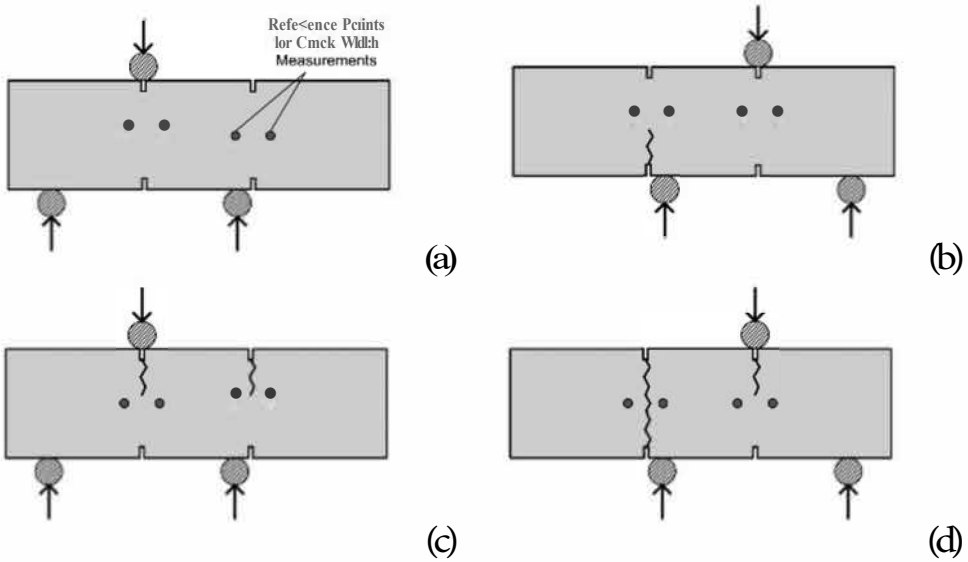


Figure 3.3. Schematic representation of applied cracking protocol; (a) first step (b) second step (c) third step (d) fourth step (beam specimens were rotated upside down between second and third step).

3.2.3.4. Curing. After the completion of the compaction process, all the specimens were demolded approximately in 24 hours, and then cured according to ASTM C192 [179] (moist cured at 23 ±2 °C), until the test age.

## 3.3. Physical Tests

To determine the physical properties; density, water absorption, and porosity values of all the concrete series were measured according to ASTM C642 [180]. Cylindrical samples with 10 cm diameter and 5 cm height sawn from 10x20 cm cylinders were used for the tests.

## 3.4. Mechanical Tests

### 3.4.1. Compressive Strength and Modulus of Elasticity

Modulus of elasticity and compressive strength tests were carried out on 10x20 cm cylindrical specimens, according to ASTM C469 [181] and ASTM C39 [182], respectively. Though, modulus of elasticity tests were done by using an MTS closed-loop servo-hydraulic test machine with 500 kN of maximum loading capacity, an automatic compression machine with 3000 kN of maximum loading capacity was used for the compressive strength tests. Test frame configuration for the modulus of elasticity tests was given in Figure 3.4.

### 3.4.2. Quasi-Static Bending for Plain Concrete

For almost all the plain concrete mixtures, load controlled 4-point bending tests on plain concrete mixtures were carried out according to ASTM C78 [183], and photo of the test frame was given in Figure 3.5. in addition, for the part related to structural performance of recycled aggregate concrete mixtures, 3-point bending tests were conducted according to Japan Concrete Institute (JCI)-8-001 [184]. All the bending tests were carried out on 10xlüx35 cm prismatic specimens by using an MTS closed-loop servo-hydraulic testing machine with 100 kN capacity.

Figure 3.4. Modulus of elasticity test frame.

### 3.4.3. Quasi-Static Bending for Fiber Reinforced Concrete

Flexural performance tests on fiber reinforced concrete mixtures were carried out on 10xlüx35 cm prismatic specimens cured for 28 days. The tests were conducted according to ASTM C1609 [185] by using an MTS closed-loop servo-hydraulic testing machine with 100 kN maximum loading capacity. Two linear variable displacement transducers (LVDTs) were used to measure the midspan deflection of the specimens, and the tests were conducted by controlling the midspan net deflection (average of two LVDTs measurements placed on front and back side of the specimens), as recommended in ASTM C1609 [185]. Photo of the test frame was given in Figure 3.6.

### 3.4.4. Quasi-Static Double-Punch

Double-punch tests were conducted on 15x15 cm cylindrical specimens sawn from 15x30 cm eylinders, and the diameters of the punches were 3.75 cm (1/4 of the diameter of the tested specimen) as recommended by Chen [68].


Figure 3.5. Plain concrete bending test frame.

For DPTs an MTS closed-loop servo-hydraulic testing machine with 500 kN capacity was used, and photo of the test frame was given in Figure 3.7. Tests were done by loading head displacement control, and displacement rate was set to 0.5 mm/min considering the recommendation given in Molins et al. [61]. It should be noted here that the top platen of the 500 kN MTS compression machine has rotating ability. However, the diameter of the punch is much lower than the upper platen, which makes hard to rotate the loading head by applying load to punch. Therefore, the spherical contact surface between the bearing block and the main frame was regularly lubricated to provide the rotation with minimum frictional resistance, as suggested by Colgrove and Chen [69].

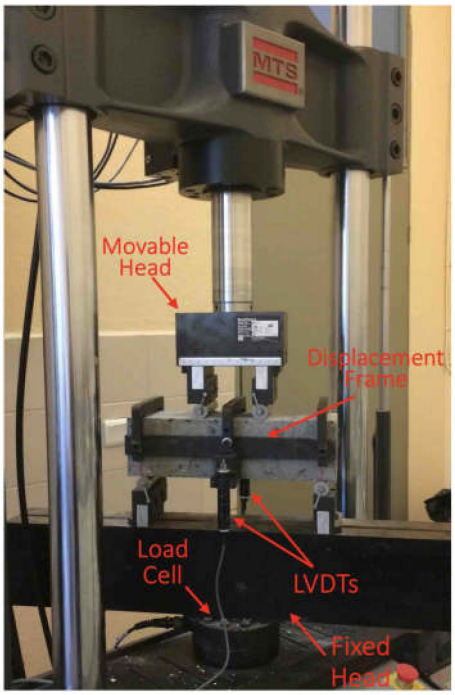


Figure 3.6. Fiber reinforced concrete bending test frame.

### 3.4.5. Abrasion

Abrasion tests were conducted according to ASTM C1747 [186], which was originally developed for pervious concrete mixtures. Considering its simplicity and strong correlation with surface abrasion tests reported in the literature [187], this test method was used in this study to compare the abrasion resistance of concrete mixtures produced with virgin and recycled aggregates. Three tests were carried out for all concrete mixtures using an automatic Los-Angeles abrasion machine. For each test, three cylindrical specimens with 10 cm diameter and 10 cm height (sawn from 10x20 cm cylinders) were put into the Los-Angeles abrasion machine, and the machine was rotated 300 times. Mass of the specimens was measured before and after each abrasion test, and mass loss due to the abrasions was calculated accordingly.

### 3.4.6. Cyclic Bending

Cyclic bending tests were carried out on 10xlüx35 cm (with '30 cm' span length) prismatic specimens by using an MTS closed-loop servo-hydraulic testing machine with

100 kN eapaeity with 10 Hz loading frequeney. Maximum stress levels were seleeted as 75% and 85% of flexural strength, while minimum stress level was 10% of flexural strength. Flexural strength mentioned here was determined from the quasi-statie flexure test results applied to the speeimens prepared for the same mixtures.


Figure 3.7. Double-puneh test frame.

### 3.4.7. Reversed Cyclic Bending

For the tests, first the beam speeimens were loaded, by using an MTS dosed-loop servo-hydraulie test maehine, in one way up to a eyde eorresponds to 30% failure probability (70% reliability), determined by assuming Weibull distribution (details were explained below). Then, survived speeimens (after eydie load applieation up to a eyde number eorresponding to 30% failure probability) were rotated 180° around their eenterlines and eydie loads were applied until the failure. Number of eydes eorresponding to failure were reeorded at the end of the tests. It should be noted here that for all loading eases minimum stress level was used as 10% of flexural strength and the tests were eondueted with 10 Hz loading frequeney. It is worth noting here that the illustrations of the applied eydie loading protoeols were given together with the loading protoeol previously [90] used to evaluate eydie loading performanee under stress reversal in Figure 3.8 Besides, the ineonvenienee of the previously applied protoeol in terms of eonerete pavements was explained in the 'Literature Review' part of the dissertation.

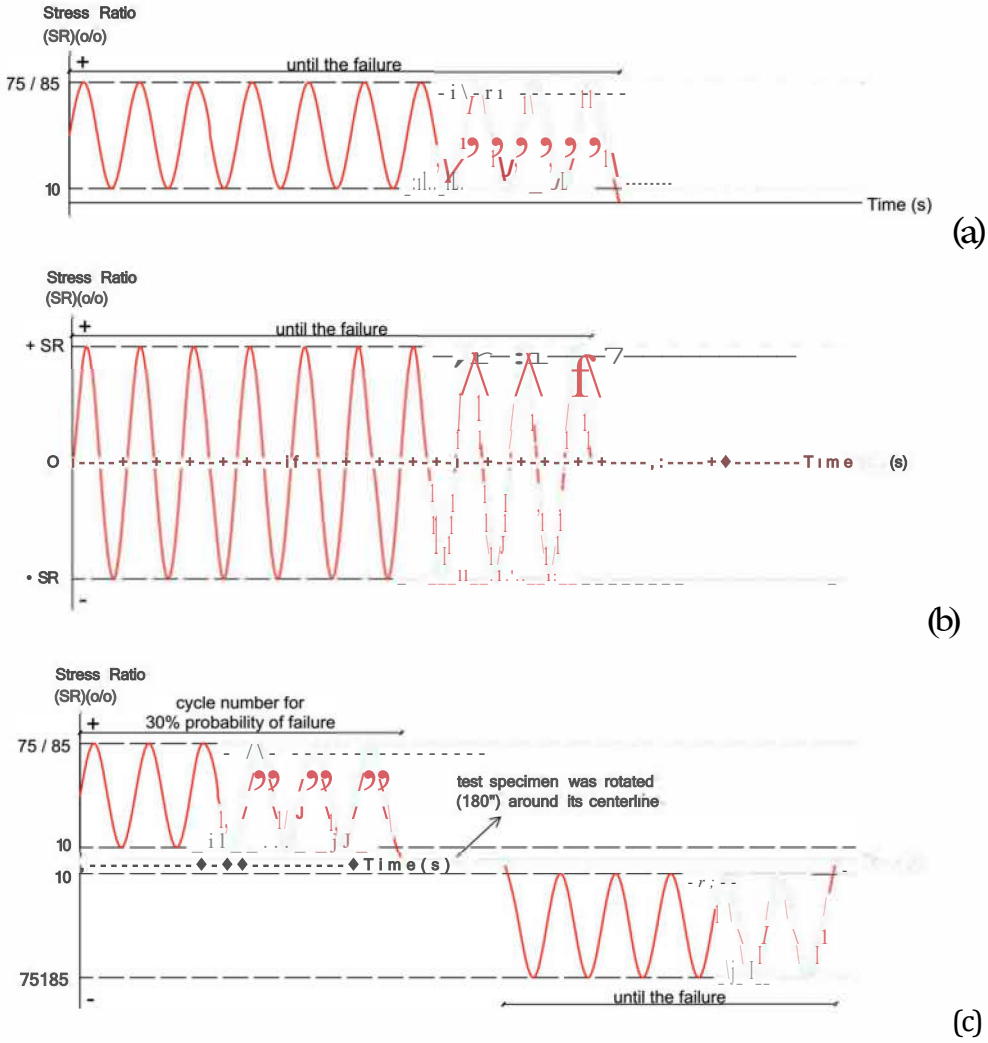


Figure 3.8. Illustrations of (a) one-way cyclic loading protocol, (b) loading protocol previously applied to measure the effect of stress reversal on cyclic bending performance, and (c) two-way cyclic loading protocol.

### 3.4.8. Cyclic Double-Punch

Cyclic double-punch tests were applied with an MTS closed-loop servo-hydraulic testing machine with 500 kN capacity. Similar maximum (0.75 and 0.85) and minimum (0.10) stress levels, as well as loading frequency (10 Hz) with flexural fatigue tests were used for the tests. On the other hand, the strength values used for cyclic DPTs were determined from the other half of the specimens. in another words, for cyclic DPTs, the maximum load that can be resisted by the one half of the specimen (15x15 cm cylinder sawn from 15x30 cm cylinder) was used to determine the maximum and minimum

stress magnitudes for the cyclic loading (which was applied to the other half of the 15x30 cm specimen). This special method was followed to eliminate the variation from specimen-to-specimen and batch-to-batch (both are in considerable amount in most of the times, as explained in the introduction part).

### 3.4.9. Cyclic Shear

Post-cracking shear tests were carried out for varying different crack widths, by using an MTS servo-hydraulic closed-loop testing machine with 100 kN maximum loading capacity following the recommendations given in Thompson [112] and Arnold et al. [113]. Drawings and photo of the test frame used were given in Figure 3.9. As it can be seen from the figures, the concrete specimen was loaded from the middle portion while portions on the sides were fixed to machine. 4 linear variable displacement transducers (LVDTs) (2 front (1 left, 1 right), 2 back (1 left, 1 right)) were placed to suitable positions two measure the deflection of middle portion compared to fixed portions of the specimen, which is closely related to the shear performance of cracked sections.

Cyclic loading was applied with 2 Hz according to the recommendation given in Arnold et al. [113], and the tests were continued for 500 cycles. To produce positive and negative '250 kPa' shear stress on each cracked surface, '+3.2 kN' maximum and '-3.2 kN' minimum load magnitudes were applied during the cyclic loadings. it should be noted that the magnitude of the shear stress was used by considering the suggestions given in Arnold et al. [113], where '250 kPa' was recommended as a typical shear stress magnitude, for concrete pavements. Additionally, number of cycles applied to the specimens (500 cycles) were selected to test specimens up to a cycle number that gives a relatively stable deflection values could be obtained, since both Thompson [112] and Arnold et al. [113] studies showed that the post-cracking shear damage propagation is considerably higher for the first a few cycles compared to following ones.

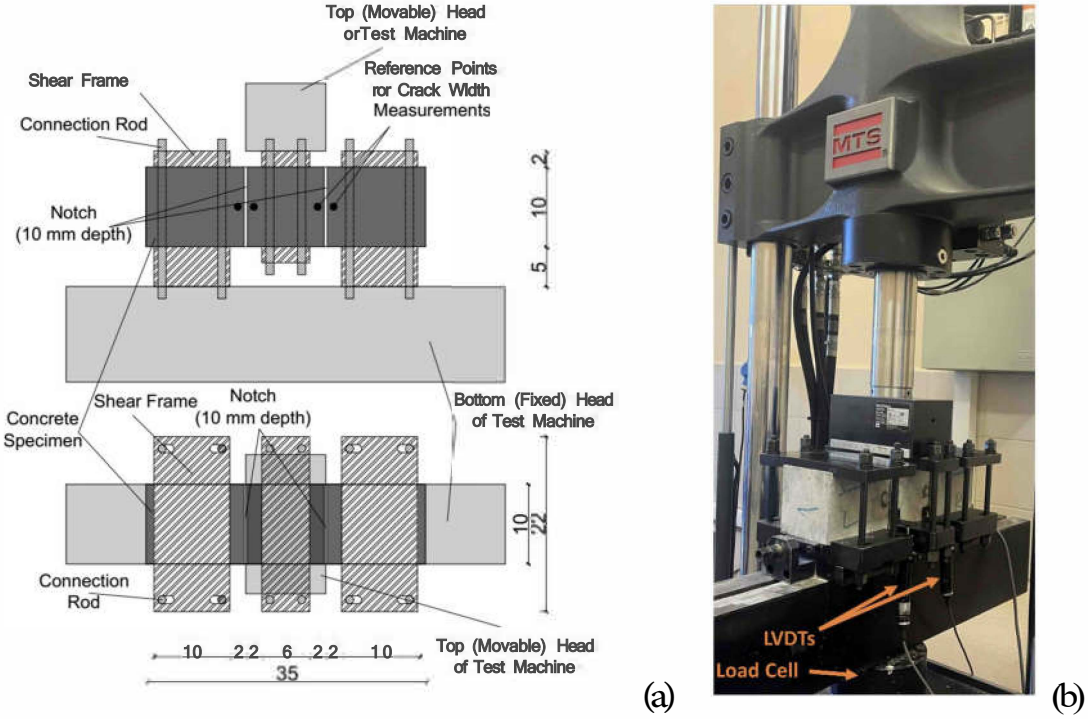


Figure 3.9. Shear frame (a) section, plan drawings (units are given in 'cm'), (b) photo.

### 3.5. Microstructural Analyses

Fiber-matrix interface properties were investigated by using an environmental scanning electron microscopy (SEM) and energy-dispersive X-ray spectroscopy (EDX) (Philips XL30 ESEM-FEG/EDX), to understand the effects of applied mixing methodology in microscale. Specimens used for the microstructural analyses were sampled from 10x10x35 cm beams used in flexural performance tests. First, the beams were crushed until a sample ('volume < 1 $cm^3$' with a maximum side length of '1 cm') was obtained with a fiber that could be separated from the cement matrix without significant damage. Then, the fibers were detached from the matrix carefully to obtain a clear interface with minimal damage. SEM images of one of the detached fibers were given in Figure 3.10 (for different magnifications: lO0x, 200x, lO00x, 500x), which shows the appearance of the surface after detaching in microscale, as well as the hydration products attached to the surface.

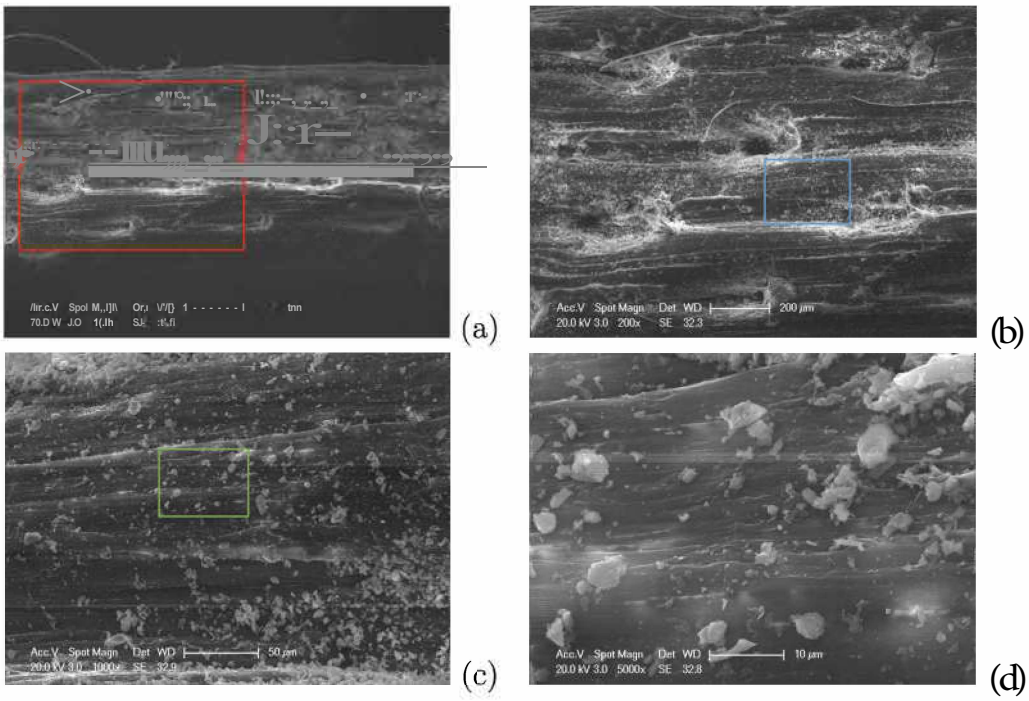


Figure 3.10. SEM images of a carefully detached fiber: (a) lO0x, (b) 200x, (c) lO00x, (d) (5000x).

Following the detaching process specimen surface that will be analyzed was covered with platinum and put into the SEM. For the analyses, first the interface was investigated by using the SEM images for the impurities and cracks. Then, EDX analyses were done to determine elemental distribution of an area free from cracks and impurities (large fiber residues, detached particles, pores, ete.). The width of embossed PP fibers used in this study was '1.2 mm', and '1/3' of this width was used as a side length of square area ('400 $\mu m$ x 400 μm') for EDX analyses. it is worth noting here that the size was also found to give reasonable (stable) elemental distribution (similar distribution with small change in size and position of analyzed surface) from trial analyses. For each of the FRC mixtures, 3 different surfaces were analyzed to avoid from the results that only explain the distribution for a local area. For one of the analyzed sample, SEM images (lO0x and 200x magnification), as well as obtained EDX spectrum and distribution of elements (both for 'weight%' and 'atomic%') were given in Figure 3.11. As given in the figure, the surfaces were analyzed for the following elements: oxygen (O), calcium (Ca), silicon (Si), magnesium (Mg), aluminum (Al), sodium (Na), iron (Fe), sulfur (S), potassium (K), and carbon (C) (to check for PP fiber residues).

As it can be seen from Figure 3.11 ((d) and (e)), in addition to oxygen, calcium (Ca) and silicon (Si) are the elements that produce significant portion of cement paste. Calcium to silicon ratio (Ca/Si) is the parameter commonly used to explain the interface characteristics in concrete mixtures [188-192]. Since, decreasing Ca/Si is attributed to high calcium silicate hydrate (C-S-H) and low calcium hydroxide *(Ca(OHh)* and ettringite at the interface [188,193] and C-S-H is the matrix component that contributes most to interface strength [194], lower Ca/Si usually associated with better interface [188,190]. Therefore, in the scope of this study, Ca/Si of the analyzed surfaces were calculated for atomic% ratios (representation given in Figure 3. 11 (e)) of the elements (Ca and Si), and the obtained values were compared to see the change in fiber matrix interface composition from mixture to mixture.

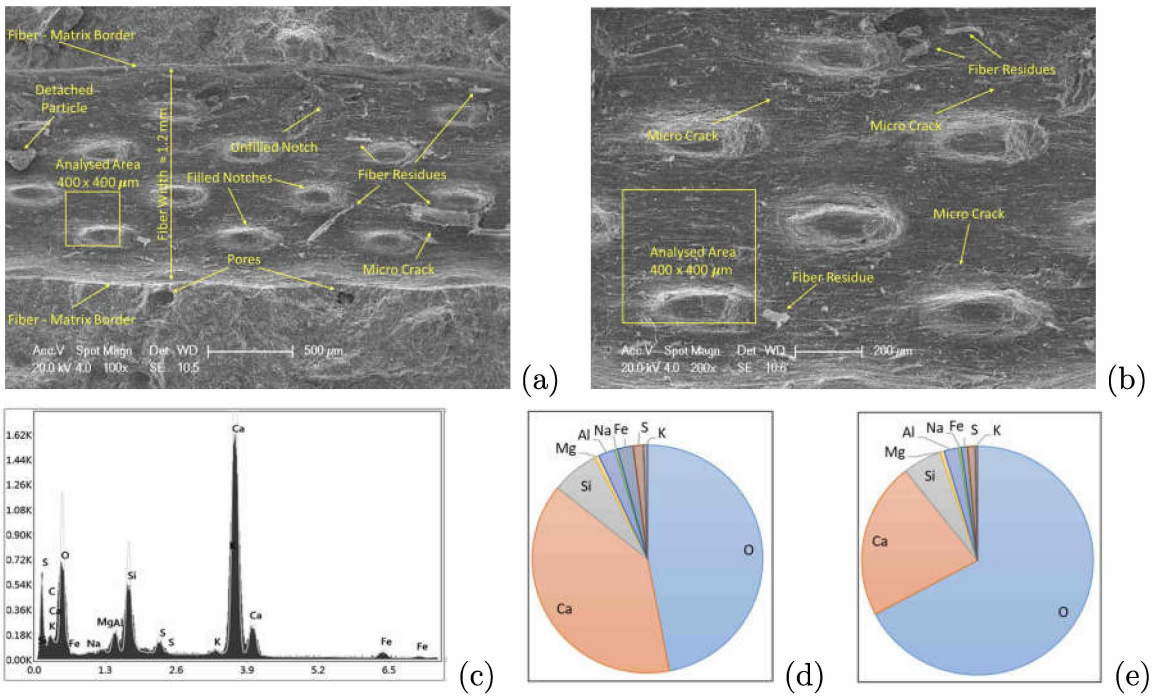


Figure 3.11. SEM/ EDX Analysis; (a) SEM image (lüüx) and analyzed area, (b) SEM image (200x) and analyzed area, (c) EDX Spectrum, (d) weight% of elements, (e) atomic% of elements.

Elemental analysis technique used in this study (EDX) gives the results by analyzing the surface up to a limited thickness, which should be taken into account while evaluating the results. Linke and Schreiner [195] reported that the depth of information that could be obtained from the EDX analysis change between 1 to 5 $\mu m$. In another studies [196,197] the depth is reported as 2 $\mu m$. In another study [198], it was reported that the depth of analysis for EDX varies between 1 and 10 $\mu m$ depending on the accelerating voltage of the electron beam as well as the chemical composition and morphology of the surface being analyzed.

## 3.6. Thickness Design

To see the effects of fibers on the thickness requirement of concrete pavements, a parametric study was carried out by using the material properties obtained from this study. Soil, traffic, and environment parameters used in all design cases were given in Table 3.4. The parameters given in Table 3.4 were determined by considering the typical values given in both American Concrete Pavement Assocoiation (ACPA) StreetPave [104] software and IRC [84] guide. For the design, major arterial road traffic spectrum given in ACPA StreetPave [104] design software was considered, and for all the trucks spacing between the front axle and first rear axle was assumed less than 4.5 m, for top-down cracking analysis. In addition, 5 ℃ of built-in negative temperature differential was added for stress analysis for top-down cracking (based on IRC 58 [84]).

IRC [84] design methodology was used to determine the thickness requirement of pavements. Based on the methodology, first, for the trial thickness, stress analysis was done for all axle load classes by considering the curling occur in the slab during the daytime and nighttime, due to temperature differential. Then, allowable axle load repetition values for calculated stress values were determined and compared with the expected number of repetitions corresponding to considered axle load, and damage due to the related axle load is determined as a ratio of the expected number of load repetition to the allowable number of load repetition.

Table 3.4. Soil, traffic, and environment parameters.

| Parameter | Value |
|---|---|
| Road Type | Major Arterial |
| Design Life (year) | 30 |
| Annual Daily Truck Traflic | 1000 |
| Annual Growth Rate (%) | 2 |
| Traffic in the Dominant Direction (%) | 50 |
| Daytime Traffic (%) | 50 |
| Nighttime Traffic (%) | 50 |
| Temperature Differential (Day) (°C) | 10 |
| Temperature Differential (Night) (°C) | 5 |
| Modulus of (Subgrade + Base) Reaction (MPa/m) | 285 |
| Transverse Joint Spacing (m) | 4.5 |
| Lane Width (m) | 3.5 |

In the next step, cumulative fatigue damage is calculated as a sum of the damage from all the axle load classes (based on Miner's hypothesis [199]). According to IRC [84]) guide, cumulative fatigue damage should be less than 100%; hence, this process is repeated until achieving this criterion by changing the trial thickness values.

For FRC mixtures, the effective modulus of rupture (MOR) approach explained in previous studies [93,101] was used. Based on the suggestions, experimentally measured MOR values were increased for FRC mixtures by

$$MOR' = MOR \times (1 + R150), \tag{3.1}$$

where $MOR$ and $MOR'$ show the modulus of rupture and effective modulus of rupture, respectively. In addition, $R_{150}$ shows the residual flexural strength (RFS) ratio corresponding to "L (span length) / 150" mid-span deflection, and it is calculated by dividing the RFS at "L/150 mm" mid-span deflection to the MOR of concrete (based on ASTM C1609 [185]).

## 3.7. Numerical Study

Finite element analysis for the material properties obtained from the experimental study was conducted by using a pavement specific 3D finite element analysis software, called EverFE (version 2.26) [200]. Increasing effect of temperature gradient on the stress occurring in the slab is a known fact, and the structural response of the pavement structure is very much dependent on the thermal expansion coefficient of concrete, which may change due to the change in the type of aggregates used in concrete. Although, effect of temperature on the structural response of concrete pavements is considered in some of the design guides [83, 84], some other design guides (such as Portland Cement Association (PCA) design guide [72]) do not consider the effect of temperature gradient in the stress computation procedure. in the scope of this study, the effect of temperature gradient was not taken into account, in order to simplify the modelling and evaluation procedure.

Structural analysis studies were done for jointed plain concrete pavements placed on a dense liquid with two different reaction moduli, as 100 and 200 MPa/m. A 1 lane pavement with 3 slabs was modelled and plan dimensions of each slab were taken as 3.6x4.5 m (width x length). For the analysis, required material parameters were determined as follows.

Modulus of elasticity and density were directly taken as average of the values from the experimental study. it should be stated that fresh density values of the mixtures were used in the models. Since, Poisson's ratios of the mixtures were not measured, and considering that the structural behaviour is not so sensitive to changes in Poisson's ratio for typical values of 0.20 to 0.25, Poisson's ratio was taken as a constant value of 0.20 in the structural analysis. Joint stiffness for the aggregate mixtures were determined as [201]

$$AGG = \left[\frac{\left(\frac{1}{LTE} - 0.01\right)}{0.012}^{-1.17786}\right] \times k \times l, \qquad (3.2)$$

where $AGG$ is joint stiffness, and $k$ and $l$ are support modulus (MPa/mm) and radius of relative stiffness (mm), respectively. in addition, $LTE$ is load transfer efficiency (%), and determined as [171]

$$LTE(\%) = 39.7 \times \log\left\{ \left[0.3689 + ATS + \left(\frac{61.5434 \times W}{C \times LA}\right)\right] \times 2.54 \times t_{eff} \right\} + 5.6, \quad (3.3)$$

where $TS$ is top aggregate size (in), $LA$ is Los Angeles abrasion (%) value of aggregates, $W$ and $C$ are water and cement amount by weight respectively, $t_{eff}$ and $CW$ represents effective depth (cm) and crack width (cm) respectively. in addition $ATS$ is aggregate top size terms and determined as

$$ATS = 0.5004 \times TS - \frac{24.5162}{LA} + 0.2049 \times TS^2 - \frac{W}{C} \times (0.0540 + 2.2665 \times TS). \quad (3.4)$$

To determine the $LTE$ by using the equation given above; $TS$, $LA$ and $W/C$ values were directly taken from the material parameters used in the study. in order to determine $t_{eff}$, saw-cut depth was assumed as 25% of total slab thickness, and $t_{eff}$ was used as a 75% of the total slab thickness. As the last parameter, $CW$ is determined by considering the possible shrinkage values of the mixtures. in this step, shrinkage value of control mixture (CStC) is assumed as 300 micro-strain by considering the typical values given in [202]. Then, by considering The lnternational Union of Laboratories and Experts in Construction Materials, Systems and Structures (RILEM) [203] recommendation shrinkage values for RCAC and RBAC are taken as 450 (1.5x300) and 600 (2x300) micro-strain respectively. For the last step, by assuming a homogeneous disribution of shrinkage strains occurring in the pavement slab, CW is calculated by multiplying the given strain values and effective slab length, that will contract and produce the crack (effective length is taken as 4.5 m (2x2.25 m)). it is worth noting here that the shrinkage values of the concrete mixtures were assumed by considering the well-known previous works, since they are not measured experimentally. However, possible deviation from the RILEM [203] recommendation might slightly alter the numerical outcomes of the study.

To investigate the effect of different loading configurations on the structural behaviour, the analysis was done for both single and tandem dual wheel axle loads. Considering the maximum axle load values allowed in Turkey, the load magnitudes for the single and tandem axles were taken as 100 and 180 kN respectively [204]. For both of the axle load cases, stress and deflection analysis were done to evaluate fatigue and faulting performance of the pavement slabs made with different materials. Axle loads were applied to the center slab (middle of the 3 slabs) on the critical locations defined in PCA design procedure [72]. Briefly, for the maximum stress analysis (critical for fatigue failure) either single or tandem axle loads were applied on the middle part of the center slab, and for the maximum deflection analysis (critical for faulting failure) the loads were applied near the transverse joints (based on the critical locations defined in PCA design guide [72]). Besides, to obtain the parameters for worst loading conditions, the loads were placed near the longitudinal joints. Illustrations for all of the critical loading cases were given in Figure 3.12. It should be noted that the loading area for each wheel is used as 150x225 $mm^2$, which corresponds to 0.74 MPa and 0.67 MPa pressure, for single axle loading of 100 kN and tandem axle loading of 180 kN, respectively.

To determine the effect of the use of different mixtures on the maximum stress and deflection occurring in the pavement slab, the analysis was done for a constant slab thickness of 15 cm for all the mixtures tested in the scope of this study. Additionally, for all of the mixtures, pavement thickness values required to resist 1 million repetitions of maximum single and tandem axle loads were determined for both fatigue and faulting criteria. it should be noted here that PCA criteria [72] was used for the fatigue and faulting life determinations, and all of the analysis were done for single and tandem axle load cases to determine the effect of different loading configurations on the life of pavements with different concrete mixtures. Details of the followed procedure explained below.

First, a trial thickness was assumed for the considered mixtures, in order to start the iterations. Then, for single and tandem axle loading cases, maximum stress and

deflection values corresponding to the trial thickness value were determined by using the finite element (EverFE [200]) model. in the third step, the maximum stress and maximum deflection values were used to calculate the allowable number of axle load repetitions for both fatigue and faulting criteria of PCA [72], explained in the next paragraph. As a final step, for all of the design cases (2 failure criteria (fatigue and faulting), 2 foundation stiffness condition (100 and 200 MPa/m), 2 axle load types (single and tandem), 5 concrete mixtures (CStC, RCAC, TRCAC, RBAC, TRBAC) the trial thickness was modified repetitively to determine the required thickness values to resist 1 million cycle of considered loading case.

For the fatigue failure analysis, in the first step, the stress ratio (SR) was determined by dividing the maximum stress for the considered axle load type to the flexural strength of the considered mixture. Then, the allowable number of load repetition was considered as infinite, if $SR$ is less than 0.45. On the other hand, the number was determined as

$$log\ (N_1) = 11.737 - 12.077 \times SR, \tag{3.5}$$

if $SR$ is higher than 0.55. Otherwise (if $SR$ is between 0.45 and 0.55) the number of load repetition was determined as

$$N_1 = \left(\frac{4.2577}{SR - 0.4325}\right)^{3.268}, \tag{3.6}$$

where $SR$ and $N_1$ represent stress ratio and number of allowable repetition for fatigue failure, respectively.

Moreover, for the faulting failure analysis, rate of work (or power) was determined as [205, 206]

$$P = 268.7 \times \left(\frac{k^{t^{2.7}} \times (5^{\circ}2)}{h}\right), \tag{3.7}$$

where $P$, $k$, $\Delta$, and $h$ are power, subgrade stiffness, corner deflection, and thickness of the slab, respectively. Then, if $C_1 \times P > 9$, the allowable number of load repetition was considered as infinite. Otherwise, the allowable repetition was determined as [205-207]:

$$loglog\ (N_e) = 14.524 - 6.777 \times (C_1 \times P - 9)^{0.1^{03}} - loglog\ (C_2), \qquad (3.8)$$

where $P$ is power (explained above), $C_1$ and $C_2$ are adjustment factors, and $N_e$ is the number of allowable road repetition for the erosion (faulting) failure criteria.

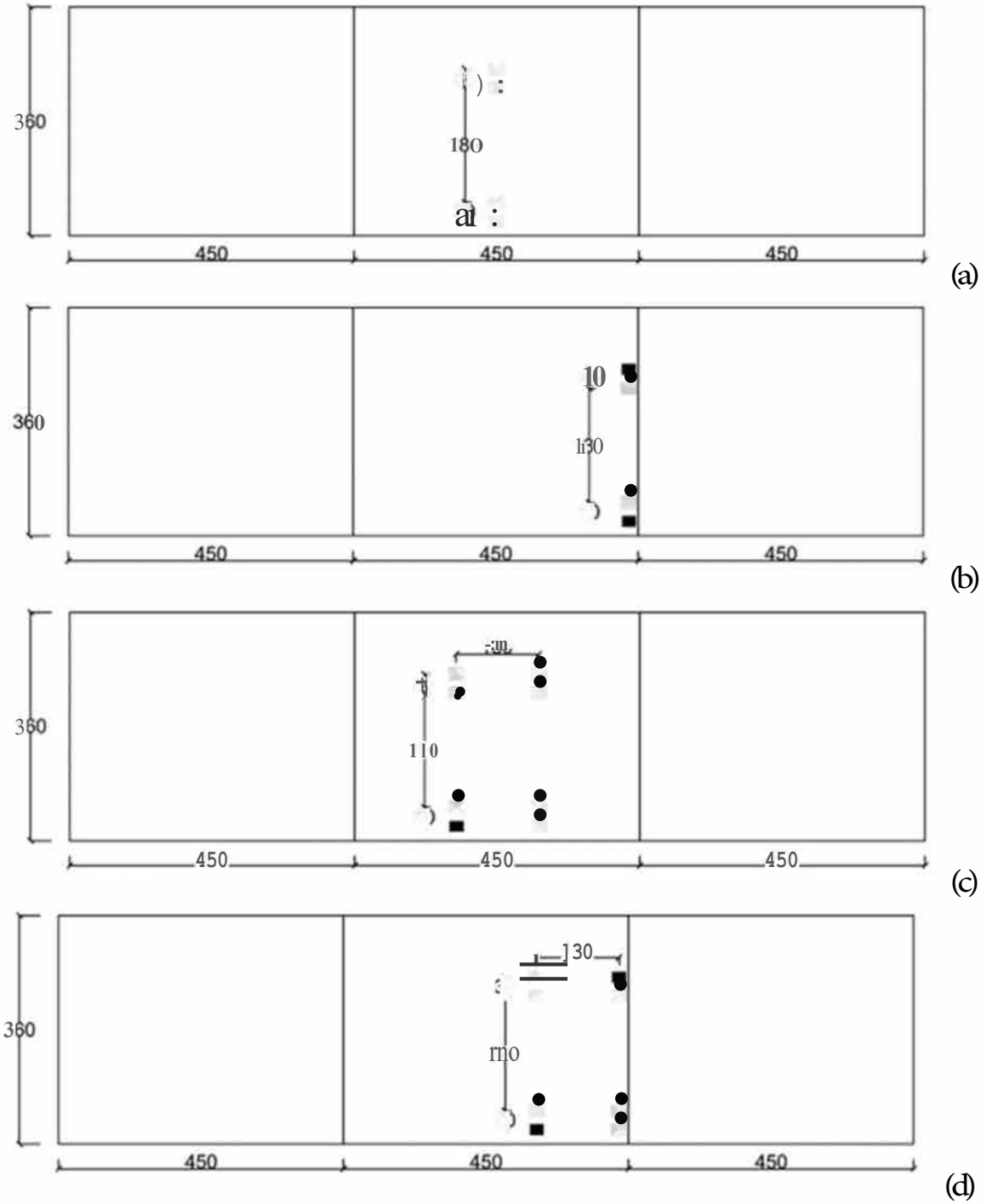


Figure 3.12. Model layouts and single / tandem axle load positions used in stress and deflection analysis (units are given in 'cm'): (a) stress analysis for single axle load of 100 kN, (b) deflection analysis for single axle load of 100 kN, (c) stress analysis for tandem axle load of 180 kN, (d) deflection analysis for tandem axle load of 180 kN.

# 4. RESULTS AND DISCUSSIONS

## 4.1. Variation in Concrete Fatigue Tests

### 4.1.1. Mixtures

Two concrete mixtures with different strengths, were designed for this part of the study. For both mixtures, cement dosage was fixed to 350 kg/m$^3$; however, water to cement ratios were used as 0.45 (named as W45) and 0.60 (named as W60). For both mixtures, amount of SP was adjusted to achieve EN 206 [208] - S2 slump class (5 - 8 cm slump value). Based on the given design methodology and nomenclature, ingredients for 1 m$^3$ concrete mixtures were given in Table 4.1.

Table 4.1. Mixture ingredients for 1 m$^3$ concrete (in kg).

| Mixture | Cement | CSt: No 1 | CSt: No 2 | es | NS | Water | SP |
|---|---|---|---|---|---|---|---|
| W45 | 350.0 | 577.9 | 480.6 | 676.2 | 192.6 | 157.5 | 2.8 |
| W60 | 350.0 | 537.2 | 446.8 | 628.6 | 179.1 | 210.0 | 1.4 |

### 4.1.2. Compressive Strength and Modulus of Elasticity

Average, standard deviation (SD) and coefficient of variation (COV), as well as maximum and minimum values for 28th day compressive strength and modulus of elasticity test results were presented in Table 4.2. As the table illustrates, by decreasing W/$C$ ratio from 0.60 to 0.45 average compressive strength value increased from 32.7 MPa to 49.6 MPa, and average modulus of elasticity value were increased from 23.7 MPa to 27.1 MPa.

Table 4.2. Compressive strength and modulus of elasticity test results.

| Parameter | W60 | | W45 | |
|---|---|---|---|---|
| | Compressive Strength (MPa) | Modulus of Elasticity(GPa) | Compressive Strength (MPa) | Modulus of Elasticity (GPa) |
| Number of Specimens | 6 | 6 | 6 | 6 |
| Maximum | 33.2 | 27.1 | 53.6 | 28.1 |
| Minimum | 32.0 | 21.5 | 46.5 | 25.1 |
| Average | 32.7 | 23.7 | 49.6 | 27.1 |
| SD | 0.5 | 1.9 | 3.1 | 1.1 |
| COV (%) | 1.5 | 8.1 | 6.2 | 4.2 |

### 4.1.3. Quasi-Static Flexure and Double-Punch Test Results

In this part, quasi-static flexure and double-punch test results were presented, and the results were compared in terms of their variations. For the comparison, first suitability of normal distribution (commonly used to evaluate concrete strength test results) assumption to the obtained results were checked by considering the median, skewness and kurtosis values, as well as 'Shapiro-Wilk significance's. The calculations were carried out by using SPSS software [209], and the results were presented in Table 4.3. To evaluate the validity of the normal distribution, the calculated values were compared with the criteria given in the literature [210-212]. The criteria used for the evaluation are:

- Median and average values of the results should be reasonably close.
- Skewness values should be between +1 and -1.
- Kurtosis values should be between +2 and -2.
- 'Shapiro-Wilk significance' value should be more than 0.05 (for '95% confidence level').

When the values given in Table 4.3 compared with the given criteria, it was seen that the results obtained for all the test cases satisfies the requirements for normal distribution. Thus, SD and COV values were calculated by assuming normal distribution,

and they were presented in Table 4.4, together with the maximum and minimum test results obtained and number of specimens tested. Based on Table 4.4, considerably lower COV values were obtained for DPT (2.1 % and 1.7 % for W60 and W45, respectively) compared to 4PBT (4.1 % and 6.5 % for W60 and W45, respectively), which validates the reports of the previous studies [61,69, 70].

Table 4.3. Normality check for quasi-static flexure and double-punch tests.

| Test Configuration | Concrete Type | Number of Specimens | Average (kN) | Median (kN) | Skewness | Kurtosis | Shapiro - Wilk | |
|---|---|---|---|---|---|---|---|---|
| | | | | | | | Sig. | Null Hypothesis |
| 4PBT | W60 | 12 | 18.0 | 18.1 | 0.136 | -0.922 | 0.832 | Accept |
| DPT | W60 | 12 | 115.3 | 115.1 | 0.248 | -1.207 | 0.612 | Accept |
| 4PBT | W45 | 6 | 22.2 | 22.4 | -0.197 | -0.692 | 0.911 | Accept |
| DPT | W45 | 6 | 151.5 | 152.0 | -0.833 | 0.490 | 0.726 | Accept |

Table 4.4. Statistical values for quasi-static test results.

| Test Configuration | Concrete Type | Number of Specimens | Max (kN) | Min (kN) | Average (kN) | SD (kN) | COV (%) |
|---|---|---|---|---|---|---|---|
| 4PBT | W60 | 12 | 19.2 | 16.8 | 18.0 | 0.73 | 4.1 |
| DPT | W60 | 12 | 119.2 | 112.1 | 115.3 | 2.38 | 2.1 |
| 4PBT | W45 | 6 | 24.1 | 20.2 | 22.2 | 1.43 | 6.5 |
| DPT | W45 | 6 | 154.5 | 147.2 | 151.5 | 2.58 | 1.7 |

### 4.1.4. Cyclic Flexure and Double-Punch Test Results

In this part, cyclic test results are presented, and a variety of statistical analyses were done to evaluate the obtained results. Based on the results of the tests and analyses several discussions were provided. Since the variations of the test results is the main interest of the study, presented results were especially examined in terms of their variations and the obtained values were compared with the literature to check the validity of the obtained / calculated results.

Cycle numbers for the failure under cyclic bending (4PBT) and double-punch (DPT) tests were given in Table 4.5 from smaller to larger eyde numbers. in the table, '*' shows the value considered as outlier (based on Chauvenet's criterion [213]), and not included in the analyses. In addition, '**' shows the value not included in the analyses due to a visible defect (an alignment problem caused by the used mold) on the specimen. As given in the table, 10 specimens were tested for each of the test cases. For the statistical analyses, first, test results for all loading configurations, maximum stress levels and concrete types were checked against normality, and results were given in Table 4.6, where bold values shows the results that might be attributed to deviation from normality. SPSS software [209] were used for the calculations, and the calculated values were compared with the criteria given in the previous section. Results showed that almost all of the results satisfies the requirements for normal distribution. However, some of the values were found really close to the boundaries that are considered as normality criteria. Therefore, it was concluded that the use of an alternative distribution function might be considered especially for some of the cases.

Table 4.5. Number of cycles for failure under cyclic 4PBT and DPT.

| Test Configuration | 4PBT | | | | DPT | | | |
|---|---|---|---|---|---|---|---|---|
| Concrete Type | W60 | | W45 | | W60 | | W45 | |
| Maximum SR (applied max stress/strength) | 85% | 75% | 85% | 75% | 85% | 75% | 85% | 75% |
| Minimum SR (applied min stress/strength) | 10% | 10% | 10% | 10% | 10% | 10% | 10% | 10% |
| 1 | 1637 | 17835 | 1551 | 76** | 293 | 9123 | 403 | 2446 |
| 2 | 1798 | 18849 | 2042 | 1569 | 397 | 9216 | 449 | 2589 |
| 3 | 2252 | 21100 | 2452 | 9706 | 437 | 9615 | 530 | 3614 |
| 4 | 2253 | 25471 | 3395 | 19803 | 452 | 10471 | 582 | 4117 |
| 5 | 3631 | 25743 | 8010 | 26498 | 515 | 11095 | 813 | 4197 |
| 6 | 4126 | 47361 | 9295 | 38987 | 544 | 11217 | 1161 | 7229 |
| 7 | 8430 | 47792 | 9792 | 46955 | 696 | 15122 | 1370 | 8442 |
| 8 | 9352 | 50615 | 10618 | 51321 | 1027 | 17616 | 1427 | 8585 |
| 9 | 13073 | 65113 | 12650 | 52648 | 1103 | 19981 | 1439 | 11854 |
| 10 | 16195 | 86407 | 12967 | 66751 | 1184 | 23873 | 2379* | 12150 |

Table 4.6. Normality check for cyclic flexure and double-punch tests.

| Test Configuration | Concrete Type | Maximum Stress Ratio (%) | Average | Median | Skewness | Kurtosis | Shapiro - Wilk | |
|---|---|---|---|---|---|---|---|---|
| | | | | | | | Sig. | Null - Hypothesis |
| 4PBT | W60 | 85 | 6275 | **3879** | **0.964** | -0.372 | **0.050** | Accept |
| 4PBT | W60 | 75 | 40629 | 36552 | 0.878 | 0.350 | 0.136 | Accept |
| 4PBT | W45 | 85 | 7277 | 8653 | 0.154 | **-1.850** | 0.119 | Accept |
| 4PBT | W45 | 75 | 34915 | 38987 | -0.203 | -1.118 | 0.813 | Accept |
| DPT | W60 | 85 | 666 | 530 | 0.720 | -1.195 | 0.089 | Accept |
| DPT | W60 | 75 | 13733 | 11156 | **1.019** | 0.188 | **0.053** | Accept |
| DPT | W45 | 85 | 908 | 813 | 0.166 | **-2.133** | 0.074 | Accept |
| DPT | W45 | 75 | 6522 | 5713 | 0.473 | 1.293 | 0.160 | Accept |

Despite the doubt for some of the cases by means of normality, since most of the results do not significantly deviates from normality, statistical values for cyclic tests first calculated assuming normal distribution and given in Table 4.7 (to see and compare the results). Based on the last column of the table (COV %) comparatively lower variations were found for cyclic DPT (between 37.7 - 56.0 %) compared to 4PBT (between 56.4 - 83.0 %) for the tested concrete series and maximum stress ratios. Additionally, when average eyde numbers given for W45 and W60 are compared for all for DPT and 4PBT, it was seen that the values were found closer for 4PBT compared to DPT (both for 85% and 75% maximum stress ratio cases).

Table 4.7. Statistical values for cyclic test results (assuming normal distribution).

| Test Configuration | Concrete Type | Maximum Stress Ratio (%) | Number of Specimens | Max | Min | Average | SD | COV (%) |
|---|---|---|---|---|---|---|---|---|
| 4PBT | W60 | 85 | 10 | 16195 | 1637 | 6275 | 5210 | 83.0 |
| 4PBT | W60 | 75 | 10 | 86407 | 17835 | 40629 | 22896 | 56.4 |
| 4PBT | W45 | 85 | 10 | 12967 | 1551 | 7277 | 4495 | 61.8 |
| 4PBT | W45 | 75 | 9 | 66751 | 1569 | 34915 | 21810 | 62.5 |
| DPT | W60 | 85 | 10 | 1184 | 293 | 666 | 323 | 48.5 |
| DPT | W60 | 75 | 10 | 23873 | 9123 | 13733 | 5179 | 37.7 |
| DPT | W45 | 85 | 9 | 1439 | 403 | 908 | 441 | 48.5 |
| DPT | W45 | 75 | 10 | 12150 | 2446 | 6522 | 3656 | 56.0 |

To compare the significance of the difference between the performances, t-tests were carried out, and the resulting p-values are presented in Table 4.8. it is worth

noting here that the p-values (calculated for t-tests) given in the table show the significance of the difference in average values, and it is calculated by considering average and standard deviation of the compared <lata series (decreasing p-value indicates the higher statistical difference between the <lata series). When the results (p-values) are examined, statistical difference between the means was obtained for only one of the comparison cases (W45 - DPT - 75 and W60 - DPT - 75), for 95% confidence level (a = 0.05). Since the mean value for W60 is higher than W45 for 75% maximum stress ratio, it can be said that the W60 (low strength) perform better under the cyclic loading with this magnitude (75% of strength) compared to W45 (high strength). For the other 3 comparison cases no statistical difference was obtained, which is the combined result of close mean values and large variations (that make hard to differentiate the means for t-test). It should be noted here that better cyclic loading performance (in terms of cyclic load resistance for similar stress ratios) for lower strength concrete mixtures were reported also in the previous studies [47,214].

Table 4.8. T-test p-values for the comparison cases.

| Case | W60 - 4PBT - 85 | W60 - 4PBT - 75 | W60 - DPT - 85 | W60 - DPT - 75 |
|---|---|---|---|---|
| W45 - 4PBT - 85 | 0.651 | - | - | - |
| W45- 4PBT - 75 | - | 0.586 | - | - |
| W45 - DPT- 85 | - | - | 0.184 | - |
| W45 - DPT- 75 | - | - | - | 0.002 |

Another thing that can be seen from the Table 4.7 is that the resulting average values were found considerably lower for DPT compared to 4PBT, for all the cases. This result might be attributed to the difference between the cracking mechanisms of these two tests. Galeote et al. [215] stated that the crack height increases progressively in bending test during the cracking, but the cracks occur abruptly in DPT (associated with the stress distribution in the DPT and bending test specimens during the loading).

To further explain the difference between the cracking mechanisms of these two cyclic tests (DPT and 4PBT), cyclic creep curves (eyde number vs peak loading head

displacement corresponding to related cycle number) obtained from the experiments were also examined in this part. Degradation of concrete under cyclic loading usually divided into three distinct stages; as crack initiation, micro-cracking (slow propagation of flaws in concrete up to a critical size), and unstable crack propagation (occurs after the flaws in concrete reach to a critical level), respectively [49]. The mentioned 3 stages of fatigue degradation were illustrated in Figure 4.1 considering one of the cyclic creep curves obtained experimentally. Moreover, cyclic creep curves for the fatigue experiments carried out in this study were presented in Figure 4.2 (curves for '4PBT / W60 - 75% - failure cycles: 21100, 47792, 50615, 65113 and 4PBT / W45 - 75% - failure cycle: 51321' were not given due to a problem occurred in the data acquisition process). It should be noted here that while preparing the curves, loading head displacement values corresponding to minimum stress of first cycle were considered as base point (taken as 'O'), to normalize the displacement values (in order to eliminate the effect of assigned zero point in the beginning of data acquisition process). Based on Figure 4.1, for almost all the examined cases, while 3rd stage of fatigue degradation clearly seen for cyclic 4PBTs, the stage was not seen for cyclic DPTs. In another words, the fatigue failure occurs in 2 and 3 visible stages for cyclic DPT and 4PBT, respectively. The appearance of 3rd stage might be associated with the crack compensation capability of test specimens under the applied loading, since the visibility of this phase means that the test specimen can carry certain number of cyclic loads of same magnitudes even after some of the cracks reach their critical level. Observed difference might be attributed to stress states of failure surfaces for the tests. Since the stress gradient formed for 4PBT in the cracking surface allowing the tensile stresses to be redistributed, but almost all parts of the cracking surfaces are under similar stress level for DPT [215]. On the other hand, for W60 mixture and 0.75 maximum stress level (the case that the largest number of cycles were obtained) case limited number of data was observed in the 3rd stage under cyclic DPT, which shows the dependence of obtained behaviors to the type of concrete mixture tested and applied stress level, in addition to testing configuration.

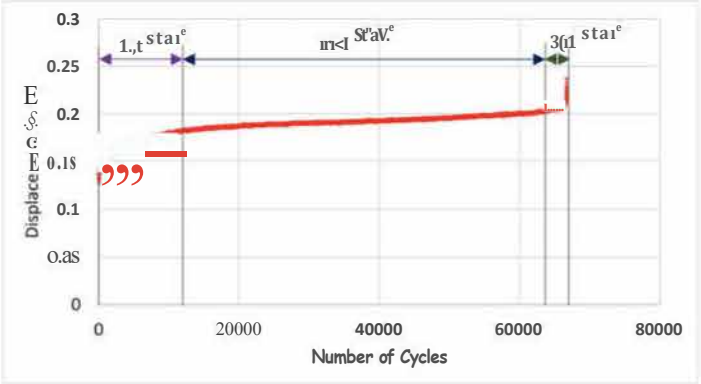


Figure 4.1. Stages of fatigue failure (test case: 4PBT - W45 - 0.85 / number of cycles to failure=66751).

As stated above, results for some of the examined cases deviates from normality in various amounts. Therefore, as an alternative distribution function 2-parameter Weibull distribution (which is mostly used to evaluate fatigue test results) is also considered in this study. The two parameters used to define Weibull distribution are scale parameter (a) and shape parameter (/3), and they are determined by using graphical method [216,217]. a and /3, as well as correlation coefficient ($R^2$) values for Weibull distribution analyses were given in Table 4.9. It should be emphasized here that the Weibull (scale (a) and shape (/3)) parameters were determined by doing regression analyses in the graphical method (used in this study), and '$R^2$' values given in the table shows the correlation coefficients for the regression analyses.

Table 4.9. Weibull distribution check and Weibull parameters.

| Test Configuration | Concrete Type | Stress Ratio (%) | R2 | Shape Factor (b) | Scale Factor (a) | Kolmogorov - Smirnov Test | | | COV (%) |
|---|---|---|---|---|---|---|---|---|---|
| | | | | | | D1 | De | Null - Hypothesis | |
| 4PBT | W60 | 85 | 0.89 | 1.10 | 7120 | 0.178 | 0.409 | Accept | 90.9 |
| 4PBT | W60 | 75 | 0.89 | 1.69 | 47300 | 0.199 | 0.409 | Accept | 60.9 |
| 4PBT | W45 | 85 | 0.91 | 1.16 | 8654 | 0.202 | 0.409 | Accept | 86.1 |
| 4PBT | W45 | 75 | 0.88 | 0.78 | 45004 | 0.257 | 0.430 | Accept | 129.6 |
| DPT | W60 | 85 | 0.91 | 2.01 | 767 | 0.206 | 0.409 | Accept | 52.1 |
| DPT | W60 | 75 | 0.82 | 2.59 | 15689 | 0.258 | 0.409 | Accept | 41.4 |
| DPT | W45 | 85 | 0.91 | 1.80 | 1063 | 0.178 | 0.430 | Accept | 57.5 |
| DPT | W45 | 75 | 0.93 | 1.61 | 7604 | 0.181 | 0.409 | Accept | 63.6 |

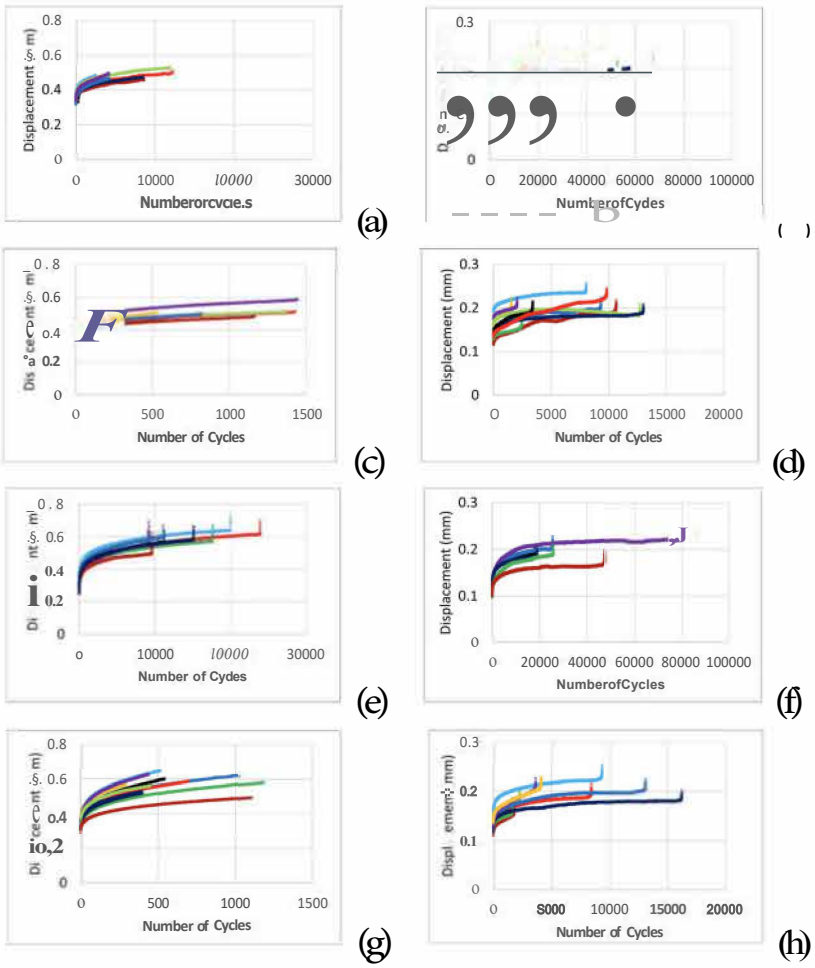


Figure 4.2. Cyclic creep curves; (a)DPT - W45 - 0.75, (b) 4PBT - W45 - 0.75, (c) DPT - W45 - 0.85, (d) 4PBT - W45 - 0.85, (e) DPT - W60 - 0.75, (f) 4PBT - W60 - 0.75, (g) DPT - W60 - 0.85, (h) 4PBT - W60 - 0.85.

High correlation coefficient ($R^2$) value ('$R^2$' close to 1.0) is one of the indicators that shows whether Weibull distribution represents the distribution of results or not [63,66,217]. Since all the $R^2$ values given in Table 4.9 reasonably close to 1.0 (all the values are above 80%), it might be said that the Weibull distribution fits well to the test results. Additionally, Kolmogorov - Smirnov test [218] [219,219] which is mostly used to check the validity of Weibull distribution, is also carried out for the results. Since the calculated D values ($D_1$) are found (considerably) lower than the critical values (De), null-hypothesis of Kolmogorov - Smirnov test that says the assumed distribution is suitable for the test results was accepted for all cases (both '$D_1$' and 'De' values were determined according to Kennedy and Neville [218]. It should be noted here that the 'De' values (given in Table 4.9) were specified for 5% significance level.

After checking the validity of Weibull distribution, COV values were calculated for all the cases from [63, 66]

$$cov = \frac{(J'}{\mu} = \sqrt{\frac{r(j+1)}{r(!+1)} - 1,} \qquad (4.1)$$

where u, $\mu$, $I'$, and $/3$ represents standard deviation, mean, gamına function, and shape parameter (one of the Weibull parameters), respectively. As the formula illustrates the COV value only depends on the shape parameter (/3), and COV decreases with an increase in $/3$.

Calculated COV values were also given in Table 4.9. Based on the given values, considerably lower variations found for DPT (between 41.4 - 63.6 %) compared to 4PBT (between 60.9 - 129.6 %).

After determination of Weibull distribution parameters, Wöhler curves are prepared for different reliability levels (from 10% to 90%) and given for 4PBT and DPT in Figure 4.3 and Figure 4.4, respectively. Based on the figures, lines that shows the numbers corresponding to different reliability levels were found closer for DPT compared to 4PBT, which is an indication of the small change in the number of cycles for increasing or decreasing level of reliability. In another words, to increase the reliability level (decrease failure probability) the number of allowable load repetition should be reduced more for 4PBT. The result might be attributed to the lower COV values found for DPT compared to 4PBT. To illustrate the point, ratio of number of cycles for 50% and 90% reliability levels are calculated for all the test cases and a scatter graph was drawn to determine the relationship between the calculated values and COV (%). The graph was given in Figure 4.5, together with the regression curve and its equation and correlation coefficient ($R^2$). It can be seen from the figure that the calculated value is increasing with an increase in COV% with a strong correlation (very high correlation coefficient ($R^2$)).

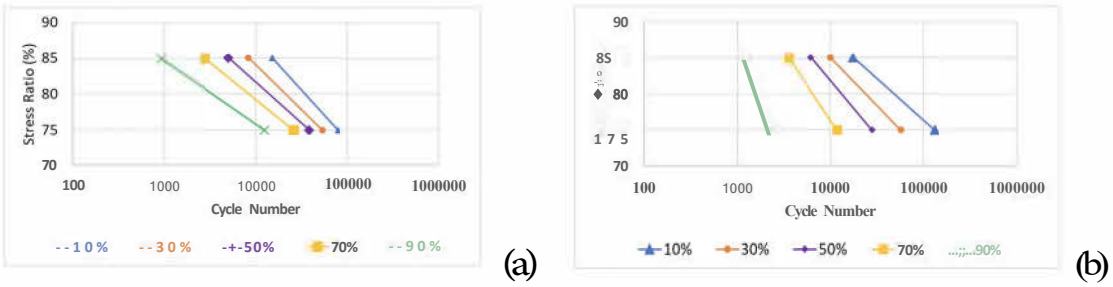


Figure 4.3. Wöhler curves for 4PBT (a) W60 (b) W45.

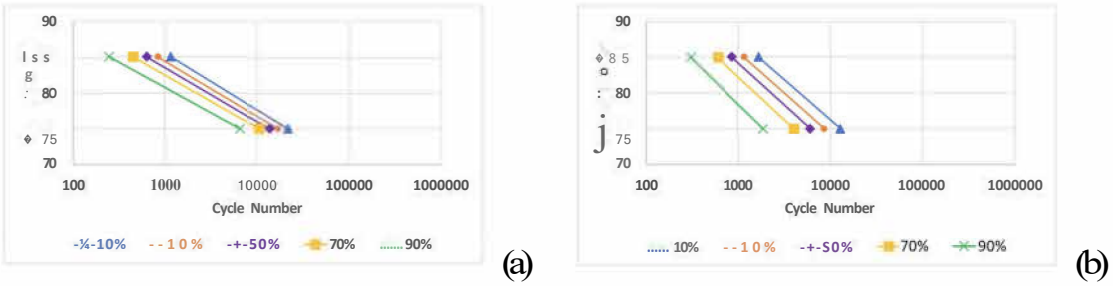


Figure 4.4. Wöhler curves for DPT (a) W60 (b) W45.

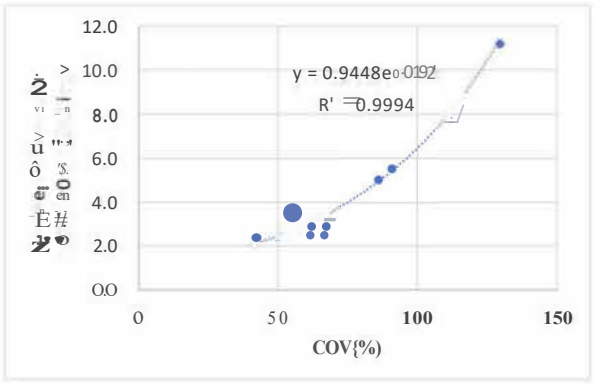


Figure 4.5. Correlation between COV (%) and number of failure cycles for 50% / 90% reliability.

Wöhler curves that correspond to '50% survival probability' were given in Figure 4.6 for all the examined cases. Based on the figure, as in normal distribution mean comparison case, considerably lower cycle numbers were obtained for DPT compared to 4PBT, which was attributed to the difference between the cracking mechanisms (or stress distributions) of these two tests. Determination of the relationship between the number of failure cycles between these two tests might be required for some design applications. For example, since pavement structures exposed to flexural loadings due to the vehicle loads applied, flexural fatigue tests are done to determine the fatigue

(Wöhler / S - N) curves used in design. For the results of the current study, relationship between the failure number of cycles of DPT and 4PBT was given in Figure 4.7, for 50% reliability (survival probability). A linear regression analysis was also done to provide an estimating equation, and the equation was given in the figure together with its correlation coefficient ($R^2$). it is worth noting here that the equation was provided by considering only 4 cases (two concrete types (W45 and W60) and two maximum stress levels (75% and 85%)) that were examined in this study, which might alter for other stress ratios and material combinations. However, if the use of DPT for fatigue performance evaluation increases, more reliable relationships could be constructed. Thus, further studies are required to better evaluate the suitability of DPT for fatigue performance evaluation.

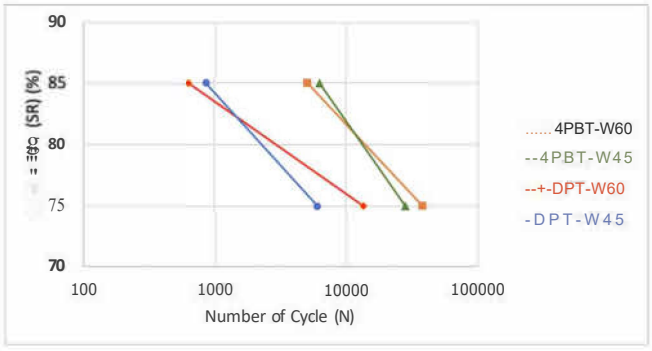


Figure 4.6. Failure cycles for 50% survival probability (assuming Weibull distribution).

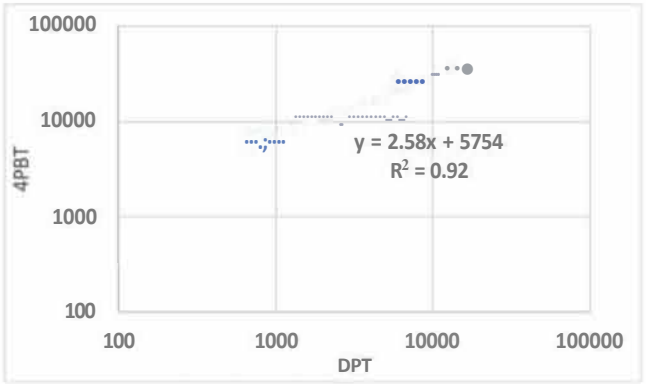


Figure 4.7. Relationship between the failure numbers for cyclic DPT and 4PBT (for 50% reliability / survival probability).

Moreover, variations found in the scope of the current study were compared with the variations of reported in literature for flexural fatigue tests. Details for the testing methodologies followed in the considered studies were presented in Table 4.10, and the calculated variations were in Figure 4.8, together with the variations obtained in this study. It should be noted here that all the COV values given in the figure were calculated assuming the Weibull distribution. Before the COV calculations the results were checked against Weibull distribution in terms of '$R^2$' and Kolmogorov - Smirnov test. For the distribution check, all the '$R^2$' values were found above '0.8' and 'D' values were found below the critical values.

According to Figure 4.8, the calculated variations for DPT found closer to lower bound of variations reported in the literature for cyclic bending tests. Besides, for all the studies considered, higher variations were found for considerable number of cases studied than the largest COV obtained for DPT (63.6%). It was also seen that the range of variations obtained for DPT were closer to each other than not only 4PBT but also flexural fatigue tests in the considered literature studies. Therefore, it can be concluded that the desirable variations were obtained for cyclic DPT, compared to cyclic flexural fatigue tests conducted in this study and literature. Furthermore, though the variations found considerably higher for 4PBT compared to DPT, they were found within the range reported in the literature (for cyclic bending tests).

Table 4.10. Test details for considered literature studies and the current study.

| Study | Specimen Type | Specimen Size (cm) | Loading Frequency (Hz) | Test Configuration | Max Aggregate Size (mm) |
|---|---|---|---|---|---|
| Current | Cylinder | 15x15 | 10 | DPT | 24.0 |
| Current | Beam | 10x10x35 | 10 | 4PBT | 24.0 |
| Harwalkar & Avanti [220] | Beam | 7.5x10x50 | 4 | 4PBT | 20.0 |
| Zhu et al. [66] | Beam | 10x10x40 | 5 | 4PBT | 10.0 |
| Arora & Singh [62] | Beam | 10x10x50 | 10 | 4PBT | 12.5 |
| Harwalkar & Avanti [64] | Beam | 7.5x10x50 | 4 | 4PBT | 20.0 |
| Mohammadi & Kaushik [63] | Beam | 10x10x50 | 20 | 3PBT | 20.0 |
| Singh & Kaushik [65] | Beam | 10x10x50 | 12 | 4PBT | 20.0 |

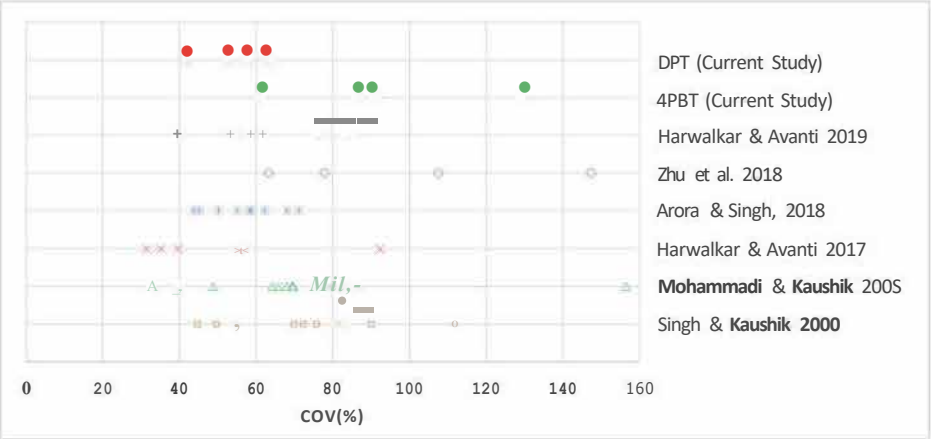


Figure 4.8. Comparison of calculated variations with literature.

## 4.2. Effects of Stress Reversal on Flexural Fatigue Life

### 4.2.1. Mixtures

A concrete mixture with a cement dosage of 350 kg/m$^3$, and water to cement ratio of 0.60 was used for the evaluation of the effects of stress reversal on the flexural fatigue performance of concrete. EN 206 [208] - 82 slump class (5-8 cm) was selected as aimed consistency for the concrete and a modified polycarboxylate based SP was used to achieve the aimed consistency. Mixture proportions of ingredients determined according to given explanations were presented in Table 4.11.

Table 4.11. Weight of ingredients for 1 m$^3$ concrete mixture.

| Ingredients | Weight (kg/m3) |
|---|---|
| Cement | 350.0 |
| Crushed Stone - No 1 | 577.9 |
| Crushed Stone - No 2 | 480.6 |
| Crushed Sand | 676.2 |
| Natural Sand | 192.6 |
| Water | 157.5 |
| SP | 2.8 |

### 4.2.2. Quasi-Static Tests

For modulus of elasticity, compressive strength and flexural strength tests average of test results were given together with minimum, maximum, and standard deviation values in Table 4.12. As mentioned previously, all the tests were carried out for 6 specimens, and the results were given for them.

Table 4.12. Quasi-static test results.

| Test | Average | Standard Deviation | Minimum | Maximum |
|---|---|---|---|---|
| Modulus of Elasticity (GPa) | 27.1 | 1.1 | 25.1 | 28.1 |
| Compressive Strength (MPa) | 49.6 | 3.1 | 46.5 | 53.6 |
| Flexural Strength (MPa) | 6.7 | 0.4 | 6.1 | 7.2 |

### 4.2.3. Cyclic Tests in One-Way

Number of cycles for failure under one-way cyclic loading, as well as average number of cycles, and coefficient of variation (COV) values were given in Table 4.13, where '*' shows the value considered as outlier according to Chauvenet's criterion [213] and not included in the analyses. In addition, it should be noted here that the average and COV % values were calculated by assuming normal distribution. Üne of the thing that can be seen from the table is that the number of cycles that can be resisted is much higher for 75% ( 5 times) maximum stress level, compared to 85%. It can be also seen from the table that 10 specimens were tested under cyclic loading, and the results are distributed in a large range, and high COV% values were found as a result. As in the current study, fatigue test results usually involve a large scatter [49, 59], and various statistical approaches are used to deal with this variation. Among them, use of Weibull probability distribution function is the most common one.

Table 4.13. Number of failure cycles far one-way loading.

| Max Stress Ratio (%) | | 85 | 75 |
|---|---|---|---|
| Specimen Number | 1 | 1551 | 76 * |
| | 2 | 2042 | 1569 |
| | 3 | 2452 | 9706 |
| | 4 | 3395 | 19803 |
| | 5 | 8010 | 26498 |
| | 6 | 9295 | 38987 |
| | 7 | 9792 | 46955 |
| | 8 | 10618 | 51321 |
| | 9 | 12650 | 52648 |
| | 10 | 12967 | 66751 |
| Average | | 7277 | 34915 |
| COV (%) | | 61.8 | 62.5 |

For the results given in Table 4.13, 2-parameter (scale ($\alpha$) and shape (/3) parameters) Weibull distribution analyses were done far both maximum stress levels (85% and 75%). To determine the parameters of Weibull distribution, graphical method [216,217] was used. According to the method, 2 parameters of Weibull distribution function are faund by doing regression analysis, and correlation coefficient ($R^2$) of conducted regression analysis is one of the measures that shows the suitability of 2-parameter Weibull distribution to the analyzed <lata set. Basically, high $R^2$ values (close to 1.00) shows that the used distribution fits well to the analyzed <lata [63, 66,217]. Moreover, in this study, suitability of Weibull distribution to the <lata set was alsa checked with a commonly applied method called Kolmogorov-Smirnov test [218].

For both maximum stress levels, scale ($\alpha$) and shape (/3) parameters faund by using graphical method were presented in Table 4.14, together with the correlation coefficients and Kolmogorov - Smirnov test results. As it can be seen from the table, since calculated D values (D1) were faund lower than the critical D values ($D_e$) (taken from Kennedy and Neville [218], considering 5% significance level and number of spec-

imens), null-hypothesis of Kolmogorov-Smirnov test that says the analyzed data set fits well to Weibull distribution was accepted for both analyzed cases.

Table 4.14. Weibull distribution analysis results for one-way cyclic loading.

| Maximum Stress Ratio (%) | Number of Specimens | R2 | Shape Factor (β) | Scale Factor (a) | Kolmogorov - Smirnov Test | | |
|---|---|---|---|---|---|---|---|
| | | | | | $D_1$ | $D_e$ | Null - Hypothesis |
| 85 | 10 | 0.91 | 1.16 | 8654 | 0.202 | 0.409 | Accept |
| 75 | 9 | 0.88 | 0.78 | 45004 | 0.257 | 0.430 | Accept |

By using the scale (a) and shape (β) parameters determined by graphical method, and given in Table 4.14, Wöhler (Stress Ratio (S) - Number of Cycles (N)) curves for 10 - 30 - 50 - 70 - 90 % reliability (1 - 'failure probability') levels were calculated for both (75% and 85%) maximum stress levels and given in Figure 4.9.

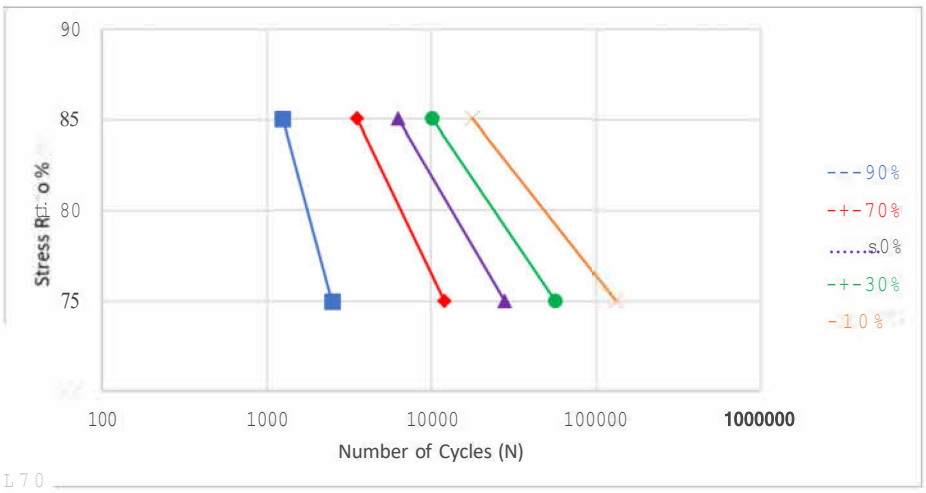


Figure 4.9. One-way cyclic loading Wöhler curves for different reliability (1 - 'failure probability') levels.

From the Wöhler curves given in Figure 4.9 (prepared by assuming Weibull distribution), cycle numbers for 30% failure probability (70% reliability) level were found as '3571' and '11996' for 85% and 75% maximum stress ratios, respectively. This values were used for the first part of the two-way cyclic loading. Details were provided in the following section.

### 4.2.4. Cyclic Tests in Two-Way

For this part, eyde numbers eorresponding to 30% failure probability ('3571' and '11996' for 85% and 75% maximum stress levels, respeetively) were used to apply eydie loading in the first direetion, means that approximately 30% of the speeimens will fail during these loadings if the fitted distribution works. For the seeond part of the tests, survived speeimens were rotated 180° around their eenterlines, and the speeimens were loaded repetitively, under the same load magnitudes used in first part. To elaborate, a speeimen was first exposed to eydie loading with 85% (or 75%) maximum and 10% minimum stress levels in one direetion up to a eyde eorresponding to 30% failure probability, then if the speeimen still alive it was rotated 180° around its eenterline and loaded eydieally until the failure with a magnitude same with applied in first part (85% or 75% maximum and 10% minimum stress level). Number of eydes eaused to failure were reeorded at the end of the tests.

For both 85% and 75% maximum stress levels 22 beam speeimens were tested in this part. For the speeimens survived in the first part of the loading, number of eydes for failure were given in Table 4.15, together with the average and COV% values. Speeimens failed in the first part of the loading were also presented in Table 4.15, together with the ratio of them to the total number of speeimens tested for relevant ease (22 speeimens were tested for both 85% and 75% maximum stress level). In Table 4.15 '-' shows the speeimens failed in the first part (loading up to the eyde number eorresponding to 30% probability of failure) of the loading. In the table the average and COV % values were ealeulated by assuming normal distribution.

As mentioned before, '3571' and '11996' eydes were applied in the first part of the loading whieh eorresponds to eyde numbers for 30% probability of failure under 85% and 75% maximum stress levels, respeetively. As the table shows, the values (27.3% and 31.8%) were found fairly dose to 30% whieh might be attributed to suitability of fitted distributions to the dealt data sets.

Table 4.15. Number of failure cycles far two-way loading.

| Specimen Number | Maximum Stress Level | |
|---|---|---|
| | 85% | 75% |
| 1 | 936 | 3010 |
| 2 | 992 | 3982 |
| 3 | 1185 | 5620 |
| 4 | 1474 | 5708 |
| 5 | 1477 | 6418 |
| 6 | 1923 | 7976 |
| 7 | 2479 | 8200 |
| 8 | 3556 | 14116 |
| 9 | 3980 | 18979 |
| 10 | 4696 | 20060 |
| 11 | 5191 | 20797 |
| 12 | 5652 | 39800 |
| 13 | 9519 | 57984 |
| 14 | 12221 | 66049 |
| 15 | 13074 | 70310 |
| 16 | 13444 | - |
| 17 | - | - |
| 18 | - | - |
| 19 | - | - |
| 20 | - | - |
| 21 | - | - |
| 22 | - | - |
| Average | 5112 | 23267 |
| COV (%) | 87.5 | 101.4 |
| Ratio of Failed Specimens to Total Specimens Tested (%) | 27.3 | 31.8 |

When the average cycle numbers obtained far one way (Table 4.13) and two-way (Table 4.15) cyclic loading were compared average cycle numbers were faund to decrease from '7277' and '34915' to '5112' and '23267' which corresponds to '29.8%' and '33.4%' far 85% and 75% maximum stress levels, respectively. Moreover, When the COV% values faund far one-way (Table 4.13) and two-way (Table 4.15) were compared, considerably higher variations were faund far two-way loading (COV% increased from 61.8% and 62.5% to 87.5% and 101.4% far 85% and 75% maximum stress levels, respectively). Effect of cyclic loadings applied in the opposite direction might be the source of increased variation; however, further studies are required to validate this hypothesis, since it was given by considering limited number of cases.

For the test results obtained under two-way cyclic loading Weibull distribution analyses were also conducted and the results were presented in Table 6. As in one-way case, graphical method was used to determine the shape (a) and scale (/3) parameters of Weibull distribution function, and Kolmogorov-Smirnov test was also done for the <lata sets to check the validity of used distribution. According to Kolmogorov-Smirnov test results, null hypothesis of the test that says the Weibull distribution fits the <lata was accepted for both 85% and 75% maximum stress levels, since calculated D values ($D_1$) were found lower than the critical values (De)- Additionally, $R^2$ values obtained for regression analyses (done for graphical method to obtain Weibull parameters) were found fairly close to '1.00' which is an another indication of suitability of Weibull distribution, as explained before.

Table 4.16. Weibull distribution analysis results for two-way cyclic loading.

| Maximum Stress Ratio (%) | Number of Specimens | R2 | Shape Factor | Scale Factor | Kolmogorov - Smirnov Test | | |
|---|---|---|---|---|---|---|---|
| | | | | | $D_1$ | De | Null - Hypothesis |
| 85 | 16 | 0.92 | 1.09 | 5568 | 0.112 | 0.327 | Accept |
| 75 | 15 | 0.91 | 0.96 | 24169 | 0.169 | 0.337 | Accept |

By using the shape and scale parameters of Weibull distribution obtained for two-way cyclic loading, Wöhler (S-N) curves for different reliability levels were produced and presented in Figure 4.10. To compare the curves with the ones obtained for one-way loading, Wöhler curves for one-way loading were also presented in the figure for the same reliability levels.

Figure 4.10 shows that for all the reliability levels lower cycle numbers were obtained for two-way loading compared to one-way loading, which shows the reduction in the number of cycles that could be resisted due to the cyclic loading applied in the opposite direction (first part of the two-way cyclic tests).

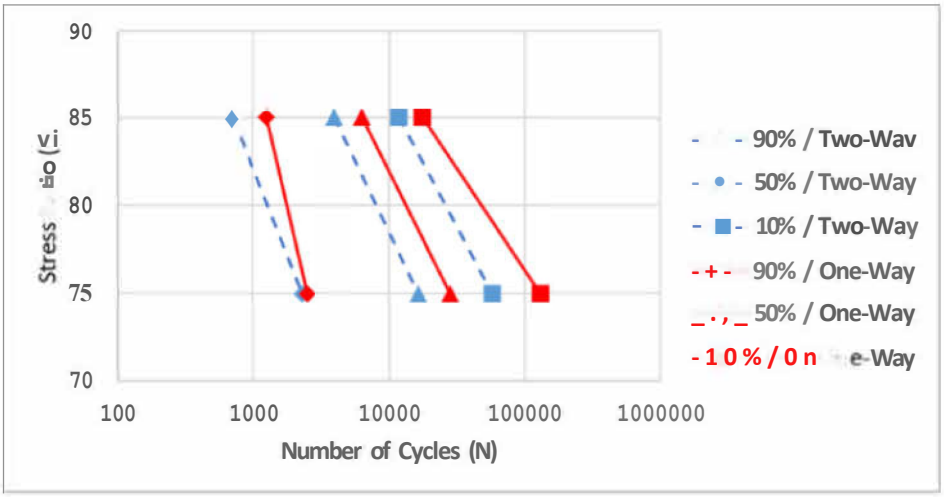


Figure 4.10. Wöhler curves for one-way and two-way cyclic loading corresponding to different reliability (1 - 'failure probability') levels.

### 4.2.5. Evaluation of Test Results in terms of Pavement Structural Design

For the design of concrete pavements various reliability levels are used by different design guides, and importance of designed road is one of the main criteria considered in the selection of reliability level. To illustrate, AASHTO ( [73] design guide recommends 85% - 99% reliability level for interstate roads, but it is decreased to 50% - 80% for local roads (both values given for 'urban road' case). in this part, based on the Wöhler curves obtained in this study, approaches given in different concrete pavement design were evaluated for 50% reliability level.

As explained above, for two-way fatigue tests, number of cycles corresponding to 30% probability of failure ('3571' and '11996' cycles for 85% and 75% maximum stress ratios, respectively) were applied to the specimens in the first way, then the specimens were loaded in the opposite direction until the failure. in this part, to consider similar scenario, it was assumed that eyde numbers corresponding to 30% failure probability were applied to the pavement slab in 1 direction. Then, number of cycles that are allowed in different design codes [73, 82, 84] in the opposite direction were calculated for various reliability levels (50%, 30%, and 10%) and given in Table 4.17 (for both 85% and 75% stress ratios), together with the one obtained experimentally (based on

the two-way cyclic loading test results) in the current study, where bold values indicate the unsafe allowable numbers (the number of allowable cycles calculated according to relevant design code higher than the allowable number of cycles calculated based on the two-way cyclic test results) given by the design codes. it is worth noting here that to determine the allowable number of load repetitions for all cases, Wöhler curves obtained in this study were used, instead of design curves given in the relevant design guide. On the other hand, number of allowable cycles on the opposite directions were calculated by using approach suggested in the design guide and given together with the allowable number of load repetitions calculated experimentally (from two-way cyclic loading). Additionally, number of cycles allowed and applied in one direction corresponding to cycle numbers calculated based on one-way cyclic loading results, and cycle numbers corresponding to 30% probability of failure for the given stress ratio (values were used for the first part of two-way cyclic loading). Number of allowed cycles in the opposite direction for current study, IRC 58 [82] AASHTO MEPDG [83], and IRC 58 [82] were calculated based on the second part of two-way cyclic loading, approaches given in IRC 58 [82] AASHTO MEPDG [83], and IRC 58 [84], respectively.

According to Table 4.17, both safe and unsafe number of allowed cycles in the opposite direction (compared to ones obtained experimentally) were found based on the approaches given in considered concrete pavement design guides. Since cyclic loading capacity in one direction were found to decrease due to the cyclic loads applied in the opposite direction in this study, the approaches given in old IRC guide [82] and AASHTO guide [83] (which neglect the reducing effect of the cyclic loading applied in the other direction) were found on the unsafe side for all the reliability cases considered. On the other hand, safe and unsafe cycle numbers were calculated for the latest version of IRC guide [84] for different reliability and stress ratio cases. in addition, since the same number of load repetitions were assumed to be applied in the first direction (to produce similar scenario applied experimentally) fatigue damages caused by the cyclic loads applied in the first direction (number of loads applied in the first direction / number of cycles allowed in one direction) was found higher for higher reliability levels, where the number of allowable load repetitions are lower.

Table 4.17. Number of applied and allowable cycles for pavement design.

| Reliability Level (%) | | 50 | | 30 | | 10 | |
|---|---|---|---|---|---|---|---|
| Stress Ratio (%) | | 85 | 75 | 85 | 75 | 85 | 75 |
| Number of Cycles Allowed in üne Direction (NI) (calculated for one-way loading assuming Weibull distribution) | | 6317 | 28126 | 10149 | 57101 | 17711 | 131162 |
| Number of Cycles Applied in üne Direction (N2) (applied in first direction for two-way loading) | | 3571 | 11996 | 3571 | 11996 | 3571 | 11996 |
| Fatigue Damage (%) Caused by the Cycles Applied in the First Direction (Fatigue Damage (%) = (N2) / (NI) x 100) | | 56.5 | 42.7 | 35.2 | 21.0 | 20.2 | 9.1 |
| Number of Allowed Cycles in the Üpposite Direction | Current Study (calculated for two-way loading assuming Weibull Distribution) | 3978 | 16499 | 6602 | 29425 | 11968 | 57619 |
| | IRC 58 [82] & AASHTü MEPDG [83] (Cycle Number = (NI)) | **6317** | **28126** | **10149** | **57101** | **17711** | **131162** |
| | IRC 58 [84] (Cycle Number = (NI) - (N2)) | 2746 | 16130 | 6578 | **45105** | **14140** | **119166** |

Moreover, when the number of allowable load repetitions on the opposite direction were compared for IRC 58 [84] and current study, IRC 58 was found on the safe side for higher reliability levels (lower allowable load cycles), but on the unsafe side for lower reliability levels (higher allowable load cycles). In another words, for lower reliability levels (higher allowable cycle numbers) approach suggested in IRC 58 [84] was found not capable to demonstrate the fatigue life degradation due to cyclic loadings applied in opposite direction.

The outcome given above might be explained with the problem related to the linear damage assumption proposed by IRC 58 [84]. As IRC 58 [84] assumes that the cyclic loading applied in one direction affect the cyclic loading capacity in the opposite direction in simple linear proportion, which might not be the case in real. Examination of cyclic creep curve (the curve that shows the relationship between the cycle numbers and peak displacement in the relevant cycles) is a reliable way to visualize the damage accumulation under cyclic loading. Therefore, cyclic creep curve obtained for one of the specimens (failed in 38987 cycles under one-way loading and 0.75 stress ratio) was

given in Figure 4.11, and phases of fatigue damage propagation were represented on the figure. The 3 phases illustrated in the figure are termed as crack initiation, micro-cracking, and unstable crack propagation, respectively [49]. Since the fatigue failure occur after reaching a level of displacement, slope of the cyclic creep curve might be associated with the damage propagation rate. Based on these issues Figure 4.11 shows that the damage propagation is fast in the beginning of the loading cycles and its rate is decreasing gradually. After a point (starting of micro-cracking phase) the rate of deterioration becomes stable and goes up to a critical point (starting of unstable crack propagation). in the last part, crack propagation rate dramatically increases, and the specimen fails after the application of a few loading cycles. Therefore, the cyclic load applied in the crack initiation phase can be considered as more damaging compared to the cycles applied in micro-cracking phase.

Based on the explanations given above, it might be hypothesized that the IRC 58 [84] approach is not able to predict the real response, as it does not take into account the non-linear deterioration rate of concrete under the application of cyclic loading. Thus, for the fatigue design of concrete pavements new approaches are needed to better represent the effect of cyclic loading applied in one direction on the fatigue performance of concrete in the other direction.

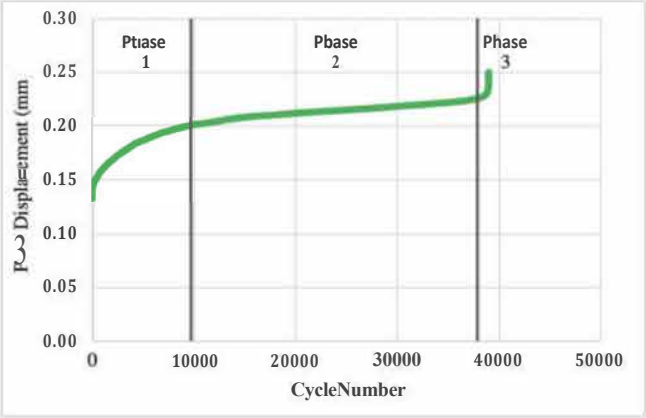


Figure 4.11. Cyclic creep curve (for the specimen that was failed in 38987 cycles under one-way loading and 0.75 stress ratio) ('peak displacement' given in 'y axes' represents the maximum displacement values obtained for each cycle).

In the end, it is worth noting here that the given discussions depend on the results of this study, which are obtained by using one type of concrete and two maximum stress levels. Since the results might change for different concrete types and stress levels, further studies are required to ensure about their validity for another design cases (different concrete mixtures and stress levels).

## 4.3. Effectiveness of Fibers in Concrete Pavement Mixtures

### 4.3.1. Mixtures

To investigate the effectiveness of fibers in different concrete pavement mixtures, 3 different concrete matrices were designed in this study, a normal strength conventional concrete (NSC), a high strength conventional concrete (HSC), and a roller compacted concrete (RCC). To achieve the aims of the study, explained in the research significance part, 3 plain and 14 fiber reinforced concrete (FRC) mixtures were designed, as given in Table 4.18. In the given table, conventional concrete series were named as "strength level (HSC / NSC) - the type of fiber - amount of fiber (%vol.)" and roller compacted concrete series were named as "RCC - the type of fiber - amount of fiber (%vol.)". Besides, the numbers show the amount of fibers used in the mixture, in terms of volume percentage (% vol.). For the type of reinforcement, plain (concrete without reinforcement) mixtures were named as "P", and polypropylene and steel fibers were named as "PPF" and "SF", respectively. As it can be seen from the table, to examine the efficiency of fibers in different concrete mixtures, for all 3 concrete types, mixtures with 0.50 % vol. fibers were designed. On the other hand, different fiber dosages were considered for normal and high strength conventional concrete mixtures, to see the effect of different fiber dosages on the performance of concrete pavement mixtures.

For all the mixtures amount of ingredients, and mixture proportions for 1 $m^3$ concrete mixtures were given in Table 4.19 and Table 4.20, respectively. It should be noted here that 'Water / Cement (%)' and 'SP' given as 'Varying' in Table 4.19 adjusted to achieve maximum dry density and aimed consistency.

Table 4.18. Concrete mixtures for fibers in concrete pavement mixtures.

| Normal Strength Concrete (NSC) | High Strength Concrete (HSC) | Roller Compacted Concrete (RCC) |
|---|---|---|
| NSC-P | HSC-P | RCC-P |
| NSC - PPF - 0.25 | HSC - PPF - 0.25 | RCC - PPF - 0.50 |
| NSC - PPF - 0.50 | HSC - PPF - 0.50 | RCC - SF - 0.50 |
| NSC - PPF - 0.75 | HSC - PPF - 0.75 | |
| NSC - PPF - 1.00 | HSC - PPF - 1.00 | |
| NSC - SF - 0.25 | HSC - SF - 0.25 | |
| NSC - SF - 0.50 | HSC - SF - 0.50 | |

Table 4.19. Amount of ingredients for concrete series.

| Concrete Series | | NSC | HSC | RCC |
|---|---|---|---|---|
| Cement Content (kg/m$^3$) | | 350 | 350 | 300 |
| Water/Cement (%) | | 60 | 45 | Varying |
| Aggregates (%wt.) | CSt: No I | 30 | 30 | 30 |
| | CSt: No II | 25 | 25 | 25 |
| | eS | 35 | 35 | 35 |
| | NS | 10 | 10 | 10 |
| SP | | Varying | Varying | Not Used |
| Fiber (%vol.) | | 0/ 0.25/ 0.50/ 0.75/ 1.00 | 0/ 0.25/ 0.50/ 0.75/ 1.00 | 0/ 0.25/ 0.50 |

### 4.3.2. Physical Tests for Fibers in Different Concrete Matrix

Results for absorption, density, and porosity tests were presented in Table 4.21 where the values presented are the average of 6 specimens and values given in parenthesis show the standard deviation of test results. Based on the given results, absorption, density, and porosity values for RCC and HSC mixtures were found very similar, but considerably different (in a negative way) values were obtained for NSC mixtures. These results could be attributed to similar water to cement ratios used in RCC and HSC, since the values investigated in the table are significantly dependent to water to cement ratio used [202,221].

Table 4.20. Mixture proportions for concrete series (kg/m$^3$).

| Concrete Mixtures | Cement | CSt: No I | CSt: No II | es | NS | Water | SP | PPF | SF |
|---|---|---|---|---|---|---|---|---|---|
| NSC- P | 350.0 | 542.3 | 451.0 | 634.6 | 180.8 | 210.0 | 1.1 | 0.00 | 0.00 |
| NSC - PPF - 0.25 | 350.0 | 547.3 | 455.2 | 640.5 | 182.4 | 210.0 | 1.2 | 2.28 | 0.00 |
| NSC - PPF - 0.50 | 350.0 | 537.2 | 446.8 | 628.6 | 179.1 | 210.0 | 1.4 | 4.55 | 0.00 |
| NSC - PPF - 0.75 | 350.0 | 545.9 | 454.0 | 638.8 | 182.0 | 210.0 | 1.6 | 6.83 | 0.00 |
| NSC - PPF - 1.00 | 350.0 | 543.9 | 452.3 | 636.4 | 181.3 | 210.0 | 1.8 | 9.10 | 0.00 |
| NSC - SF - 0.25 | 350.0 | 547.3 | 455.2 | 640.4 | 182.4 | 210.0 | 1.2 | 0.00 | 19.50 |
| NSC - SF - 0.50 | 350.0 | 539.9 | 449.0 | 631.8 | 180.0 | 210.0 | 1.8 | 0.00 | 39.00 |
| HSC-P | 350.0 | 577.9 | 480.6 | 676.2 | 192.6 | 157.5 | 2.8 | 0.00 | 0.00 |
| HSC- PPF - 0.25 | 350.0 | 588.4 | 489.4 | 688.5 | 196.1 | 157.5 | 2.8 | 2.28 | 0.00 |
| HSC- PPF - 0.50 | 350.0 | 578.8 | 481.3 | 677.2 | 192.9 | 157.5 | 3.2 | 4.55 | 0.00 |
| HSC- PPF - 0.75 | 350.0 | 578.5 | 481.1 | 676.9 | 192.8 | 157.5 | 3.5 | 6.83 | 0.00 |
| HSC- PPF - 1.00 | 350.0 | 581.9 | 483.9 | 680.9 | 194.0 | 157.5 | 3.9 | 9.10 | 0.00 |
| HSC- SF - 0.25 | 350.0 | 586.4 | 487.7 | 686.1 | 195.5 | 157.5 | 3.2 | 0.00 | 19.50 |
| HSC- SF - 0.50 | 350.0 | 578.8 | 481.3 | 677.2 | 192.9 | 157.5 | 3.5 | 0.00 | 39.00 |
| RCC- P | 300.0 | 613.6 | 510.3 | 718.0 | 204.5 | 138.2 | 0.0 | 0.00 | 0.00 |
| RCC - PPF - 0.50 | 300.0 | 609.3 | 506.7 | 712.9 | 203.1 | 137.9 | 0.0 | 4.55 | 0.00 |
| RCC - SF - 0.50 | 300.0 | 603.4 | 501.8 | 706.0 | 201.1 | 139.5 | 0.0 | 0.00 | 39.00 |

When FRC mixtures were compared with control mixtures, similar absorption and porosity values were found. On the other hand, though similar density values were found for PPF reinforced concrete mixtures and control mixtures, the values were found higher for SF reinforced concrete mixtures. The increase in the density values due to the addition of SF could be attributed to high densities of SF (7800 kg/m$^3$) compared to all other ingredients of concrete.

### 4.3.3. Mechanical Tests for Fibers in Different Concrete Matrix

Average compressive strength, MOE, and flexural strength (MOR) values for plain and fiber reinforced (0.5%vol.) conventional and roller compacted concrete mixtures given in Table 4.22.

Table 4.21. Absorption, density, and porosity test results for fibers in different mixtures.

| Concrete Mixture | Absorption after immersion (%) | Absorption after immersion and boiling (%) | Bulk density, dry ($g/cm^3$) | Bulk density after immersion ($g/cm^3$) | Bulk density after immersion and boiling ($g/cm^3$) | Apparent density ($g/cm^3$) | Porosity (%) |
|---|---|---|---|---|---|---|---|
| HSC-P | 4.7 (0.7) | 4.8 (0.7) | 2.35 (0.03) | 2.46 (0.02) | 2.46 (0.02) | 2.64 (0.01) | 11.1 (1.5) |
| HSC-PPF-0.50 | 4.9 (0.2) | 5.0 (0.2) | 2.33 (0.01) | 2.45 (0.01) | 2.45 (0.01) | 2.64 (0.01) | 11.7 (0.4) |
| HSC-SF-0.50 | 4.6 (0.4) | 4.7 (0.4) | 2.38 (0.02) | 2.49 (0.01) | 2.49 (0.01) | 2.68 (0.02) | 11.3 (0.8) |
| NSC-P | 7.5 (0.5) | 7.6 (0.5) | 2.22 (0.03) | 2.38 (0.02) | 2.38 (0.02) | 2.66 (0.01) | 16.7 (0.9) |
| NSC-PPF-0.50 | 7.3 (0.3) | 7.4 (0.2) | 2.22 (0.01) | 2.38 (0.01) | 2.38 (0.01) | 2.65 (0.01) | 16.3 (0.5) |
| NSC-SF-0.50 | 7.1 (0.1) | 7.2 (0.1) | 2.26 (0.01) | 2.42 (0.01) | 2.42 (0.01) | 2.70 (0.01) | 16.3 (0.2) |
| RCC-P | 4.2 (0.3) | 4.3 (0.3) | 2.39 (0.01) | 2.49 (0.01) | 2.49 (0.01) | 2.66 (0.01) | 10.3 (0.6) |
| RCC-PPF-0.50 | 4.4 (0.4) | 4.6 (0.5) | 2.37 (0.03) | 2.48 (0.02) | 2.48 (0.02) | 2.66 (0.01) | 10.8 (1.1) |
| RCC-SF-0.50 | 4.4 (0.1) | 4.6 (0.4) | 2.39 (0.03) | 2.50 (0.03) | 2.51 (0.02) | 2.69 (0.01) | 11.1 (0.9) |

In Table 4.22, all the values were given as an average of 6 specimens and values given in parenthesis show the standard deviation of test results. As it can be seen from the table, for all the performance parameters, the highest values were found for HSC mixtures. On the other hand, while compressive strength and MOE values were found higher for RCC mixtures compared to NSC mixtures, MOR values were found similar for these two types of concrete.

To see whether fibers significantly affect strength and stiffness properties or not, t-tests (for 95% confidence level) were carried out to compare the plain and FRC mixtures of each concrete series, and the results were also given in Table 4.22 (boldface numbers represent the statistical difference with respect to the control mixtures of the same type of concrete (as a result of t-test for 95% confidence level)). Though statistical differences were observed for some comparison cases, performance parameters for plain and FRC mixtures were found similar for most of the cases. Besides, for the cases that statistical differences were seen, the amount differences between the average values were found very small (Table 4.22).

Table 4.22. Compressive strength, modulus of elasticity (MOE), and modulus of rupture (MOR) test results.

| Concrete Mixture | Compressive Strength | | MOE | MOR |
|---|---|---|---|---|
| | 7 days (MPa) | 28 days (MPa) | 28 days (GPa) | 28 days (MPa) |
| HSC- P | 41.2 (3.7) | 49.6 (3.1) | 27.1 (1.1) | 7.54 (0.3) |
| HSC-PPF-0.50 | 38.1 (1.8) | 47.1 (2.2) | **26.0 (0.4)** | 7.84 (0.5) |
| HSC-SF-0.50 | 42.2 (2.7) | 49.9 (3.8) | 26.8 (1.1) | 7.85 (0.8) |
| NSC-P | 27.8 (1.7) | 32.7 (0.5) | 23.7 (1.9) | 6.00 (0.3) |
| NSC-PPF-0.50 | 28.1 (1.5) | 34.3 (1.0) | 23.7 (0.8) | 5.84 (0.2) |
| NSC-SF-0.50 | 27.9 (0.8) | 33.3 (1.7) | 24.4 (1.8) | 6.13 (0.3) |
| RCC-P | 35.4 (1.3) | 40.0 (3.4) | 25.6 (2.0) | 6.15 (0.2) |
| RCC-PPF-0.50 | 32.9 (3.2) | 38.1 (3.4) | 25.3 (1.3) | 6.07 (0.7) |
| RCC-SF-0.50 | **33.9 (0.6)** | 40.3 (2.1) | 25.3 (1.7) | **6.62 (0.3)** |

It is known that the contribution of fibers can specifically be seen in the post-cracking region and the effect of fibers on the strength and stiffness properties of concrete is very low, especially for small amounts (less than 1 %vol.) [93,99,222]. Besides, the post-cracking performances of fiber-reinforced concrete mixtures depend on several factors, such as fiber type and amount, as well as concrete matrix properties. RFS values obtained in this study, from 4-point bending tests [185], were given in Figure 4.12 for various mid-span deflection values (0.5, 1.0, 1.5, and 2.0 mm), together with the MOR values. Since RFS ratio (RFS / MOR) is a good indicator of the effectiveness of fibers in the concrete matrix and it is used in concrete pavement structural design applications (explained in chapter 2.4.), these values were presented in Table 4.23, where the values presented are the average of 6 specimens and values given in parenthesis show the standard deviation of test results. Results given in Figure 4.12 and Table 4.23 indicate that the use of a similar amount (in volume) of SF gives considerably higher residual performance values compared to PPF, which could be attributed to their higher modulus of elasticities (200 GPa (SF), 8.5 GPa (PPF)), as well as their geometries with hooked end (which improves the pull-out resistance of fibers).

For the RFS ratio values given in Table 4.23, t-tests (with 95% confidence level) were performed within PPF and SF reinforced concrete mixtures to see whether efficiencies of fibers are similar in the concrete mixtures considered in this study or not, and results were given in the table, where statistical differences were obtained between the values with '*' and '**' (as a result of t-test for 95 % confidence level). Based on the statistical comparisons, efficiencies of polypropylene fibers were found very similar for all the concrete matrices considered in this study; however, efficiencies of SF were found higher for NSC compared to HSC (t-test results indicated that the obtained average RFS ratio values are different for NSC and HSC with 95% confidence). Even though, t-tests represent no significant statistical difference between efficiencies of fibers in RCC and HSC mixtures (mainly due to the large variation of results, as large variation makes hard to statistically distinguish the results), considerable differences between the RFS ratio values were observed for these two. Besides, despite the considerable difference in mixture proportions, consistency, and compaction effort, average RFS ratio values of both PPF and SF reinforced RCC mixtures were found very similar to NSC mixtures.

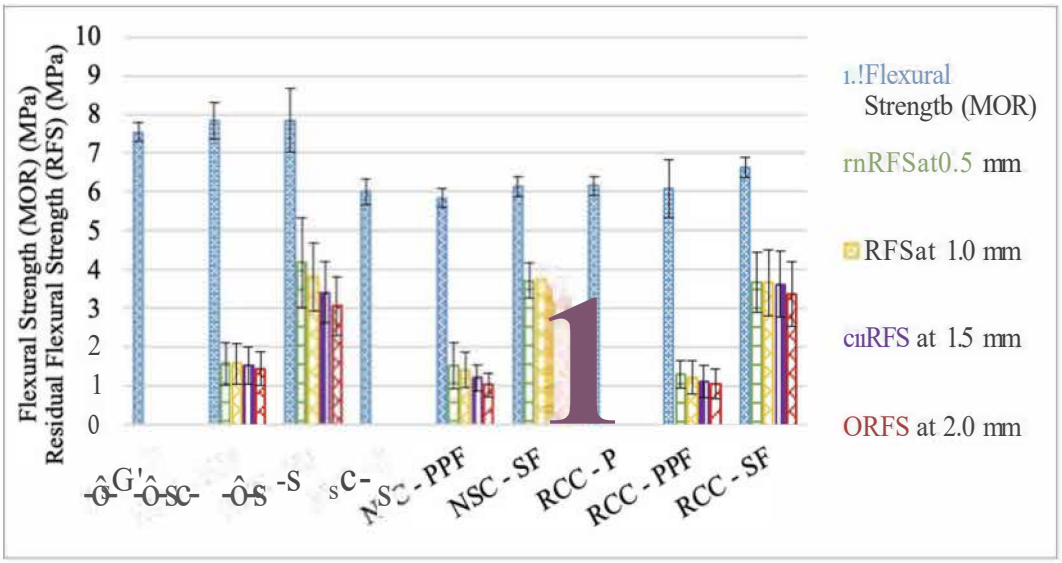


Figure 4.12. Flexural strength (modulus of rupture) (MOR) and residual flexural strength (RFS) values (for different mid-span deflections).

Table 4.23. Residual flexural strength (RFS) ratio values for different mid-span deflections.

| Concrete Mixture | Midspan Deflection (mm) | | | |
|---|---|---|---|---|
| | 0.5 | 1.0 | 1.5 | 2.0 |
| HSC- PPF - 0.50 | 19.7 (6.1) | 19.8 (5.7) | 19.2 (5.4) | 18.2 (4.9) |
| NSC - PPF - 0.50 | 25.8 (10.0) | 23.7 (8.0) | 20.6 (5.7) | 17.4 (5.0) |
| RCC - PPF - 0.50 | 21.2 (3.7) | 19.8 (5.2) | 18.2 (5.1) | 17.0(4.8) |
| HSC- SF - 0.50 | 52.5 (10.6) | 48.1 (7.9)* | 42.9 (7.0)* | 38.6 (7.0)* |
| NSC - SF - 0.50 | 60.6 (8.0) | 61.5 (7.8)** | 59.0 (7.5)** | 54.1 (8.4)** |
| RCC - SF - 0.50 | 55.6 (12.4) | 55.5 (13.7) | 55.0 (13.2) | 51.0 (13.1) |

Average values of abrasion resistance test results (for 3 tests for each concrete series) in terms of mass loss after the abrasion exposure were given in Figure 4.13. Based on the figure, similar abrasion resistance values were found for RCC and NSC mixtures, but the resistance of HSC was found higher. Since average flexural strength values were found similar for RCC and NSC, and higher for HSC, obtained results validate the strong relationship reported previously [223] for flexural strength and abrasion resistance of concrete. When the effect of fibers on the abrasion mass loss values were examined, reduced mass loss values were observed for both PPF and SF reinforced concrete mixtures, and the amount of decrease was found higher for SF reinforced concrete mixtures. Additionally, based on the figure the amount of decrease in mass loss due to the addition of fibers was found low for RCC mixtures compared to conventional concrete mixtures.

### 4.3.4. Thickness Requirements for Fibers in Different Concrete Matrix

IRC [84] design guide was used to determine the pavement thickness for a sample road, and road parameters used were given in thickness design part of experimental and numerical study chapter. As mentioned previously, material parameters used in the design were taken from the results of the experiments carried out in the scope of this study.

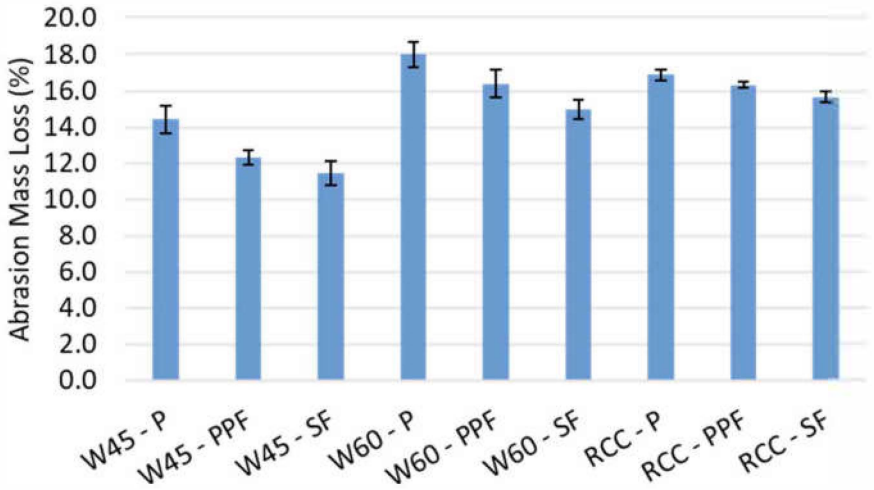


Figure 4.13. Abrasion resistance test results.

It should be stated here that in IRC [84] method 90-day characteristic MOR value is used for the design of concrete pavements, but only 28-day MOR values were measured in this study. Therefore, measured average 28-day MOR values were converted to 90-day characteristic MOR values. To this end, measured average MOR values were first multiplied by 1.10 to convert the 28-day MOR to 90-day MOR [84], then the values were multiplied by 0.70 to obtain characteristic values [95].

Required thickness values for all concrete types were presented in Table 4.24, together with the material properties used in the design. To show how the addition of fibers affects the required thickness values, the reduction in required thickness (%) values obtained by the addition of fibers were also added to the last column of Table 4.24. Based on the results, lowest thickness requirement values were found for HSC mixtures, and thickness requirement values were found similar for NSC and RCC. The result could be associated with the flexural strength of the mixtures. For the fiber reinforced mixtures, a higher amount of reduction in required thickness was found for SF reinforced concrete mixtures compared to PPF reinforced concrete mixtures ( 20-27% for SF vs. 9-10% for PPF) as expected. Though reduction in thickness values due to the addition of PPF were found very similar for the concrete series considered in the study, the reduction for SF was found lower for HSC, compared to the other two mixtures (NSC and RCC). These results could be directly associated with the obtained

RFS ratios (given in Table 4.23) (the main parameter that is used to reflect the fiber contribution to the performance), due to the addition of the corresponding fiber type.

Table 4.24. Material properties and required thickness values.

| Concrete Mixture | Density ($t/m^3$) | MOE (GPa) | MOR (MPa) | RFS (2 mm) | MOR' (MPa) | Characteristic Strength (90 days) (Flexural) (MPa) | Required Thickness (cm) | Thickness Reduction (%) |
|---|---|---|---|---|---|---|---|---|
| HSC-P | 2.44 | 27.1 | 7.54 | 0.00 | 7.54 | 5.81 | 18.2 | - |
| HSC-PPF-0.50 | 2.45 | 26.0 | 7.84 | 1.44 | 9.27 | 7.14 | 16.3 | 10.4 |
| HSC-SF-0.50 | 2.48 | 26.8 | 7.85 | 3.05 | 10.90 | 8.39 | 14.5 | 20.3 |
| NSC-P | 2.37 | 23.7 | 6.00 | 0.00 | 6.00 | 4.62 | 22.9 | - |
| NSC-PPF-0.50 | 2.36 | 23.7 | 5.84 | 1.02 | 6.86 | 5.28 | 20.7 | 9.6 |
| NSC-SF-0.50 | 2.40 | 24.4 | 6.13 | 3.31 | 9.44 | 7.27 | 16.6 | 27.5 |
| RCC-P | 2.48 | 25.6 | 6.15 | 0.00 | 6.15 | 4.74 | 21.6 | - |
| RCC-PPF-0.50 | 2.47 | 25.3 | 6.07 | 1.05 | 7.12 | 5.48 | 19.6 | 9.3 |
| RCC-SF-0.50 | 2.49 | 25.3 | 6.62 | 3.37 | 9.99 | 7.69 | 15.7 | 27.3 |

### 4.3.5. Cost and Environmental Impact for Fibers in Different Concrete Matrices

In this part, first cost and $CO_2$ emission (CE) of the mixtures per unit amount (1 $m^3$) were determined, then required thickness values found in the previous section were used together with the cost and emission values of unit mixtures to find material cost and environmental impact corresponding to 1 $m^2$ concrete pavement. Details of the followed methodology and results were given below.

First, CE and cost of all concrete ingredients were determined as given in 4.25. It should be noted here that all the cost values were taken from local suppliers (Turkey) (in June, 2021). However, the CE values were taken from local suppliers (Cement), Hammond and Jones [224] (CSt: No I, CSt: No II, CS, NS, ater, SP, steel mesh), Korol et al. [225] (PPF), and Stengel and SchieBl [226] (SF). Then, cost and CE values were multiplied with the corresponding material amount for 1 $m^3$ of concrete given in Table 4.20. Cost and CE values for unit products were given in Table Besides, the cost and

CE of 1 $m^3$ of concrete were given in Table 4.26. Based on the results presented in Table 4.26, compared to the conventional concrete mixtures both lower cost and lower CE values were obtained for RCC mixtures. These results could be attributed to lower amount of cement used in RCC mixtures, as well as the absence of SP, as the cement and SP are the ingredients of (plain) concrete that contribute most to the cost and CE (see Table 9). Furthermore, it can be seen from the table that the use of both PPF and SF increases the cost and CE of unit concrete mixtures, and the amount of increase in both values are much larger for SF compared to PPF.

Table 4.25. CE and cost values for unit product.

| Parameter | Cement | Crushed Stone: No I | Crushed Stone: No il | Crushed Sand | Natura! Sand | Water | SP | PPF | SF | Steel Mesh |
|---|---|---|---|---|---|---|---|---|---|---|
| CE (kg C02-eq / kg product) | 0.707 | 0.004 | 0.004 | 0.004 | 0.009 | 0.0003 | 1.880 | 3.430 | 2.680 | 1.990 |
| Cost ($/kg product) | 0.032 | 0.005 | 0.005 | 0.005 | 0.006 | 0.001 | 0.517 | 6.000 | 1.900 | 0.940 |

Table 4.26. CE and cost values for 1 $m^3$ concrete.

| Parameter | CE (kg C02-eq) | Cost ($) |
|---|---|---|
| HSC-P | 262.1 | 22.2 |
| HSC-PPF | 278.4 | 49.7 |
| HSC-SF | 368.0 | 96.6 |
| NSC- P | 258.3 | 20.7 |
| NSC -PPF | 274.4 | 48.1 |
| NSC - SF | 364.1 | 95.2 |
| RCC- P | 222.1 | 19.7 |
| RCC - PPF | 237.6 | 46.9 |
| RCC- SF | 326.4 | 93.6 |

For the next step, by using the required thickness values given in Table 4.24, the volume of concrete required for 1 $m^2$ of pavement construction was calculated for each of the concrete series. Lastly, by multiplying the calculated volumes with the cost and CE of the unit amount of corresponding concrete (Table 4.26), cost and CE for all concrete series were calculated for 1 $m^2$ pavement production. Results for CE and cost for 1 $m^2$ pavement production were given in Figure 4.14 and Figure 4.15, respectively. It should be stated here that for plain conventional concrete mixtures (HSC- P and NSC - P) steel mesh reinforcement was also considered, as crack control performance similar to FRC mixtures could only be possible by the use of steel reinforcements in plain concrete mixtures. Amount of steel meshes required for the plain mixtures were determined according to IRC 58 [84], and use of Q106/106 [227] steel meshes was found suitable for both concrete mixtures (HSC-P and NSC-P). It should be also stated here that the use of steel meshes in RCC pavement applications is not practical, and dimensional stabilities of RCC mixtures are usually much higher than conventional concrete mixtures (due to the decreased cement and increased aggregate content); thus, steel meshes were not considered for plain RCC mixture (RCC-P).

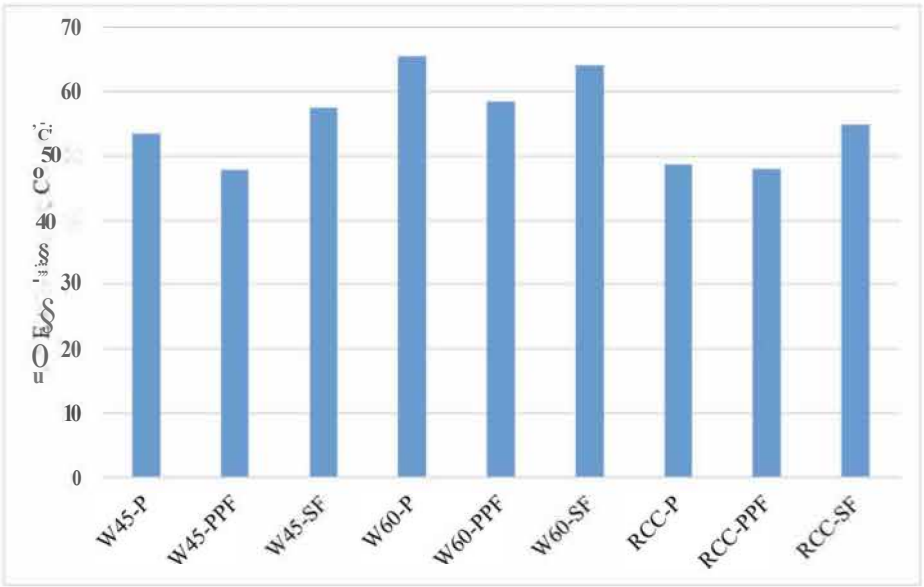


Figure 4.14. Material CE for 1 $m^2$ pavement.

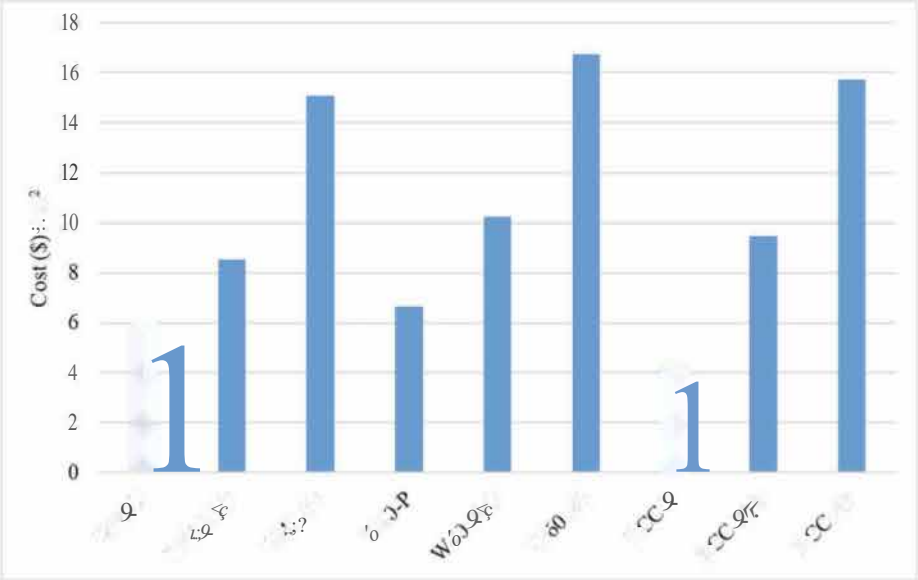


Figure 4.15. Material cost for 1 $m^2$ pavement.

Based on the figures, for plain concrete mixtures, though highest MOR and lower thickness requirement were found for HSC- P, lower CE values were obtained for RCC - P, which could be attributed to both low amount of cement used in RCC mixture and absence of steel mesh reinforcement for RCC. Additionally, due to increased required thickness, higher cost and environmental impact values were found for NSC - P mixture compared to HSC - P mixture.

For FRC mixtures, considerably increased pavement material cost values were found, and the amount of increase was found much higher for SF. On the other hand, both decreased and increased CE values were found for FRC mixtures. Amount of decrease in CE due to the addition of PPF was found lower for RCC mixture compared to HSC and NSC mixtures, which is mainly due to the absence of mesh reinforcement in RCC plain mixture. Similarly, amount of increase in cost due to the addition of PPF was found higher for RCC mixture compared to the conventional concrete mixtures.

For CE of SF reinforced concrete mixtures, though lower CE was found for NSC - SF mixture when compared to NSC-P (due to the addition of steel mesh into plain matrix and decreased thickness owing to addition of fibers into NSC -SF), higher emis-

sion values were found for HSC- SF and RCC - SF mixtures when compared to their control mixtures since reduction in thickness due to fiber addition was relatively low. Reduction in the emission value on NSC - SF mixture could be attributed to higher RFS ratio value obtained from it (refer to Table 8). Although, similar RFS ratio values were found also for RCC - SF mixture, since steel meshes were not considered for RCC - P mixture, no reduction in the emission value was observed. These results could be attributed to dependence of the results to the type of concrete mixture considered.

Furthermore, this study only focused on the cost and CE of materials, and cost and environmental impact of construction activities were not considered, but it is a known fact that the effort needed to construct steel mesh reinforced concrete slab is considerably higher compared to FRC slab. According to a previous study [98], cost of construction process for the FRC slab is almost half of the cost for steel mesh reinforced concrete slab. Increase in the cost of the construction process could be attributed to the additional effort required for laying, cutting, and tying activities required for steel meshes [97].

In the end, it should be noted that the cost values presented in Figure 4.15 are determined by considering the costs of the concrete ingredients valid in Turkey. On the other hand, though fiber prices in Turkey are comparable with most of the countries around the world, prices for cement and aggregates are considerably lower for Turkey. For example, aggregate and cement prices are almost 2 and 4 times higher for the United States with respect to the prices in Turkey [228]. Since the use of fibers might considerably decrease the amount of cement and aggregates used to produce concrete pavements (which is due to increased flexural capacity), a further cost advantage could be achieved for FRC for the countries with higher cement and aggregate prices.

### 4.3.6. Mechanical and Physical Tests for Fibers in Varying Amounts

Since the amount of fiber used to produce FRC mixture is the main parameter that affects not only the performance that could be obtained from the mixture but also

the cost and the environmental impact of materials, further studies have been carried out to see the effects of using different fiber volumes on the investigated performance criteria. For this part of the study, 0.25 - 0.50 - 0.75 and 1.00 %vol. PPF and 0.25 and 0.50 %vol. SF were taken into account. Selection for upper limits for fiber amounts was done by considering the results of previous part. Since the use of 0.50 %vol. SF dramatically increased the cost and marginally affect the environmental impact of concrete mixtures, this amount is considered as maximum for SF. On the other hand, since the use of 0.50 %vol. PPF affects the CE in positive way for all mixtures and it affects the cost much lower than same volume of SF, maximum amount for PPF was increased to 1.00 %vol. for PPF to see how further increase in the amount of fibers affects the results. In this part of the study, only the conventional concrete mixtures (HSC and NSC) were considered.

Mechanical and physical test results for plain and different amount of fiber reinforced normal strength and high strength conventional concrete mixtures were presented in Table 4.27 and Table 4.28, respectively. In both tables, values were given as average of 6 specimens for plain and 0.5%vol. fiber mixtures, but for the other mixtures results were given as average of 3 specimens. Besides, values given in parenthesis show the standard deviation of test results. To see the significance of the differences in performance parameters obtained for plain and FRC mixtures, t-tests were also carried out for all parameters investigated in this part, and in the tables bold values represent the statistical difference with control mixtures (as a result of t-test for 95 % confidence level). Based on the Table 4.27 and Table 4.28, for strength (compressive strength MOR), stiffness (MOE), absorption, density and porosity values were found similar for plain and FRC mixtures for all fiber types and amounts. Although, some statistical differences were obtained in both tables only marginal differences were seen in terms of means. This means that, fibers did not affect the performance in positive or negative way in terms of strength, stiffness, density, and porosity. On the other hand, varying post cracking contributions were obtained from the fibers based on the type and amount of fiber, as well as concrete matrix that they are used in. However, since the RFS value given in Table 4.27 is not applicable for control mixtures, no statistical

comparison was done for the values given in last column of the table. On the other hand, significant increases with an increasing fiber volume ratio in the RFS can be clearly seen from the table, for both concrete mixtures and fiber types.

Table 4.27. Mechanical test results for different fiber amounts.

| Concrete Mixture | Compressive Strength (MPa) | MOE (GPa) | MOR (MPa) | RFS (2 mm) (MPa) |
|---|---|---|---|---|
| HSC-P | 49.6 (3.7) | 27.1 (1.1) | 7.54 (0.25) | - |
| HSC-PPF-0.25 | 50.6 (0.9) | 27.1 (0.4) | 7.76 (0.35) | 0.97 (0.20) |
| HSC-PPF-0.50 | 47.1 (2.2) | **26.0 (0.4)** | 7.84 (0.47) | 1.44 (0.43) |
| HSC-PPF-0.75 | 47.8 (2.7) | 25.8 (1.1) | 7.95 (0.43) | 2.59 (0.99) |
| HSC-PPF-1.00 | 46.7 (1.6) | **25.0 (1.9)** | 7.93 (0.40) | 3.51 (0.53) |
| HSC-SF-0.25 | 52.5 (2.8) | 27.2 (0.5) | 7.88 (0.40) | 1.99 (0.29) |
| HSC-SF-0.50 | 49.2 (5.5) | 26.8 (1.1) | 7.85 (0.82) | 3.05 (0.75) |
| NSC-P | 32.7 (0.5) | 23.7 (1.9) | 6.00 (0.33) | - |
| NSC-PPF-0.25 | 32.1 (2.2) | 23.6 (0.8) | 5.87 (0.32) | 0.60 (0.09) |
| NSC-PPF-0.50 | 34.3 (1.0) | 23.7 (0.8) | 5.84 (0.24) | 1.02 (0.30) |
| NSC-PPF-0.75 | 32.7 (1.0) | 24.1 (0.4) | 6.01 (0.08) | 1.33 (0.33) |
| NSC-PPF-1.00 | 33.2 (1.2) | 23.3 (0.9) | 5.98 (0.07) | 2.30 (0.66) |
| NSC-SF-0.25 | 33.7 (2.3) | 23.8 (0.9) | 6.06 (0.43) | 2.26 (0.13) |
| NSC-SF-0.50 | 33.4 (1.7) | 24.4 (1.8) | 6.13 (0.27) | 3.31 (0.50) |

### 4.3.7. Thickness Requirements for Fibers in Varying Amounts

For different fiber volume cases, required thickness values were presented in Table 4.29, together with the material properties considered in the design. Last column of the table was given to show the change in the required thickness values due to the addition of different types and amount of fibers.

Table 4.28. Absorption, density, and porosity test results far different fiber amounts.

| Concrete Mixture | Absorption after immersion (%) | Bulk density, dry ($g/cm^3$) | Bulk density after immersion ($g/cm^3$) | Apparent density ($g/cm^3$) | Porosity (%) |
|---|---|---|---|---|---|
| HSC-P | 4.71 (0.73) | 2.35 (0.03) | 2.46 (0.02) | 2.64 (O.Ol) | 11.13 (1.51) |
| HSC-PPF-0.25 | 4.81 (0.26) | 2.36 (0.02) | 2.48 (0.02) | **2.67 (O.Ol)** | 11.49 (0.48) |
| HSC-PPF-0.50 | 4.92 (0.19) | 2.33 (O.Ol) | 2.45 (O.Ol) | 2.64 (O.Ol) | 11.69 (0.38) |
| HSC-PPF-0.75 | 4.97 (0.09) | 2.35 (0.00) | 2.47 (0.00) | **2.67 (0.00)** | 11.84 (0.18) |
| HSC-PPF-1.00 | 5.10 (0.22) | 2.34 (0.02) | 2.46 (O.Ol) | **2.66 (O.Ol)** | 12.08 (0.44) |
| HSC-SF-0.25 | 5.03 (0.31) | 2.36 (0.03) | 2.48 (0.02) | **2.69 (O.Ol)** | 12.02 (0.59) |
| HSC-SF-0.50 | 4.65 (0.40) | **2.38 (0.02)** | **2.49 (O.Ol)** | **2.68 (0.02)** | 11.26 (0.83) |
| NSC-P | 7.47 (0.46) | 2.22 (0.03) | 2.38 (0.02) | 2.66 (O.Ol) | 16.73 (0.87) |
| NSC-PPF-0.25 | 7.23 (0.41) | 2.23 (0.03) | 2.39 (0.02) | 2.66 (O.Ol) | 16.23 (O.70) |
| NSC-PPF-0.50 | 7.26 (0.26) | 2.22 (O.Ol) | 2.38 (O.Ol) | **2.65 (O.Ol)** | 16.34 (0.45) |
| NSC-PPF-0.75 | 7.04 (0.33) | 2.23 (0.02) | 2.39 (0.02) | 2.65 (O.Ol) | 15.86 (0.57) |
| NSC-PPF-1.00 | 7.24 (0.59) | 2.22 (0.04) | 2.38 (0.03) | 2.65 (0.02) | 16.23 (0.99) |
| NSC-SF-0.25 | 7.01 (0.28) | **2.26 (0.02)** | **2.41 (O.Ol)** | **2.68 (O.Ol)** | 15.96 (0.51) |
| NSC-SF-0.50 | 7.13 (0.08) | **2.26 (O.Ol)** | **2.42 (O.Ol)** | **2.70 (O.Ol)** | 16.26 (0.20) |

Based on the presented values, varying required thickness values were obtained far the FRC mixtures depending on the type and amount of fibers, and amount of decrease in the required thickness values were faund higher far the mixtures that includes higher amount of fibers, as expected. For the similar amount (in terms of volume) of fiber, higher reduction in required thickness values were obtained far SF reinfarced concrete mixtures compared to PPF reinfarced ones. Although, far HSC mixtures, O.75 %vol. PPF was faund enough to achieve similar thickness reduction with 0.25 %vol. SF, 1.00 %vol. PPF was required to achieve similar thickness requirement with 0.25 %vol. SF far NSC mixtures, which clearly demonstrate the dependence of the perfarmance to the concrete matrix properties.

Table 4.29. Material properties and required thickness values for different fiber amounts.

| Concrete Mixture | Density ($t/m^3$) | MOE (GPa) | MOR (MPa) | RFS (2 mm) | MOR' (MPa) | Characteristic MOR (90 days) (MPa) | Required Thickness (cm) | Thickness Reduction (%) |
|---|---|---|---|---|---|---|---|---|
| HSC-P | 2.44 | 27.1 | 7.54 | 0.00 | 7.54 | 5.81 | 18.2 | - |
| HSC-PPF-0.25 | 2.48 | 27.1 | 7.76 | 0.97 | 8.73 | 6.72 | 17.8 | 2.2 |
| HSC-PPF-0.50 | 2.45 | 26.0 | 7.84 | 1.44 | 9.27 | 7.14 | 16.3 | 10.4 |
| HSC-PPF-0.75 | 2.45 | 25.8 | 7.40 | 2.59 | 10.00 | 7.70 | 15.6 | 14.3 |
| HSC-PPF-1.00 | 2.46 | 25.0 | 7.93 | 3.51 | 11.44 | 8.81 | 14.6 | 19.8 |
| HSC-SF-0.25 | 2.49 | 27.2 | 7.88 | 1.99 | 9.87 | 7.60 | 15.3 | 15.9 |
| HSC-SF-0.50 | 2.48 | 26.8 | 7.85 | 3.05 | 10.90 | 8.39 | 14.5 | 20.3 |
| NSC-P | 2.37 | 23.7 | 6.00 | 0.00 | 6.00 | 4.62 | 22.9 | - |
| NSC-PPF-0.25 | 2.39 | 23.6 | 5.87 | 0.60 | 6.47 | 4.98 | 21.7 | 5.2 |
| NSC-PPF-0.50 | 2.36 | 23.7 | 5.84 | 1.02 | 6.86 | 5.28 | 20.7 | 9.6 |
| NSC-PPF-0.75 | 2.39 | 24.1 | 6.01 | 1.33 | 7.33 | 5.65 | 19.7 | 14.0 |
| NSC-PPF-1.00 | 2.38 | 23.3 | 5.98 | 2.30 | 8.28 | 6.37 | 18.4 | 19.7 |
| NSC-SF-0.25 | 2.41 | 23.8 | 6.06 | 2.26 | 8.32 | 6.41 | 18.2 | 20.5 |
| NSC-SF-0.50 | 2.40 | 24.4 | 6.13 | 3.31 | 9.44 | 7.27 | 16.6 | 27.5 |

### 4.3.8. Cost and Environmental Impact for Fibers in Varying Amounts

By using the required thickness values determined in the previous section and cost and environmental impacts of the unit materials (given in Table 4.26), costs and CE of the mixtures considered in this part were presented in Table 4.30. in the table, change (%) values for FRC mixtures were given relative to control mixture of the corresponding mixture, and negative and positive values represent decrease and increase in the considered parameter, respectively.

Although, decreased CE values were found for increasing PPF for both concrete types, varying emission values were obtained for increasing amount of SF. For both types of concrete mixtures, reduction in CE was observed for the use of 0.25 %vol. SF, but for the use of 0.50 % vol. SF increased and decreased CE values were obtained for HSC and NSC, respectively. Despite the decrease in required pavement thickness values, increased cost values were found for FRC mixtures compared to plain concrete mixtures, which could be attributed to higher costs of the fibers. However, it should be

noted here again that this study only considers the effect of fibers on the CE and cost of the materials and construction process for FRC mixtures is much easy, compared to mesh reinforced plain concrete mixtures. Therefore, by considering the construction effort and cost, further benefit could be obtained for FRC mixtures compared to plain ones.

Furthermore, concrete pavements are mostly exposed to harsh environmental conditions during their service lives, and corrosion of steel meshes might be considered as one of the pavement durability issues. In this respect the corrosion free nature of PPF can also be advantageous in terms of durability, against both steel fibers and steel mesh.

Table 4.30. Cost and CE values for different fiber amounts.

| Concrete Mixture | CE (kg $CO_2$-eq) / $m^2$ | Change in CE (%) | Cost ($) / $m^2$ | Change in Cost (%) |
|---|---|---|---|---|
| HSC-P | 51.6 | - | 5.9 | - |
| HSC-PPF-0.25 | 48.1 | -6.8 | 6.4 | 9.1 |
| HSC-PPF-0.50 | 45.4 | -12.0 | 8.1 | 37.8 |
| HSC-PPF-0.75 | 44.7 | -13.3 | 9.9 | 68.7 |
| HSC-PPF-1.00 | 43.1 | -16.4 | 11.3 | 92.4 |
| HSC-SF-0.25 | 48.2 | -6.5 | 9.1 | 55.1 |
| HSC-SF-0.50 | 53.4 | 3.4 | 14.0 | 138.6 |
| NSC-P | 63.0 | - | 6.6 | - |
| NSC-PPF-0.25 | 57.8 | -8.3 | 7.5 | 13.9 |
| NSC-PPF-0.50 | 56.8 | -9.9 | 10.0 | 51.3 |
| NSC-PPF-0.75 | 55.7 | -11.6 | 12.2 | 85.5 |
| NSC-PPF-1.00 | 53.5 | -15.1 | 13.9 | 111.5 |
| NSC-SF-0.25 | 56.6 | -10.2 | 10.5 | 60.1 |
| NSC-SF-0.50 | 60.4 | -4.1 | 15.8 | 139.8 |

## 4.4. Effects of Fibers on the Joint Performance of Concrete Pavements

### 4.4.1. Mixtures

3 different concrete mixtures with varying polypropylene fiber amounts (0.0%, 0.5%, and 1.0%) were designed for this part of the study. For all the mixtures cement dosage and water to cement ratios were fixed to 350 kg/m$^3$ and 0.60, respectively. To adjust the workability of mixtures, which is selected as EN 206 [208] - S2 slump class (5 - 8 cm) in this study, a modified polycarboxylate based SP was used. Polypropylene fibers (PPF) were used for fiber reinforced concrete mixtures for 2 different volume ratios (0.5% and 1.0%). In this study, plain concrete mixture was named as PC, but fiber reinforced concrete mixtures with 0.5%vol. 1.0%vol. were named as FRC - 0.5 and FRC - 1.0, respectively. Based on the explained methodology and nomenclature, mixture proportions for plain and fiber reinforced concrete mixture were determined as given in Table 4.31.

Table 4.31. Mixture proportions for 1 m$^3$ plain and fiber reinforced concrete mixtures.

| Ingredients | PC | FRC-0.5 | FRC-1.0 |
|---|---|---|---|
| Cement | 350.0 | 350.0 | 350.0 |
| CSt: No I | 542.3 | 537.2 | 543.9 |
| CSt: No II | 451.0 | 446.8 | 452.3 |
| es | 634.6 | 628.6 | 636.4 |
| NS | 180.8 | 179.1 | 181.3 |
| Water | 210.0 | 210.0 | 210.0 |
| SP | 1.1 | 1.4 | 1.8 |
| PPF | 0.00 | 4.55 | 9.10 |

### 4.4.2. Quasi-Static Tests

Results for compressive strength, modulus of elasticity and flexural performance tests were presented as average values in Table 4.32, together with the standard de-

viation of test results (in parenthesis). it should be noted here that the results for PC and FRC - 0.5 mixtures were given for 6 specimens, but the results were given for 3 specimens for FRC - 1.0 mixture. Additionally, all the tests were applied to the specimens cured for 28 days.

As the table shows average compressive strength, modulus of elasticity and flexural strength values were found very similar (with some marginal changes) for plain (PC) and fiber reinforced concrete mixtures, which is consistent with the relevant literature [60,229,230] that used polypropylene fibers with similar amounts. When the residual flexural strength values (a widely accepted indicator of post-cracking performance of FRC mixtures) were examined for FRC mixtures (FRC-0.5 and FRC-1.0), it was seen that the residual flexural strength values were found doubled for the FRC with 1.0%vol. fiber (FRC - 1.0), compared to FRC with 0.5%vol. fiber (FRC - 0.5).

Table 4.32. Compressive strength, modulus of elasticity and flexural performance test results.

| Property | | PC | FRC - 0.5 | FRC - 1.0 |
|---|---|---|---|---|
| Compressive Strength (MPa) | | 32.7 (0.5) | 34.3 (1.0) | 33.2 (1.2) |
| Modulus of Elasticity (GPa) | | 23.7 (1.9) | 23.7 (0.8) | 23.3 (0.9) |
| Flexural Strength (MPa) | | 6.00 (0.33) | 5.84 (0.24) | 5.98 (0.07) |
| Residual Flexural Strength (MPa) | 0.5mm | - | 1.51 (0.58) | 2.99 (0.87) |
| | 1.0 mm | - | 1.40 (0.46) | 2.97 (0.85) |
| | 1.5 mm | - | 1.20 (0.34) | 2.59 (0.78) |
| | 2.0mm | - | 1.02 (0.30) | 2.30 (0.66) |

### 4.4.3. Cyclic Shear Tests

in this part, post-cracking shear performance test results applied to plain (PC) and fiber reinforced concrete (FRC - 0.5 and FRC - 1.0) mixtures were presented. it should be noted here that the post-cracking shear tests were applied to 4 specimens for each concrete series, and the results were presented for these 4 specimens.

Peak differential displacement, which is defined as the difference between the displacement measured for maximum and minimum stress levels at the specified cycle number, is a reasonable indication of post-cracking shear performance of concrete. The value (peak differential displacement) demonstrates the shear load transfer capability of cracked section under the applied load magnitudes. Basically, better shear load transfer capability results in lower peak differential displacement. in another words, magnitude of peak differential displacement decreases with an increasing shear performance. Figure 4.16 shows the hysteresis curves for a selected concrete specimen (FRC - 1.0 - 1) at 500 cycle for various crack widths, and representation of peak differential displacement was given in the figure for the given crack width and cycle. As it can be seen from the figure that the peak differential displacement value is represented as the difference between the maximum and minimum displacement values observed for the relevant cycle, and crack width considerably affect the magnitude of the peak differential displacement increases dramatically (peak differential displacement increases with increasing crack width).

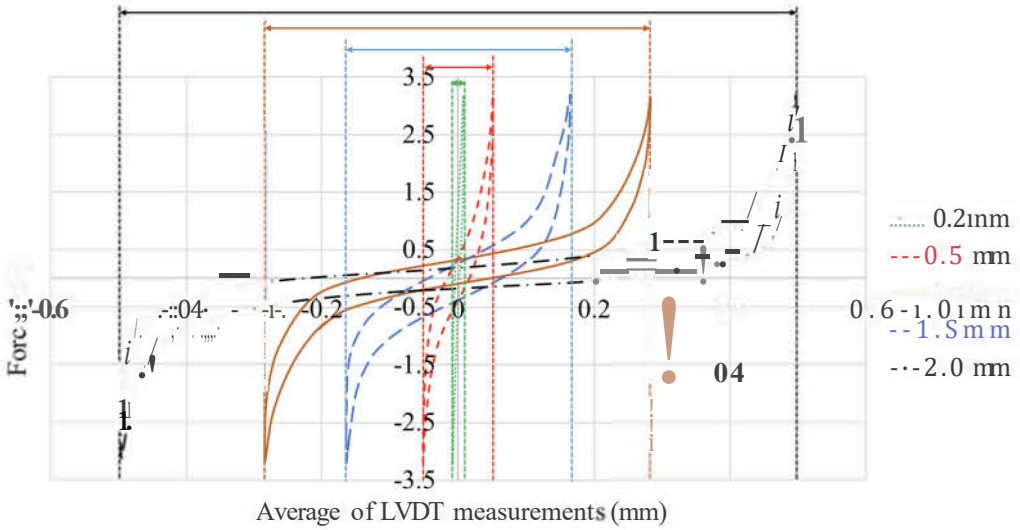


Figure 4.16. Hysteresis curves for 'FRC - 1.0 - 1' at 500 cycle for different crack widths (0.2 - 0.5 - 1.0 - 1.5 - 2.0 mm) and representation of peak differential displacements for the relevant crack widths at 500 cycle.

For the post-cracking performance tests 4 specimens were tested for each of the concrete mixtures (PC, FRC - 0.5, and FRC - 1.0) for 5 different crack widths (0.2, 0.5, 1.0, 1.5, and 2.0 mm), and based on the definition given above, peak differential displacement for all cases and cycles were calculated and presented in Figure 6. As explained above, peak differential displacement is an important indication of post-cracking shear performance of tested specimen, an increasing peak displacement can be associated with the decreased shear performance.

Figure 4. 17 shows that the peak differential displacement increases with the application of cyclic loading; however, it can be noticed that the amount of change in peak differential displacement is much higher for a few number of initial cycles and reaches an approximately constant value after that. Figure 4. 17 also shows that the increasing crack widths considerably increase the magnitudes of peak differential displacements calculated. in addition, it can be seen from the figure that for the similar crack widths use of fibers in increasing amount tend to increase the shear performance (decrease the peak differential displacement).

To compare the obtained peak differential displacement values for plain and fiber reinforced concrete mixtures, peak displacement values corresponding to 500 eyde were specified for all test cases. Then, by using the obtained values average peak displacement values corresponding to different concrete mixtures (PC, FRC - 0.5, and FRC - 1.0) and crack widths (0.2, 0.5, 1.0, 1.5, 2.0 mm) were presented together with the standard deviations of the results in Figure 4.18. it can be seen from the figure that for all the crack widths considered in this study lower average peak displacement values were found for fiber reinforced concrete mixtures (FRC - 0.5 and FRC - 1.0) compared to plain one (PC).

Moreover, for all the crack widths, amount of decrease in peak differential displacement value was found higher for FRC - 1.0 compared to FRC - 0.5, which shows that the amount of increase in fiber amount further decrease the peak differential displacement (increase the post-cracking shear performance).

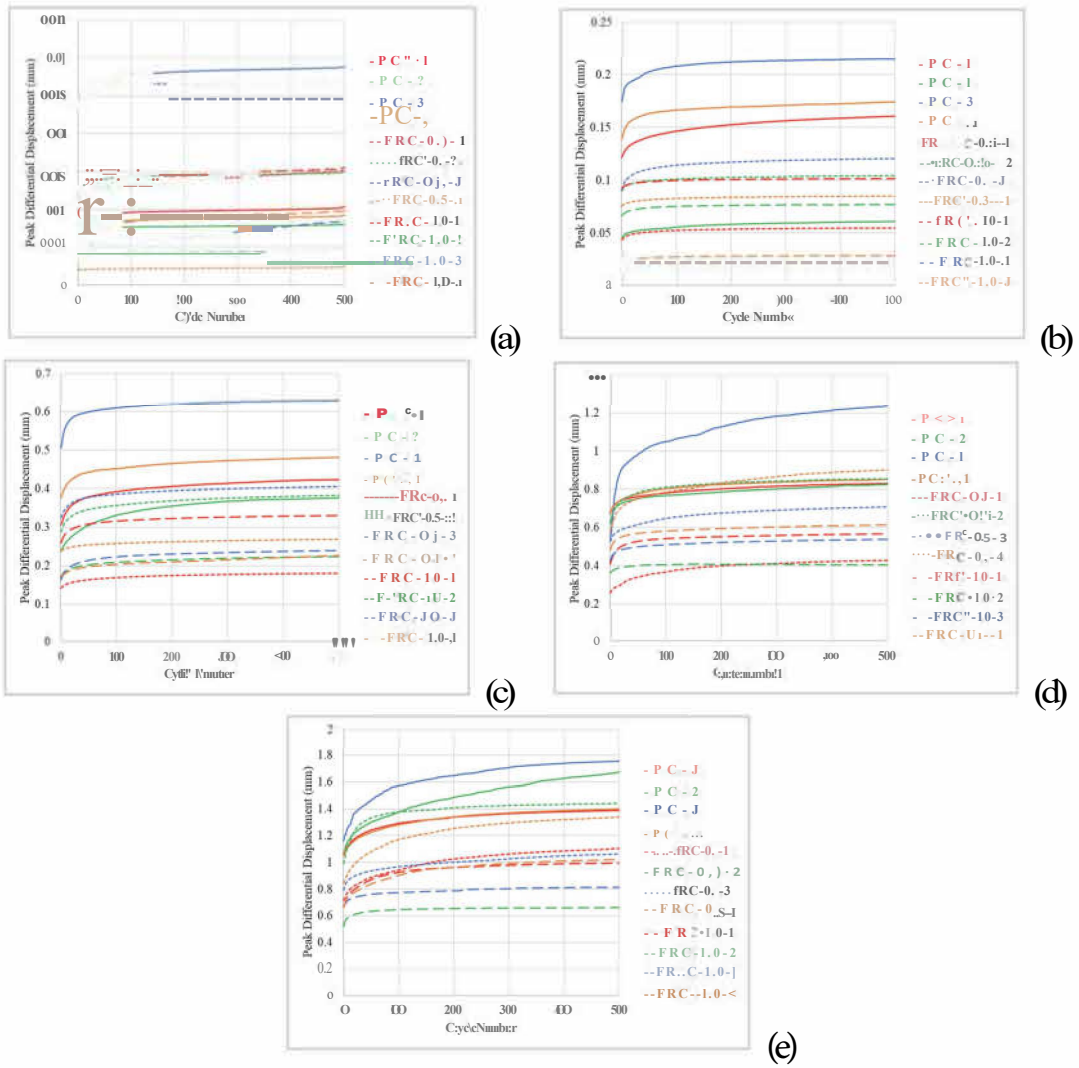


Figure 4.17. Cycle number and peak differential displacement relationships for different crack widths (CW) up to 500 cycles; (a) 0.2 mm, (b) 0.5 mm, (c) 1.0 mm, (d) 1.5 mm, (e) 2.0 mm.

In order to see if the obtained differences in post-cracking shear performance values are statistically meaningful, t-tests were carried out to compare the obtained peak differential displacements for all concrete mixtures (PC vs FRC - 0.5, PC vs FRC - 1.0, and FRC - 0.50 vs FRC - 1.0) and crack widths (0.2, 0.5, 1.0, 1.5, 2.0 mm). P-values obtained as a result of t-tests and the values that emphasize the statistical difference (for 95% confidence level) were presented in Table 4.33 for all the cases mentioned here, where bold values represents the statistical difference between the compared mixtures.

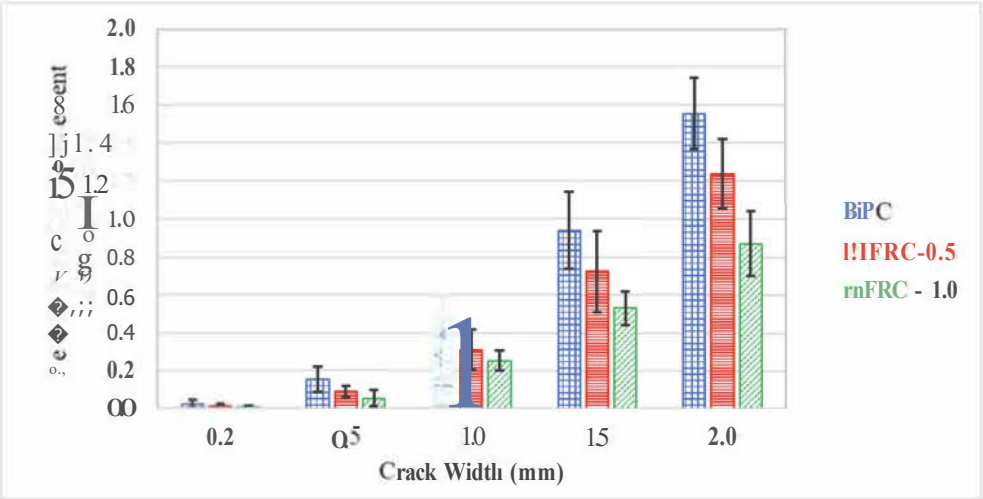


Figure 4.18. Peak differential displacement at 500 eyde.

Based on the Table 4.33 it can be said that there is a tendency to increase in statistical difference (decrease in p-value) with an increasing crack widths, which might be associated with the increasing contribution of fibers to the shear performance with increasing crack widths. For '2 mm' crack width, differences in average peak differential displacement values were found significant for all the comparison cases (with 95% confidence level). On the other hand, for other crack widths, statistical difference was observed for only between PC and FRC - 1.0 (mixture with no fiber and maximum fiber), but no statistical difference was observed for other comparison cases (for 95% confidence level). Despite the visible difference in average peak displacement between the concrete series for all crack widths (in reference to Figure 4.18), the absence of statistical difference (in reference to Table 4.33) for most of the comparison case, might be attributed to large variation of the test results, which makes hard to distinguish the results statistically. Though each of the test requires considerable time and effort, to deal with this large variation use of larger number of specimens might be recommended to examine the post-cracking shear performance of mixtures with the test method employed in this study.

Table 4.33. P-values obtained as a result of t-tests.

| Compared Concrete Series | Crack Widths (mm) | | | | |
|---|---|---|---|---|---|
| | 0.2 | 0.5 | 1.0 | 1.5 | 2.0 |
| PC / FRC - 0.5 | 0.90 | 0.13 | 0.07 | 0.19 | **0.05** |
| PC / FRC - 1.0 | 0.45 | **0.05** | **O.OI** | **O.OI** | **0.00** |
| FRC - 0.5 / FRC - 1.0 | 0.37 | 0.20 | 0.38 | 0.15 | **0.03** |

Moreover, by using the peak differential displacements obtained (experimentally) for 500 cycles of cyclic shear stress repetition, regression analyses were done for all the concrete mixtures (PC, FRC - 0.5, FRC - 1.0) to show the relationship between crack width and peak differential displacement. Regression curves obtained for the concrete mixtures were given in Figure 4.19, together with the regression equations and their correlation coefficients ($R^2$). The figure demonstrate that the regression curves obtained for the data sets shift in downward direction for with the increasing amount of fiber reinforcements. Obtained curves basically represents that the peak differential displacement obtained for similar scenarios (crack widths and load magnitudes) are lower for FRC mixtures, which is another indication of increased shear stiffness for FRC mixtures. In addition, Figure 4.19 shows that the vertical distance between the regression curves increase with increasing crack widths, which represents the increasing contribution of fibers with increasing crack widths, and support the outcome obtained for Table 4.33 (explained in previous paragraph).

As explained above, peak differential displacement values were determined in this study for varying crack widths, fiber ratios. To propose a model that defines the peak differential displacement as a function of crack width and fiber amount, linear model fitting tool of MATLAB [231] was used and obtained as

$$\hat{O}_{peak,e} = - 0.083016 + 0.19709 \times e^{c\,w} + 0.16113 \times e^{P\,P\,F\,R}, \qquad (4.2)$$

where $\hat{O}_{peak,e}$ shows estimated peak differential displacement, $CW$ represents crack width ('mm'), and PPFR is volume ratio of polypropylene fibers to the total volume of concrete in percent (between OO - 1.0).

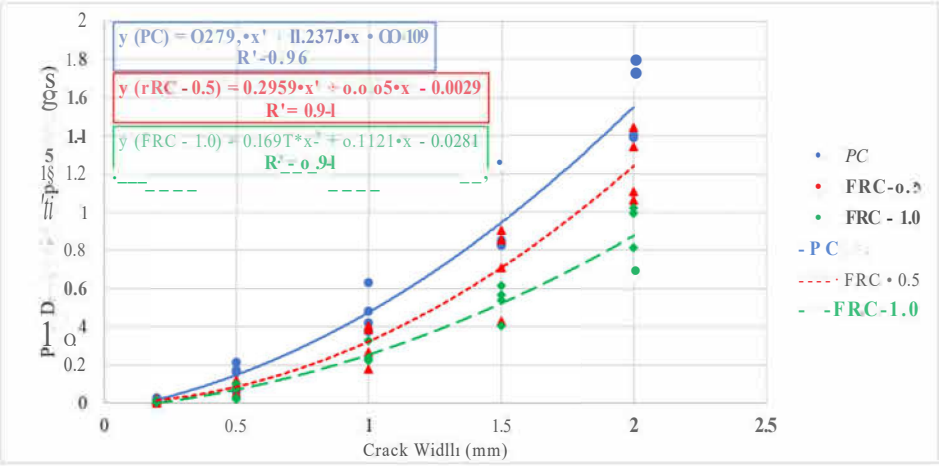


Figure 4.19. Relationship between crack width and peak differential displacement for varying fiber amounts.

Additionally, correlation coefficient ($R^2$), which is an indication of suitability of proposed model to the actual data ($R^2$ value close to '1.000' indicates better fit), for the given equation was found as 0.904. Besides, the scatter graph that represent the relationship between the estimated and measured peak differential displacement values was presented in Figure 4.20, together with the equilibrium line. When the correlation coefficient coefficient scatter graph given in Figure 4.20 examined together, it could be concluded that the proposed model reasonably explains the experimentally obtained results. It should be emphasized here that the model parameters proposed above are dependent on the properties of the concrete mixture used, as well as the fiber type used in this study.

## 4.5. Two-Stage Mixing Approach to Improve Fiber-Matrix Interface

### 4.5.1. Mixtures and Mixing Protocols

For this part, 4 different concrete mixtures were designed: one plain mixture without fibers and MS, one FRC mixture without MS, and two FRC mixtures with MS (2% and 4% of cement by weight was replaced with MS, respectively). The plain mixture was named as 'Control', and the FRC mixtures were named based on the weight percent of MS used in binder, as 'MS-0' (100% cement), 'MS - 2' (98% cement

and 2% MS), and 'MS-4' (96% cement and 4% MS). It should be stated here that both standard and modified mixing methodologies (explained in the following section) were applied to the FRC mixtures, and while presenting the results, mixtures produced with standard mixing protocol were given with 'Std' extension and mixtures produced with modified mixing protocol were given with 'Mod' extension. To elaborate the statement, 'MS-0' (FRC without MS) concrete was produced with standard and modified mixing protocol, and they are named as 'MS-0-Std' and 'MS-0-Mod', respectively. Based on the mixing methodology and nomenclature given, ingredients for 1 $m^3$ concrete mixtures were given in Table 4.34.

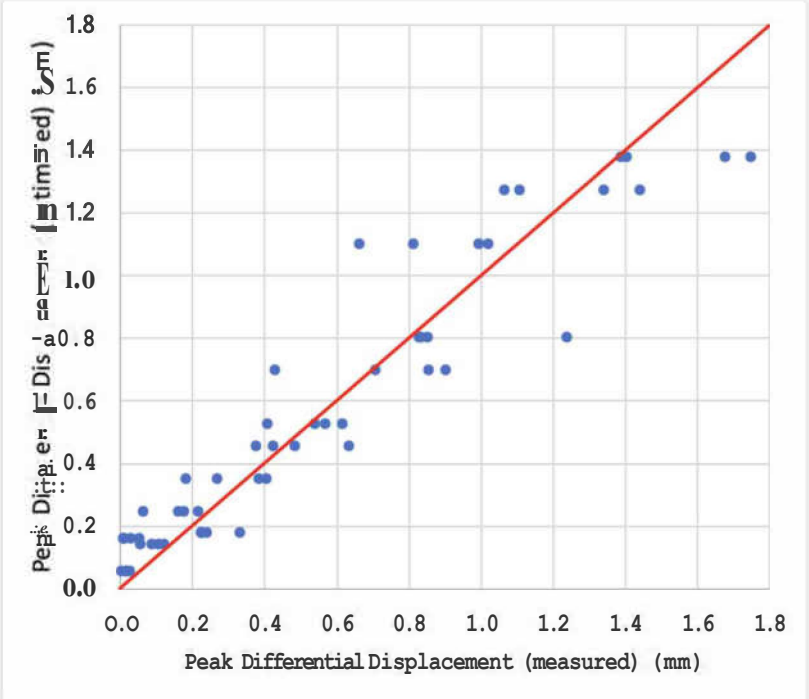


Figure 4.20. Measured and estimated (based on the proposed model) peak differential displacement values.

As explained above the aim of this study is to see if fiber-matrix interface can be improved by modifying the mixing method. With this aim two different mixing protocols were used in this study, as (i) standard mixing protocol and (ii) modified mixing protocol.

Table 4.34. Ingredients of concrete mixtures for 1 $m^3$ volume.

| Mixture Name | Control | MS-0 | MS-2 | MS-4 |
|---|---|---|---|---|
| Cement | 350.0 | 350.0 | **343.0** | 336.0 |
| SF | - | - | 7.0 | 14.0 |
| CSt: No I | 542.3 | **537.2** | **536.7** | 535.9 |
| CSt: No il | 451 | 446.8 | 446.4 | 445.7 |
| **eS** | 634.6 | **628.6** | **628.0** | 627.0 |
| NS | 180.8 | 179.1 | 178.9 | 178.7 |
| Water | 210.0 | 210.0 | 210.0 | 210.0 |
| **SP** | 1.1 | 1.4 | 1.5 | 1.6 |
| **PPF** | - | 4.55 | 4.55 | 4.55 |

Four different concrete mixtures were prepared with standard mixing protocol, as plain (Control), FRC without MS (MS-0-Std), FRC with 2% MS (MS-2-Std), and FRC with 4% MS (MS-4-Std). On the other hand, three different concrete mixtures were prepared with modified mixing protocol; FRC without MS (MS-0-Mod), FRC with 2% MS (MS-2-Mod), and FRC with 4% MS (MS-4-Mod). It should be emphasized here that the SF was used in this study due to its well-known positive impact on the ITZ of cementitious composites, caused by its pozzolonic activity (change ITZ composition and thickness), as well as filler effect (reduce ITZ porosity) [193,232,233].

4.5.1.1. Standard Mixing Protocol. First, dry ingredients (aggregates and binders) were put into the pan mixer (from coarse to fine) and mixed for two minutes. Then, while the mixer is still running water and SP mixture was added to the mixer in one minute gradually, and wet mix was mixed for additional one minute. Following this, for plain concrete mixture, formed mix was mixed for two more minutes. On the other hand, for FRC mixtures, fibers were added gradually in one minute and then final (FRC) mixture was mixed for one more minute. Therefore, mixing operation was completed in six minutes, for both plain and fiber reinforced concrete mixtures.

4.5.1.2. Modified Mixing Protocol. The aim of modified mixing methodology is to coat the fibers with a high-performance binder matrix (with low water/binder and MS). For this purpose, the fibers were coated with three different binder slurry, with or without MS, following the mixing methodology explained below.

In the beginning, required amount of binder ('cement' or 'cement + MS'), aggregate, water and SP to produce aimed volume of concrete were weighted, and water and SP was mixed in a bucket. Then, aggregates and cement corresponding to 80% of total binder was separated and put into pan mixer. After that water - SP mixture corresponding to the 35%wt. of binder was separated to prepare the binder slurry (water/binder ratio for the main mix was 60%). Following this, remaining cement and MS (if any) were put into the small mixer and mixed with separated water and SP mixture in two minutes the mixer to obtain binder slurry. At the same time, dry materials inside the pan mixer were mixed for two minutes to achieve uniformity. After that water and SP mixture remaining from the slurry was added into the pan mixer in one minute while the mixer is running, and formed mix was mixed for one additional minute. At the same time (in the small mixer) fibers were mixed with slurry until ensuring that all the fibers were covered with the slurry (approximately in two minutes). Then, slurry coated fibers were added to the pan mixer in one minute while the mixer is running. In the final step, formed wet mix was mixed for one more minute to achieve uniformity. Thus, as a total of six minutes was spent for modified mixing protocol.

Schematic representations of standard and modified mixing protocols were given in Figure 4.21. It is worth noting here that though the FRC mixtures were named considering the weight percent of MS compared to total binder (MS-0, MS-2, and MS-4), for the modified mixing protocol, weight percent of MS by means of slurry binder weight corresponding to 0% (for MS-0), 10% (for MS-10), and 20% (for MS-20).

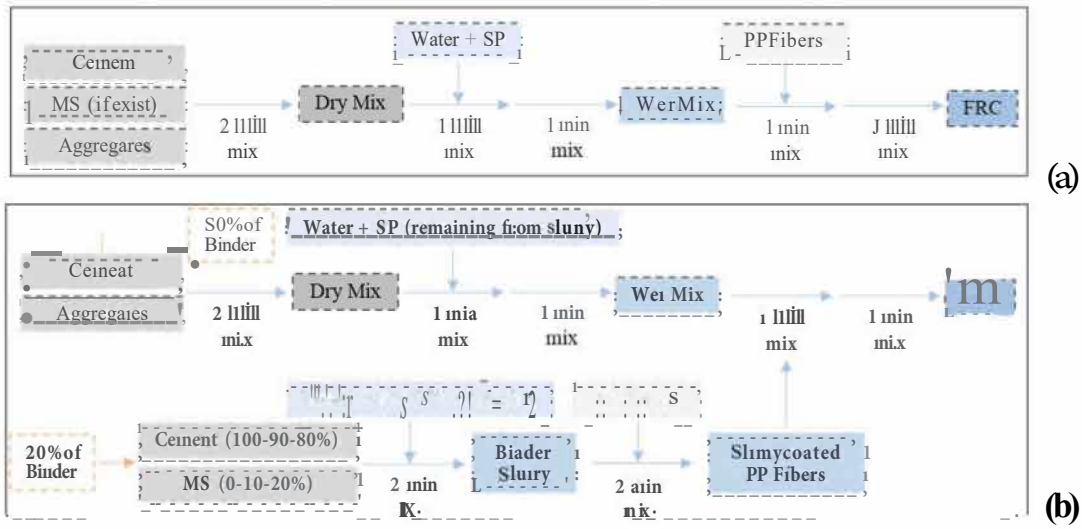


Figure 4.21. Concrete mixing protocols; (a) standard mixing, (b) modified mixing.

### 4.5.2. Quasi-Static Tests

Compressive strength and modulus of elasticity test results for all concrete mixtures were presented in Table 4.35, where the average values given for 6 specimens, and values given in parenthesis show the standard deviation of results. Accordingly, similar compressive strength and modulus of elasticity values were obtained for plain (Control) concrete and FRC mixtures produced with standard and modified mixing methodology. Therefore, based on the results modified mixing methodology was found not to affect the compressive strength and modulus of elasticity of concrete mixtures in positive or negative way. In addition, for the amounts of MS used in this study (2% and 4%) no considerable change in compressive strength and modulus of elasticity was observed.

Load - midspan deflection graphs obtained for FRC mixtures prepared by using standard and modified mixing method with 0%, 2%, and 4% MS presented in Figure 4.22. In addition, average flexural strength (MOR) and residual flexural strength (RFS) values obtained for all the mixtures were given in Table 4.36, where values given in the parenthesis show the standard deviation of test results and all the values given for 5 specimens.

Table 4.35. Compressive strength and modulus of elasticity test results.

| Mixture Name | Compressive Strength (MPa) | Modulus of Elasticity (GPa) |
|---|---|---|
| Control | 32.9 (0.4) | 23.9 (2.1) |
| MS-0-Std | 33.1 (0.6) | 23.7 (1.2) |
| MS-0-Mod | 35.0 (1.4) | 25.3 (1.1) |
| MS-2-Std | 35.3 (0.7) | 25.6 (0.5) |
| MS-2-Mod | 35.2 (1.1) | 25.0 (1.9) |
| MS-4-Std | 36.3 (0.9) | 24.0 (0.8) |
| MS-4-Mod | 35.8 (1.1) | 24.8 (0.8) |

According to Table 4.36, there was no noticeable increase or decrease in the average flexural strength values for FRC mixture (prepared using either standard or modified mixing methodology) compared to Control mixture. On the other hand, the average residual flexural strength values for FRC mixtures prepared with modified mixing methodology were higher than those obtained using standard mixing methodology.

Table 4.36. Average flexural performance test results.

| Mixture Name | Flexural Strength (MOR) (MPa) | Residual Flexural Strength (MPa) | | | |
|---|---|---|---|---|---|
| | | 0.5mm | 1.0 mm | 1.5 mm | 2.0mm |
| Control | 5.96 (0.34) | - | - | - | - |
| MS-0-Std | 5.61 (0.38) | 1.33 (0.23) | 1.11 (0.26) | 0.96 (0.26) | 0.83 (0.22) |
| MS-0-Mod | 5.67 (0.61) | 1.49 (0.25) | 1.39 (0.25) | 1.21 (0.25) | 1.05 (0.23) |
| MS-2-Std | 5.62 (0.24) | 1.34 (0.28) | 1.18 (0.24) | 1.00 (0.24) | 0.86 (0.23) |
| MS-2-Mod | 5.73 (0.50) | 1.72 (0.46) | 1.77 (0.37) | 1.60 (0.35) | 1.38 (0.32) |
| MS-4-Std | 6.05 (0.39) | 1.63 (0.13) | 1.52 (0.19) | 1.32 (0.20) | 1.16 (0.17) |
| MS-4-Mod | 6.30 (0.45) | 1.70 (0.39) | 1.65 (0.37) | 1.51 (0.26) | 1.34 (0.17) |

Moreover, average residual flexural strength ratio (RFSR) (RFSR = RFS / MOR) values corresponding to 0.5, 1.0, 1.5, and 2.0 mm midspan deflections were given in Figure 4.23, together with the standard deviations.

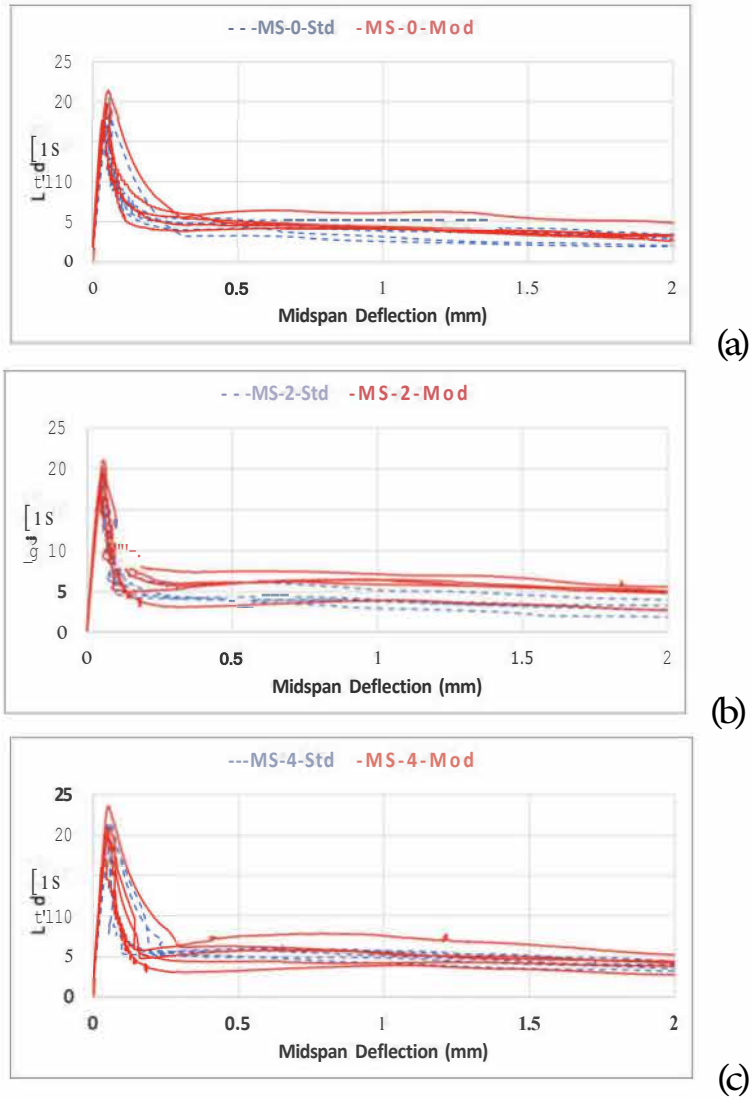


Figure 4.22. Load - midspan defl.ection graphs for FRC mixtures; (a) without MS, (b) with 2% MS, (c) with 4% MS.

Based on Figure 4.23, modified mixing methodology was found to increase the average RFSR values for all 3 mixture cases (with 0%, 2%, and 4% MS) and 4 midspan defl.ection values considered. To show the magnitude of increase in average RFSR and its statistical significance, change in RFSR values obtained by using modified mixing were given in Table 4.37, together with the results of t-tests (p-values that represents the significance of obtained changes), where bold values represents statistical difference between the compared mixtures. Table 4.37 shows that the increase in RFSR varies between 0.1 and 30.6% according to the considered mixture, as well as midspan defl.ection value. For all the midspan defl.ections largest change in RFSR values were obtained for

MS-2 followed by MS-0 and MS-4, respectively. Additionally, for all the comparison cases, change in RFSR values were found to be increased with an increase in midspan deflection values, which might be attributed to increasing contribution obtained due to modified mixing methodology with increasing midspan deflections. Based on the p-values given in Table 4.37, change in average RFSR values were found significant (95% significance) for only the comparison case of 'MS-2-Std MS-2-Mod' and midspan deflections of 1.0 mm, 1.5 mm, and 2.0 mm. Despite considerable changes (up to 24.9%) in average RFSR for other case, comparatively large p-values obtained for other comparison cases ('MS-0-Std MS-0-Mod' and 'MS-4-Std MS-4-Mod') might be attributed to large variations of flexural performance test results (see Figure 8) which make hard to distinguish the compared mixtures statistically. Furthermore, despite similar changes obtained for MS-0 and MS-2 mixtures by using modified mixing methodology, lower changes obtained for MS-4 mixtures might be related to relatively high performance obtained for the companion mixture, as well as the excessive amount of MS (20%) used in cement slurry for both secondary (pozzolanic) reaction and filler effect [232] which are the main effects of MS that improve the performance of cementitious matrices, as previous studies suggested lower MS amounts (less than 10%) to obtain maximum performance [232-234]. Therefore, further studies are recommended to determine the optimum amount of SF (or other supplementary cementitious materials) to maximize the benefit obtained from the modified mixing methodology.

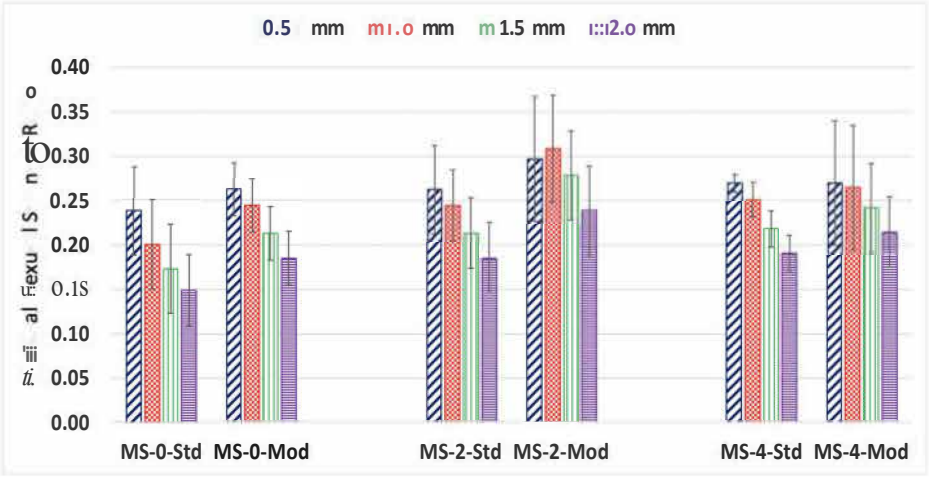


Figure 4.23. Average residual flexural strength ratios for different midspan deflections.

Table 4.37. Change in residual flexural strength ratio (%) and results (p-values) of t-tests.

| Compared Mixtures | 0.5 mm | | 1.0 mm | | 1.5 mm | | 2.0mm | |
|---|---|---|---|---|---|---|---|---|
| | Change (%) | p | Change (%) | p | Change (%) | p | Change (%) | p |
| MS-0-Std & MS-0-Mod | 10.3 | 0.36 | 22.3 | 0.11 | 23.4 | 0.14 | 24.9 | 0.12 |
| MS-2-Std & MS-2-Mod | 13.1 | 0.16 | 26.2 | 0.01 | 30.6 | 0.01 | 29.0 | 0.02 |
| MS-4-Std & MS-4-Mod | 0.1 | 0.99 | 5.5 | 0.68 | 11.1 | 0.36 | 12.4 | 0.22 |

### 4.5.3. Microstructural Analyses

Using the 'atomic%' of elements obtained from EDX for fiber-matrix interface, Ca/Si for all the FRC mixtures and analyzed surfaces (3 surfaces for each mixture) were calculated, and the average Ca/Si were given together with their standard deviations in Figure 4.24. Accordingly, for the mixtures produced with standard mixing protocol, decreasing Ca/Si values were observed with increasing use of MS. In addition, considerable reductions in Ca/Si were observed for the MS mixtures produced with modified mixing protocol compared to those produced with standard mixing protocol. Obtained reductions in Ca/Si values for the given comparison cases might be attributed to higher amount of C-8-H gel and MS particles within the interface, both provided by high silicon dioxide ($SiO_2$) content of MS particles put into the mixtures ( 90%).

In contrast, despite considerable improvements in mechanical performance obtained for non-SF mixture by using modified mixing protocol (see Figure 4.23 and Table 4.37), Ca/Si was found similar for non-MS mixtures produced with standard (MS-0-Std) and modified (MS-0-Mod) mixing protocol. Similar interface compositions (similar Ca/Si) obtained for the mixtures might be due to the incapability of the investigation methodology (EDX analysis on the matrix surface) to capture the thickness and overall composition of fiber-matrix interface. Since EDX analysis give an idea about the surface to a limited depth (1-10 *μm),* while the thickness of interface in cementitious composites usually greater than that (usually reported between 10 to 80 *μm* [192,193, 235-238]) and being significantly affected by change in water/cement ra-

tio [192,193]. Therefore, further studies are recommended to investigate the efficiency of the applied mixing methodology on the overall depth and composition of fiber-matrix interface.

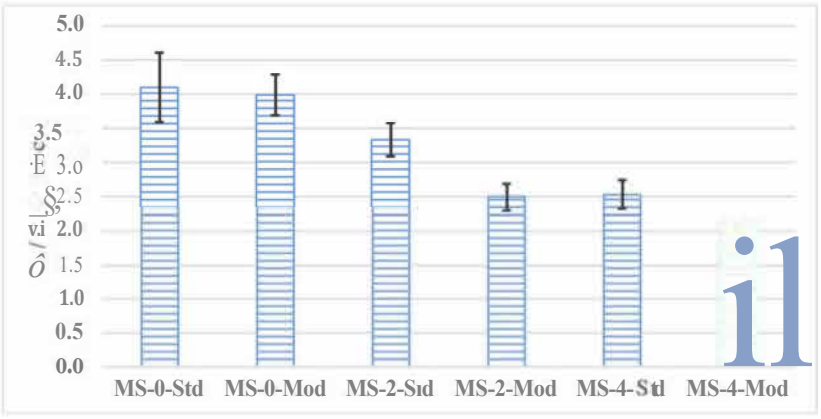


Figure 4.24. Calcium to silicon ratio (Ca/Si) of FRC mixtures.

### 4.5.4. Thickness Requirements

For the sample pavement considered, thickness requirements corresponding to different concrete mixtures were given in Table 4.38, together with the material properties used in design and reduction in thickness requirements. According to the table, thickness reductions changing from 5.2% to 17.9% was obtained for FRC mixtures, and the use of MS was found to reduce required thickness. In addition, lower thickness requirements (up to 6.0% reduction in required thickness) were obtained for the mixtures prepared with modified mixing protocol than those prepared with standard mixing protocol, which might be associated with the better flexural performance obtained for them (see Figure 4.23).

### 4.5.5. Cost and Environmental Impact Analyses

By using the thickness requirements determined for the concrete mixtures, cost and $CO_2$ emission (CE) analyses were done to show the effect of change in concrete ingredients and mixing methodology on the cost and environmental impact of sample pavement.

Table 4.38. Material parameters, thickness requirements and thickness reductions.

| Mixture Name | MOE (MPa) | MOR (MPa) | RFS (MPa) (2mm) | MOR' (MPa) | Characteristic MOR' (90 days) (MPa) | Required Thickness (cm) | Thickness Reduction Compared to Plain (%) | Thickness Reduction Compared to Standard Mixing (%) |
|---|---|---|---|---|---|---|---|---|
| Control | 23.9 | 5.96 | - | 5.96 | 4.59 | 22.9 | - | - |
| MS-0-Std | 23.7 | 5.61 | 0.83 | 6.44 | 4.96 | 21.7 | 5.2 | - |
| MS-0-Mod | 25.3 | 5.67 | 1.05 | 6.72 | 5.17 | 20.4 | 10.9 | 6.0 |
| MS-2-Std | 25.6 | 5.62 | 0.86 | 6.48 | 4.99 | 20.8 | 9.2 | - |
| MS-2-Mod | 25.0 | 5.73 | 1.38 | 7.11 | 5.47 | 19.7 | 14.0 | 5.3 |
| MS-4-Std | 24.0 | 6.05 | 1.16 | 7.21 | 5.55 | 19.9 | 13.1 | - |
| MS-4-Mod | 24.8 | 6.30 | 1.34 | 7.64 | 5.88 | 18.8 | 17.9 | 5.5 |

First, cost and CE of the unit volume (1 $m^3$) of concrete mixtures were calculated by considering the mixture ingredients corresponding to '1 $m^3$' concrete (given in Table 4.34), as well as cost and CE ofthe ingredients. Cost and CE of the mixture ingredients and '1 $m^3$' concrete mixtures were given in Table 4.39 and Table 4.40, respectively. It should be noted here that all the cost values were taken from local suppliers (Turkey) (in July 2022). On the other hand, the CE values were taken from local suppliers (Cement), Hammond and Jones [224] (CSt: No I, CSt: No il, CS, NS, ater, SP, steel mesh), Korol et al. [225](PPF), and Thilakarathna et al. [239] (MS).

Afterward, amount of concrete required to produce unit area (1 $m^2$) concrete pavement was calculated for each of the concrete mixture considering the thickness requirement corresponding to relevant mixture. Finally, to determine the cost and environmental impact of concrete pavements produced with the different concrete mixes considered in this study, the amount of concrete required to produce the concrete pavements (determined in the second step) and the cost and CE of the respective mixes were multiplied.

Furthermore, to compare the pavements with similar performances cost and CE of steel meshes were also considered for plain (Control) concrete mixture, as mesh reinforcements are needed for the plain concrete mixtures to achieve a cracking performance similar to FRC mixtures. For the plain concrete mixture, TS 4559 [227] - Q106/106

steel mesh was found suitable to meet the amount of reinforcement required based on IRC 58 [84] design guide, and both cost and CE of the steel mesh corresponding to 1 $m^2$ of concrete pavement were added to the total cost and CE of the concrete mixture.

Table 4.39. Cost and CE of the unit weight of concrete ingredients.

| Parameter | CE (kg CO2 - eq / kg product) | Cost ($ / kg product) |
|---|---|---|
| Cement | 0.707 | 0.067 |
| MS | 0.024 | 0.400 |
| CSt: No I | 0.004 | 0.006 |
| CSt: No il | 0.004 | 0.006 |
| es | 0.004 | 0.006 |
| NS | 0.009 | 0.009 |
| Water | 0.0003 | 0.001 |
| SP | 1.880 | 0.600 |
| PPF | 3.430 | 6.000 |
| Steel Mesh | 1.990 | 1.000 |

For the cost and environmental impact calculations, first volume of concrete required to produce 1 $m^2$ pavement was calculated for each mixture by using the thickness requirements given in Table 4.38 and cost and environmental impact of concrete mixtures for unit volume (given in Table 4.40), and resulting values were presented in Table 4.41.

Table 4.41 represents that while increasing the cost (up to 35. 1%), the use of fibers reduces the CE (up to 20.9%) caused by the materials used. Besides, in line with the reduced thickness requirements (see Table 4.38), use of modified mixing methodology was found to decrease both cost and CE (up to 6.0%) compared to those prepared with standard mixing methodology.

Table 4.40. Cost and CE of the unit volume (1 $m^3$) of concrete.

| Mixture Name | CE (kg C02-eq) | Cost ($) |
|---|---|---|
| Control | 257.7 | 35.7 |
| MS-0-Std | 273.8 | 63.1 |
| MS-0-Mod | 273.8 | 63.1 |
| MS-2-Std | 269.2 | 65.5 |
| MS-2-Mod | 269.2 | 65.5 |
| MS-4-Std | 264.6 | 67.8 |
| MS-4-Mod | 264.6 | 67.8 |

Table 4.41. Cost and CE of unit pavement area (1 $m^2$) for plain and FRC mixtures.

| Mixture Name | Cost ($/$m^2$) | Change (%) in Cost Compared to Control | Change (%) in Cost Compared to Standard Mixing | CE (kg $CO_2$-eq /$m^2$) | Change (%) in CE Compared to Control | Change (%) in CE Compared to Standard Mixing |
|---|---|---|---|---|---|---|
| Control | 10.1 | - | - | 62.9 | - | - |
| MS-0-Std | 13.7 | 35.1 | - | 59.4 | -5.5 | - |
| MS-0-Mod | 12.9 | 27.0 | -6.0 | 55.9 | -11.2 | -6.0 |
| MS-2-Std | 13.6 | 34.4 | - | 56.0 | -11.0 | - |
| MS-2-Mod | 12.9 | 27.3 | -5.3 | 53.0 | -15.7 | -5.3 |
| MS-4-Std | 13.5 | 33.2 | - | 52.7 | -16.3 | - |
| MS-4-Mod | 12.8 | 25.9 | -5.5 | 49.7 | -20.9 | -5.5 |

## 4.6. Structural Behavior of Recycled Aggregate Concrete for Pavements

### 4.6.1. Mixtures

Control concrete mixture (CStC) was produced using 321.4 kg/$m^3$ Portland cement, 128.6 kg/$m^3$ slag, 85.05 kg/$m^3$ and 693.25 kg/$m^3$ natural and crushed sand, respectively, 476.61 kg/$m^3$ No-1 and No-II crushed stone each and 212.14 kg/$m^3$ water at a w/c of 0.50. in line with the recommendation by Lee et al. [240] for the optimum cement replacement ratio of slag, 40% of cement, by weight, was replaced by slag in

the concrete mixture with a total cementitious material content of 450 kg/m$^3$. The cement equivalence factor of 0.8 for slag. The control concrete was designed to have a compressive strength of 40-50 MPa. Four recycled aggregate concrete mixtures were produced by volume replacing both the No-1 and No-11 crushed stone coarse aggregates in the control concrete by recycled aggregates, which were used as plain (RBA, RCA) and surface treated (TRBA, TRCA) by slag slurry as given in Table 4.42. A sufficient amount of SP was added to get a slump of 18 ± 2 cm.

To minimize the slump loss due to the high water absorption of the recycled aggregates, they were first saturated in water for 24 hours and then surface dried on large sieves for 1 hour. Concrete mixtures of CStC, RBAC and RCAC were cast according to ASTM C192 [179]; however, a modified concrete mixing method as given in Figure 4.25 was followed to cast TRBAC and TRCAC mixtures in reference to the previous studies [130,241,242].

Table 4.42. Mixture ingredients for concrete mixtures (kg/m$^3$).

| Ingredients | Concrete Series | | | | |
|---|---|---|---|---|---|
| | CStC | RCAC | TRCAC | RBAC | TRBAC |
| CemenLA | 321.4 | 321.4 | 321.4 | 321.4 | 321.4 |
| Slag | 128.6 | 128.6 | 128.6 | 128.6 | 128.6 |
| CSt: No LA | 476.6 | - | - | - | - |
| CSt: No ILA | 476.6 | - | - | - | - |
| RCA:Nol | - | 423.7 | 423.7 | - | - |
| RCA: No II | - | 429.0 | 429.0 | - | - |
| RBA:Nol | - | - | - | 367.2 | - |
| RBA: No II | - | - | - | 370.7 | - |
| NS_A | 85.1 | 85.1 | 85.1 | 85.1 | 85.1 |
| CS_A | 693.3 | 693.3 | 693.3 | 693.3 | 693.3 |
| Water | 212.1 | 212.1 | 212.1 | 212.1 | 212.1 |

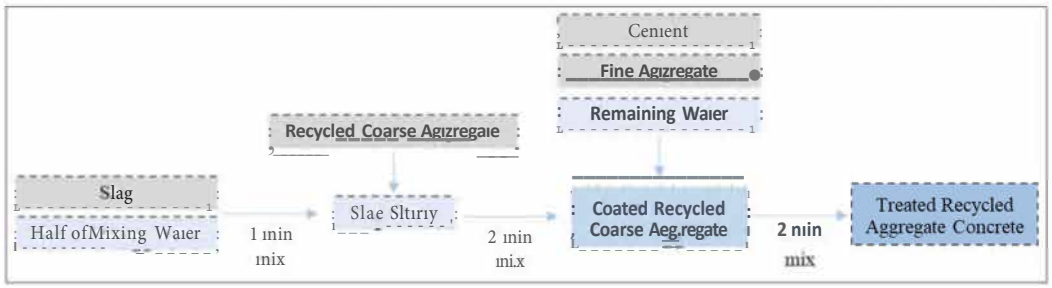


Figure 4.25. Modified mixing method for the production of treated recycled aggregate concrete.

### 4.6.2. Fresh State Properties

eoncrete mixes were cast by using a SP at the required dosage for achieving a slump of 18±2 cm. The highest amount of SP, by weight of cementitious material, was used to get the target slump value for e s t e (0.85%) followed by R e A e (0.75%) and R B A e (0.65%) that may be attributed to the fact that e S t has the lowest roundness with the highest flakiness index followed by R e A and RBA. The higher the flakiness index, the greater the surface area to volume ratio and so the water requirement to produce workable concrete. eoncrete mixes were workable and cohesive, and segregation was not observed. When R e A and RBA totally replaced the e s t, the unit weight of the concrete series decreased from 2410 kg/m$^3$ to 2260 kg/m$^3$ and 2120 kg/m$^3$, respectively. There was no change in the fresh unit weight of T R B A e and T R e A e due to the change in the concrete production process. Replacing the crushed stone coarse aggregate fully with recycled aggregates reduced the fresh density of the concrete up to 12%, whereas compressive strength values conformed to the limitation for structural use.

### 4.6.3. Hardened State Properties

eompressive strength, modulus of elasticity and flexural strength values of all mixtures were given in Table 4.43, where values given in the parenthesis shows the standard deviation of test results. eompressive strength and modulus of elasticity test results presented in the table for e s t e, R e A e, T R e A e, R B A e, and T R B A e were

given for 12, 13, 14, 14, and 13 specimens respectively. On the other hand, flexural strength tesr results were given for 12 specimens for all the mixtures.

Based on Table 4.43 eompressive strength of concrete mixtures decreased from 45.51 MPa for control concrete (este) and varied between 33.91 and 27.61 MPa for the recycled aggregate concrete mixtures due to the higher porosity and lower strength of the recycled aggregates. Among the recycled aggregate concrete mixtures, higher compressive strength was obtained with TReAe followed by ReAe, TRBAe and RBAe having the performance of 75, 69, 66 and 61 % of este, respectively. Similarly, modulus of elasticity of concrete mixtures decreased from 35.51 GPa for este and varied between 27.14 and 23.44 GPa for the recycled aggregate concrete mixtures. Higher modulus of elasticity was obtained with TReAe followed by ReAe, TRBAe and RBAe having the performance of 76, 74, 69 and 66% of este, respectively. Flexural strength of concrete mixtures decreased from 6.93 MPa for este and varied between 4.70 and 3.96 MPa for the recycled aggregate concrete mixtures. Higher flexural strength was obtained with TReAe followed by ReAe, TRBAe and RBAe having the performance of 68, 66, 61 and 57% of este, respectively.

Table 4.43. Mechanical properties of concrete mixtures.

| Concrete Mixtures | Compressive Strength | | Modulus of Elasticity | | Flexural Strength | |
|---|---|---|---|---|---|---|
| | Average (MPa) | Change (%) | Average (GPa) | Change (%) | Average (MPa) | Change (%) |
| CStC | 45.51 (3.87) | - | 35.51 (0.90) | - | 6.93 (0.63) | - |
| RCAC | 31.42 (3.17) | 31 | 26.2 (1.16) | 26.2 | 4.54 (0.28) | 34.5 |
| TRCAC | 33.91 (2.95) | 25.5 | 27.14 (0.82) | 23.6 | 4.7 (0.27) | 32.2 |
| RBAC | 27.61 (2.35) | 39.3 | 23.44 (0.79) | 34.0 | 3.96 (0.20) | 42.9 |
| TRBAC | 29.85 (1.93 | 34.4 | 24.41 (0.67) | 31.3 | 4.22 (0.21) | 39.1 |

### 4.6.4. Structural Analyses

Structural analyses of the pavements were realized in two parts as analyses for constant slab thickness of 15 cm and analyses to determine the slab thickness required to resist 1 million load repetition.

Material properties used in design are given in Table 4.44. It should be noted here that to obtain flexural strength values for 4-point bending test configuration (from 3-point bending test results), measured flexural strength values were modified based on the [243] recommendation (4-point flexural strength = measured 3-point flexural strength / 1.20). In addition, LTE (%) values are given foran effective slab thickness of '11.25 cm (15 x 0.75 cm)', these values are modified to use in variable slab thicknesses used in the second part (required thickness for 1 million load repetition) of the analyses.

As the last column of the Table 4.44 illustrates, significantly decreased LTE (%) values were found for recycled aggregate concrete mixtures (≅ 22% reduction for RCAC, ≅ 38% reduction for RBAC). Since the largest aggregate sizes for control and recycled aggregate mixtures are kept same (16 mm), reduced LTE (%) values for recycled aggregate concrete mixtures can be attributed to the lower Los Angeles abrasion and higher shrinkage (that increases the crack width) values of recycled aggregate mixtures compared to virgin ones.

4.6.4.1. Results for Constant Pavement Thickness of 15 cm. For all of the concrete mixtures tested in this study, stress and deflection analysis was done for a constant thickness of 15 cm. The analyses were done for single and tandem axle load cases and for two different foundation support conditions, as 100 and 200 MPa/m. Illustrations for the stress and deflection analysis results are given in Figure 4.26, and maximum stress and defl.ection values for all the cases were given in Table 4.45.

Table 4.45 shows that maximum stress and defl.ection values were decreased with increasing stiffness of the foundation that supports the pavement. Additionally, increasing foundation stiffness has a higher effect for maximum deflection values (57 - 64 %), compared to maximum stress values (12 - 15%). Furthermore, for the axle load values considered in the analysis (100 kN for single axle and 180 kN of tandem axle), significantly lower maximum stress values were found for tandem axle load cases, but similar maximum deflection values were found for both types of the axle loads.

Table 4.44. Material properties used in analyses.

| eoncrete Series | Modulus of Elasticity (GPa) | Fresh State Density (kg/m$^3$) | Flexural Strength (MPa) | Shrinkage Strain (SS) (x10-6) | erack Width (SSx4500) (mm) | LTE (%) |
|---|---|---|---|---|---|---|
| este | 35.51 | 2410 | 5.78 | 300 | 1.35 | 85.1 |
| ReAe | 26.20 | 2260 | 3.78 | 450 | 2.03 | 66.5 |
| TReAe | 27.14 | 2260 | 3.92 | 450 | 2.03 | 66.5 |
| RBAe | 23.44 | 2120 | 3.30 | 600 | 2.7 | 52.5 |
| TRBAe | 24.41 | 2120 | 3.52 | 600 | 2.7 | 52.5 |

The results given in Table 4.45 also show that the use of different concrete mixtures results in different maximum stress and maximum deflection values. Maximum stress values for both RCAC and RBAC mixtures were 5-8 % lower, respectively, compared to CStC mixture. On the other hand, maximum deflection values were found to be 21-38 % higher for the recycled aggregate concrete mixtures. Additionally, slight increase in maximum stress and a slight decrease in maximum deflection values were found for treated RCAC and RBAC mixtures, with respect to untreated versions. In the previous studies [46,105], similar results were attributed to decrease in elastic modulus of slab, as decreased stiffness increases the deflection and decreases the stress that occurs in the slab. But, it is worth noting that different joint stiffness (or LTE) values were calculated for different concrete series with different mixture ingredients. Therefore, the overall results commented here are due to the combined effect of change in both slab and joint stiffness (or LTE). Although, decrease in maximum stress value is advantageous for the design in terms of fatigue failure analysis, increase in maximum deflection has an inverse impact on the design for faulting (erosion) failure analysis. Additionally, the effect of thermal gradient on the stress calculations were not considered in this study to simplify the analyses and evaluation of the results. Similar, higher and lower thermal expansion coefficient values were reported in previous studies for recycled aggregate concrete mixtures compared to virgin aggregate ones [244-246]. It is worth noting here that pavement stress values are increasing with an increased thermal expansion coefficient of pavement material [246,247].

Table 4.45. Stress and deflection values for 15 cm slab thickness.

| Concrete Series | Single Axle (SA) | | | | Tandem Axle (TA) | | | |
|---|---|---|---|---|---|---|---|---|
| | k = 100 MPa/m | | k = 200 MPa/m | | k = 100 MPa/m | | k = 200 MPa/m | |
| | Max Stress (MPa) | Max Deflection (mm) | Max Stress (MPa) | Max Deflection (mm) | Max Stress (MPa) | Max Deflection (mm) | Max Stress (MPa) | Max Deflection (mm) |
| CStC | 3.33 | 0.70 | 2.89 | 0.44 | 2.45 | 0.66 | 2.15 | 0.40 |
| RCAC | 3.14 | 0.85 | 2.72 | 0.54 | 2.31 | 0.80 | 2.05 | 0.49 |
| TRCAC | 3.16 | 0.84 | 2.74 | 0.53 | 2.32 | 0.79 | 2.06 | 0.48 |
| RBAC | 3.07 | 0.96 | 2.66 | 0.61 | 2.26 | 0.89 | 2.00 | 0.55 |
| TRBAC | 3.09 | 0.95 | 2.68 | 0.61 | 2.27 | 0.89 | 2.02 | 0.55 |

Maximum stress and maximum deflection values discussed above are important parameters that represent the structural behaviour of pavement slab. On the other hand, in the design procedures, instead of these two parameters, stress ratio (SR) (applied flexural stress/flexural strength) and power (P) (rate of work) parameters are used for the fatigue and faulting analysis [72, 84]. Therefore, SR and P values are alsa calculated in this part, and presented in Figure 4.27 and Figure 4.28 respectively, for all of the mixtures and loading cases. As previously explained, the SR parameter includes the effect of not only the flexural stress occurring in the slab but alsa the flexural strength of the pavement material. On the other hand, the P parameter includes the effect of maximum deflection and pavement support characteristics.

As stated above, due to their lower stiffness values, lower maximum stress values are found for recycled aggregate mixtures, and it is an advantage for the fatigue design. But, Figure 4.27 clearly demonstrates that for all types of the recycled aggregates higher SR (flexural stress / flexural strength) values were found for recycled aggregate concrete mixtures. Therefore, in terms of fatigue failure analysis, the effect of decrease in flexural strength was found to be higher compared to the effect of decrease in maximum stress. Furthermore, it can be seen from Figure 4.28 that higher P values were obtained for recycled aggregate concrete mixtures, and the amount of increase in the P value (with respect to CStC mixture) is found to be higher for RBAC mixtures. As an addition, for the treated recycled aggregate mixtures (TRCAC and TRBAC) slightly decreased SR and P values were found, compared to their untreated versions (RCAC and RBAC).

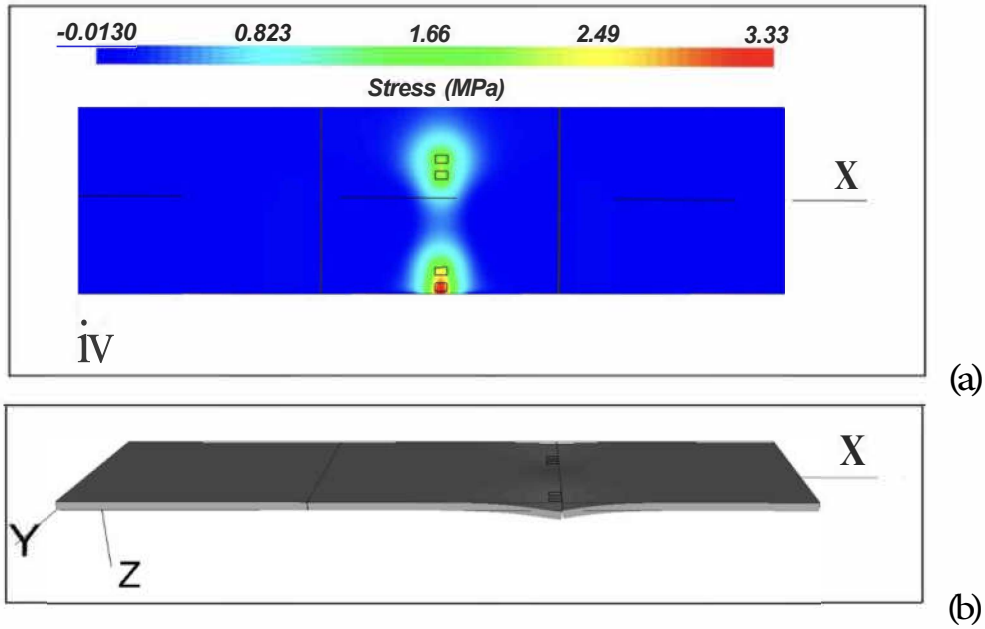


Figure 4.26. Results for (a) stress (at the bottom plane of the concrete slab), (b) deflection (at the construction joint) analyses of 15 cm CStC slabs under 100 kN of dual wheel single axle loadings (for 100 kN/m support stiffness) (not to scale).

When Figure 4.27 and Figure 4.28 are examined together, it can be said that increase in foundation support value decreases both the SR and P. As previously stated, the effect of increase in foundation support was found higher for maximum defl.ection, compared to maximum stress.

On the contrary, when the foundation support increased from 100 MPa/m to 200 MPa/m, the amount of decrease in SR values was found to be higher (13-15%), compared to decrease in power values (3-10%), depending on the mixture and loading condition. Based on the results, an increase in foundation stiffness was found more pronounced for fatigue failure, compared to faulting failure.

4.6.4.2. Required Thicknesses for 1 Million Load Repetition. in this part, pavement thickness required to resist 1 million cycles of single or tandem axle loadings are determined and presented in Table 4.46. Results given in Table 4.46 show that depending on the type of the load and support condition, pavement thickness required to resist 1 million cycles of load changes from 12.5 cm to 23.0 cm.

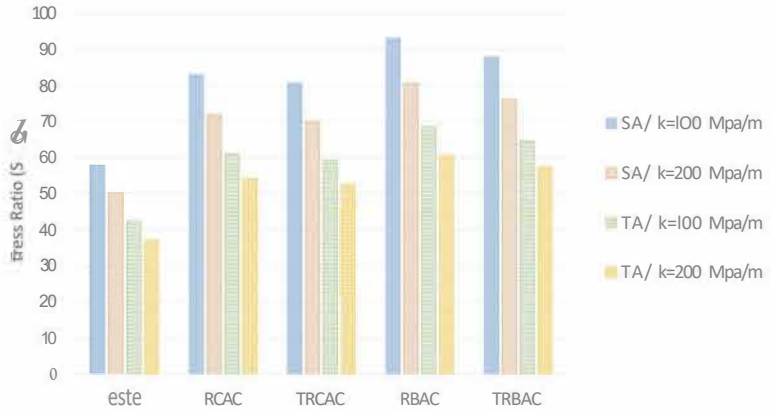


Figure 4.27. Stress ratio (SR) values for 15 cm slab thickness.

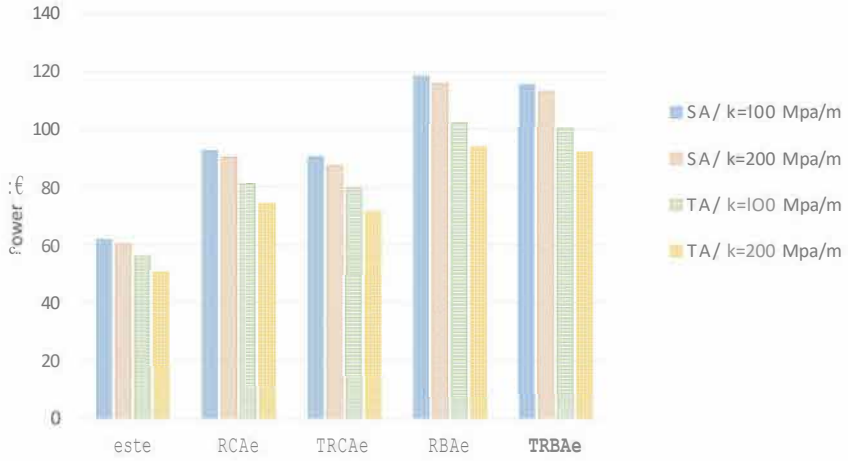


Figure 4.28. Power (P) values for 15 cm slab thickness.

Compared to control mixture, recycled concrete aggregate mixtures require 10-40 % larger pavement thickness to resist 1 million cycles of axle load applications. Additionally, a higher (20 - 40 %) increase in the required pavement thickness was found for RBAC mixtures compared to (10 - 30 %) increase in RCAC mixtures. On the other hand, negligible amount of decrease in required pavement thickness (both for fatigue and faulting failure cases) was found for treated recycled aggregate concrete mixtures, which can be attributed to slight increase in flexural strength (advantageous for fatigue failure analysis) and modulus of elasticity (advantageous for faulting failure analysis) obtained with slurry treatment.

Table 4.46. Required thickness (cm) values to resist 1 million cycle of single and tandem axle loads.

| Concrete Series | Single Axle (SA) | | | | Tandem Axle (TA) | | | |
|---|---|---|---|---|---|---|---|---|
| | k = 100 MPa/m | | k = 200 MPa/m | | k = 100 MPa/m | | k = 200 MPa/m | |
| | Fatigue | Faulting | Fatigue | Faulting | Fatigue | Faulting | Fatigue | Faulting |
| CStC | 16.5 | 16.5 | 15.0 | 16.5 | 13.5 | 16.5 | 12.5 | 15.5 |
| RCAC | 21.5 | 19.0 | 19.5 | 18.5 | 17.5 | 18.5 | 16.0 | 17.5 |
| TRCAC | 21.0 | 18.5 | 20.0 | 18.5 | 17.0 | 18.5 | 15.5 | 17.5 |
| RBAC | 23.0 | 20.0 | 21.0 | 20.0 | 19.0 | 20.0 | 17.0 | 19.0 |
| TRBAC | 22.5 | 20.0 | 20.5 | 19.5 | 18.5 | 20.0 | 16.5 | 19.0 |

For the single axle load case and CStC mixture, thickness requirement for faulting was found similar to the thickness requirement for fatigue. But for the other cases of single axle loading, the thickness requirement to allow 1 million cycles of load repetition was higher for the fatigue case. However, for the tandem axle loading case, higher thickness values were found for the faulting compared to fatigue case. Therefore, for the considered design cases, tandem axle loading configuration was found to be more critical for faulting analysis and single axle loading configuration was found to be more damaging for fatigue failure analysis, which was also stated in previous reports [72,105].

Additionally, as in the 15 cm constant thickness case, the effect of increase in foundation stiffness was found to be higher for the fatigue failure analysis case for almost all of the mixtures compared to faulting failure analysis case.

In the end, required thickness values given in Table 4.46, for the single axle loading and 100 MPa/m foundation support case, were used to calculate the amount of materials required to produce 1 lane and 1 km of pavement. First, required thickness values given for fatigue and faulting analysis cases were compared for each mixture, and higher one was used in calculations. Then, in order to determine the amount of concrete required to produce 1 km (1 lane) pavement, these values were multiplied by the length (1 km) and width (3.6 m) of the pavement for each of the mixtures, and the results were given in Table 4.47.

Table 4.47. Materials required to produce 1 lane and 1 km pavement (tons).

| Ingredients | | CStC | RCAC | TRCAC | RBAC | TRBAC |
|---|---|---|---|---|---|---|
| 1 | Cement | 190.9 | 248.8 | 243.0 | 266.1 | 260.3 |
| 2 | Slag | 76.4 | 99.5 | 97.2 | 106.5 | 104.2 |
| 3 | No-I (4-8 mm) | 283.1 | 327.9 | 320.3 | 306.9 | 300.3 |
| 4 | No-II (8-16 mm) | 283.1 | 332.0 | 324.3 | 304.0 | 297.4 |
| 5 | Crushed Sand | 411.8 | 536.6 | 524.1 | 574.0 | 561.5 |
| 6 | Natural Sand | 50.5 | 65.8 | 64.3 | 70.4 | 68.9 |
| 7 (3+4) | Total Coarse | 566.2 | 659.9 | 644.6 | 611.0 | 597.7 |
| 8 (5+6) | Total Fine | 462.3 | 602.4 | 588.4 | 644.4 | 630.4 |

As seen in Table 4.47, the amount of each ingredient, required to resist the same number of load repetition, was found higher for recycled aggregate concrete mixtures, compared to virgin aggregate mixtures, which can be attributed to increase in the required thickness values. In this respect, a huge amount of virgin coarse aggregate can be replaced with recycled aggregates, which protects both natural raw materials and landfill areas. However, recycled concrete mixtures also require a higher amount of virgin fine aggregates. Besides, the use of recycled concrete pavements, which need more cement for the similar performance, might be disadvantageous, since the significant portion of the environmental impact of concrete stems from the cement used in the production of concrete [46,248].

Additionally, cement is the ingredient of concrete that contributes most to the material cost. To illustrate, for 2020, while the cost of cement in the U.S.A. was reported as 124 $/tonne, it was given as 12.2 $/tonne and 9.6 $/tonne for crushed stone and sand gravel (average) aggregates, respectively [228]. Prices given for the U.S. demonstrate that the increase in the use of cement considerably increases the total cost of concrete. On the other hand, since production of recycled aggregates from construction wastes also requires a considerable amount of effort, it only marginally decreases the aggregate cost, currently. As Table 4.47 illustrates, while reducing the virgin aggregate requirement, recycled aggregate concrete pavements require higher amounts of cement to achieve similar structural performance with virgin aggregate

concrete. Therefore, for the current situation, use of recycled aggregate can also be disadvantageous in terms of cost.

In contrast, due to the scarcity of earth resources and increasing demand of the construction industry, virgin aggregate costs are increasing in most of the countries. For example, between 2010 and 2020, 42% and 31 % increase in crushed stone and sand gravel (average) costs were reported [228], respectively. Besides, there is a tendency to increase in aggregates prices for the upcoming years, which will make recycled aggregates more attractive in terms of cost in the future.

To sum up, despite the presented environmental impact and cost disadvantages of recycled concrete pavements that occur due to the requirement of higher amounts of cement to achieve similar performance, recycled aggregate concrete pavements can still be a viable alternative for countries with limited natural resources and landfills. Additionally, results given here are valid for the recycled coarse aggregate types and amounts used in this study, as well as applied treatment method. Different results could be obtained with different recycled aggregate sources and amounts, as well as application of different treatment methods explained in the introduction part. To illustrate the point, Shi et al. [154] compared the mechanical properties and field performance of recycled and virgin aggregate concrete mixtures (for similar slab size (3.5 m x 4.6 m) and replacement level with current study), and they reported much closer performance parameters (compared to current study) for those two kinds. In another study [249] that compares the field performance of recycled and virgin aggregate pavements, considerably decreased performances for the most of the recycled aggregate concrete pavement sections were reported; however, in the study comparable performances for some other types of aggregates. These kinds of conflicting results can be mainly attributed to the differences in the properties of the recycled aggregates used.

Table 4.48. Ingredients of the mixtures for 1 $m^3$ concrete.

| Ingredients (kg) | NAC | RAC - 50 | RAC - 100 |
|---|---|---|---|
| Cement | 380.0 | 380.0 | 380.0 |
| CSt: No LA | 412.3 | 206.2 | - |
| CSt: No ILA | 618.5 | 309.2 | - |
| RA:Nol | - | 183.3 | 366.5 |
| RA: No il | - | 278.3 | 556.6 |
| cs_A | 558.1 | 558.1 | 558.1 |
| NS_A | 272.8 | 272.8 | 272.8 |
| Water | 171.0 | 171.0 | 171.0 |

## 4.7. Joint Performance of Recycled Aggregate Concrete for Pavements

### 4.7.1. Mixtures

3 different concrete mixtures were designed in this study as follows: one control mixture without recycled aggregates (NAC), one mixture with 50% recycled coarse aggregate (RAC - 50), and one mixture with 100% recycled coarse aggregate (RAC - 100). For all the concrete mixtures, fine aggregates were used as 100% natural aggregates (CS and NS). Compositions of concrete mixtures corresponding to unit volume (1 $m^3$) of concrete were given in Table 4.48.

### 4.7.2. Physical Tests

Average values of density, absorption and porosity with the standard deviations were presented in Table 4.49 for 6 specimens. Increasing the replacement amount of virgin coarse aggregate with recycled aggregates increased the porosity (up to 40.5%) and absorption (up to 51.8%) while it decreased the density (up to 7.1%). in terms of mentioned physical properties, RAC-100 was found to be more disadvantageous than RAC-50 compared to NAC. The results were found consistent with the ones given in the literature [250-252], and they might be attributed to the lower densities and porous structures of recycled aggregates used in the mixtures (RCA-50 and RCA-100).

Table 4.49. Average density, absorption, and porosity test results.

| Mixture | Absorption after immersion (%) | Bulk density, dry ($g/cm^3$) | Bulk density after immersion ($g/cm^3$) | Apparent density ($g/cm^3$) | Porosity (%) |
|---|---|---|---|---|---|
| NAC | 5.38 (0.16) | 2.32 (0.00) | 2.44 (0.00) | 2.65 (O.Ol) | 12.60 (0.36) |
| RAC - 50 | 6.82 (0.19) | 2.23 (0.02) | 2.38 (O.Ol) | 2.63 (O.Ol) | 15.31 (0.35) |
| RAC - 100 | 8.16 (0.18) | 2.15 (O.Ol) | 2.33 (O.Ol) | 2.61 (O.Ol) | 17.70 (0.30) |

### 4.7.3. Abrasion Resistance

The average mass loss values of the concrete mixtures were presented in Table 4.50, along with the standard deviations and relative increment (%) in mass loss compared to the control mixture (NAC). Even though a slight increase in mass loss (as an indication of abrasion resistance) was found for RAC-50 compared to NAC, a considerable increase in the mass loss was found for RAC-100. Moreover, to see whether the obtained differences in abrasion values are statistically significant, t-tests were performed to compare the results. As a result of t-tests, p-values for the pairwise comparisons of NAC vs. RAC-50, NAC vs. RAC-100, and RAC-50 vs. RAC-100 were found as 0.39, 0.02, and 0.03, respectively. The results represent that though the difference in mass loss between NAC and RAC-50 is not statistically significant ($0.39 > 0.05$), the difference is significant for the pairwise comparisons of NAC vs. RAC-100, as well as RAC-50 vs. RAC-100. Therefore, partial replacement of coarse virgin aggregates with recycled aggregates seems to be a good alternative to reduce the loss in abrasion resistance.

Table 4.50. Abrasion resistance test results.

| Mixture | Mass Loss (%) | Change (%) |
|---|---|---|
| NAC | 11.4 (0.5) | - |
| RAC - 50 | 11.7 (0.4) | 3.1 |
| RAC - 100 | 12.9 (0.5) | 13.8 |

Table 4.51. Compressive strength, modulus of elasticity, and flexural strength test results.

| Mixture | Compressive Strength | | Modulus of Elasticity | | Flexural Strength | |
|---|---|---|---|---|---|---|
| | Average (MPa) | Reduction (%) | Average (GPa) | Reduction (%) | Average (MPa) | Reduction (%) |
| NAC | 53.1 (0.7) | - | 30.1 (0.6) | - | 7.08 (0.45) | - |
| RAC - 50 | 46.7 (1.4) | 12.1 | 27.9 (0.8) | 7.3 | 6.37 (0.07) | 10.0 |
| RAC - 100 | 41.3 (1.5) | 22.2 | 26.0 (0.7) | 13.6 | 5.58 (0.18) | 21.2 |

### 4.7.4. Quasi-Static Test Results

Compressive strength, modulus of elasticity, and flexural strength values, all as an average of the results for three specimens, were given in Table 4.51, where values given in the parenthesis shows standard deviation of the results, and reduction (%) values were given compared to control (NAC) mixture. The standard deviation and relative strength reduction (%) values compared to the control mixture (NAC) were also presented. As explained above, Poisson's ratio was also measured for each mixture on one of the cylindrical specimens, and the values were found as follows: 'NAC=0.21', 'RAC-50 = 0.20', and 'RAC-100 = 0.21'.

Results in Table 4.51 represent that the mechanical performance parameters measured in the mixtures were found lower for the mixtures that include recycled aggregates, which is consistent with the relevant studies [253-255]. The reduction in mechanical performance was double for RAC-100 compared to RAC-50. in addition, the reduction in compressive and flexural strength values due to replacing virgin coarse aggregates with recycled aggregates was found to be higher than that in modulus of elasticity.

### 4.7.5. Cyclic Shear Tests

Peak differential displacement, the difference between the maximum and minimum displacement (average of 4 LVDTs measurements) measured in a cycle, is an

indication of the post-cracking shear performance of concrete. Basically, lower peak differential displacements under the same load magnitude are associated with better load transfer, as it means that the displacement that occurs under the same load magnitude is low. Since '±3.2 kN' was applied in each cycle in this study, peak differential displacement in a cycle was calculated as the difference between the average of 4 LVDTs measurements at '+3.2 kN' and '-3.2 kN'.

Cycle number - peak differential displacement relationships for all the crack widths tested in this study (0.2 mm, 0.5 mm, 1.0 mm, and 1.5 mm) were presented in Figure 4.29 for NAC, RAC-50, and RAC-100 mixtures. Figure 4.29 represents that for all the crack widths and concrete mixtures increase rate in the peak differential displacement (as an indication of shear degradation rate) is higher at the beginning of the cyclic shear load application compared to following cycles. Besides, the rate of change decreases in a few cycles, and it stabilizes over time and goes to 500 cycles at a constant rate. Similar tendencies for the post-cracking cyclic shear degradation were also reported in Thompson [112] and Arnold et al. [113]. Additionally, despite some slight differences, the change in peak displacement values (an indicator of shear degradation rate) was found similar for both initial and subsequent cycles for control and recycled aggregate concrete mix up to 500 cycles (maximum number of cycles applied in this study). However, though it is not covered in this study, lower abrasion resistance of recycled aggregates may lead to early failure of recycled aggregate concrete specimens compared to virgin ones. Since this is an important issue in terms of pavement joint life, further studies are required to test the hypothesis and to determine the extent of the difference in the number of cycles for failure numerically.

Moreover, average peak displacement values obtained at 500 cycles were given in Figure 4.30 which shows the dependence of the post-cracking shear performance on the width of the crack and aggregate type used. As seen in Figure 4.30, considerable increments in peak differential displacements were obtained with increasing crack width. In addition, for all the crack widths, the highest average peak differential displacements were obtained for RAC-100, while the lowest values were obtained for NAC.

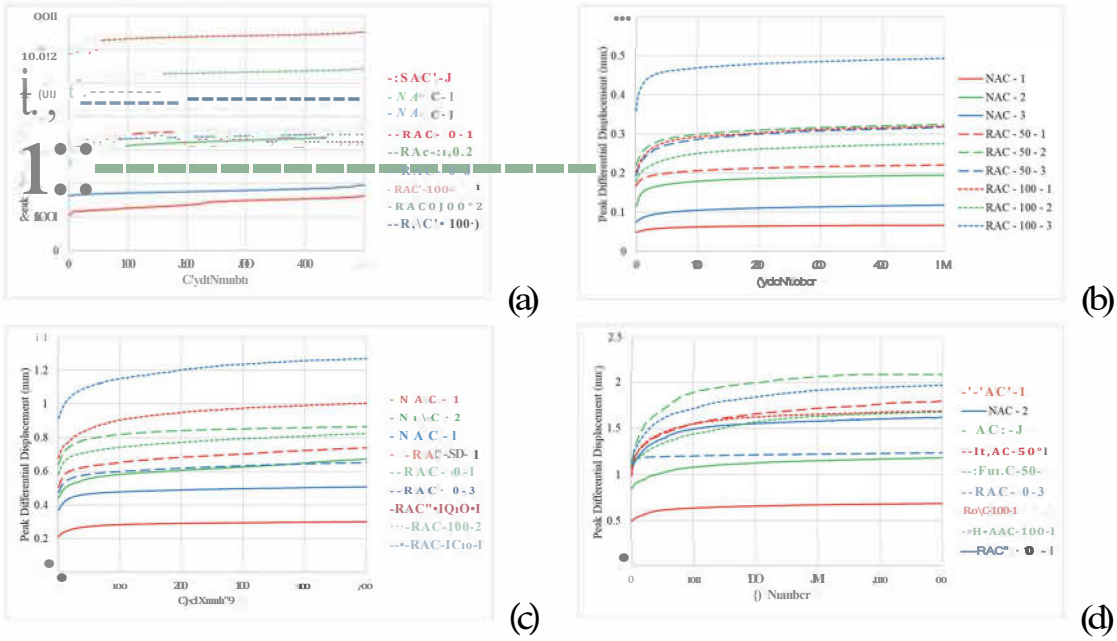


Figure 4.29. Cycle number - peak differential displacement relationships for different crack widths up to 500 cycles: (a) 0.2 mm, (b) 0.5 mm, (c) 1.0 mm, (d) 1.5 mm.

Additionally, regression analyses were done to determine the relationship between crack width and peak differential displacement at 500 cycles for all concrete mixtures. The resulting regression curves were given together with their equations in Figure 4.31, which shows the effect of crack width and a varying amount of recycled aggregate usage on the peak differential displacement of concrete mixtures. it can also be inferred from the figure that increasing the amount of recycled aggregate increases the peak differential displacement of concrete mixture, and crack width has a considerable impact on the obtained displacement values.

To compare the obtained average values and to see whether the difference obtained for 500 cycles is statistically significant or not, t-tests were also carried out, and the resulting p-values (indicate the significance of the obtained differences) were presented in Table 4.52. Given values represent that for most of the crack widths, the differences in peak differential displacement values of different concrete mixtures were statistically insignificant except for the pairwise comparison of the concrete mixtures of NAC and RAC-100. Üne of the main reasons behind this outcome is the large variation of the test results, making it hard to distinguish the obtained average values.

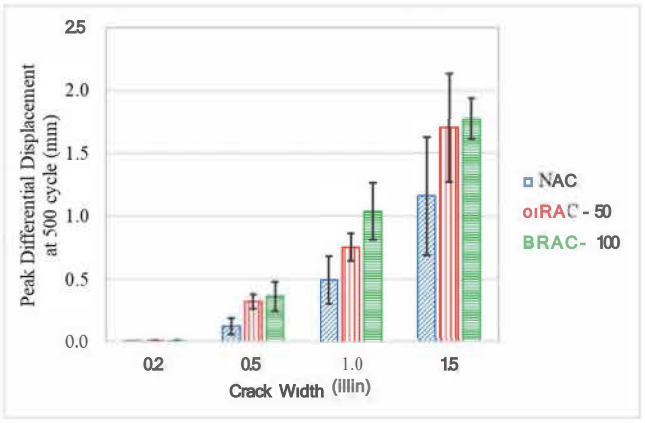


Figure 4.30. Average peak differential displacement at 500 cycles for different crack widths.

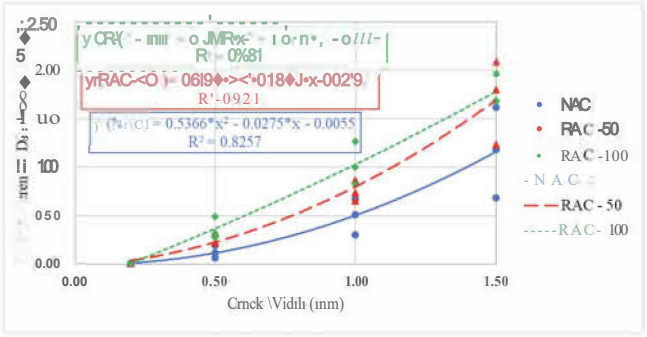


Figure 4.31. Crack width - peak differential displacement regression equations.

Testing a higher number of test specimens might be beneficial to distinguish the concrete mixtures for further studies. However, testing a single concrete specimen requires a considerable amount of time and afford with the test method used in this study. Therefore, the development / use of alternative test methods might be recommended for further studies.

Furthermore, in order to represent peak differential displacement values obtained at 500 cycles in a single equation as a function of crack width and recycled aggregate replacement level, linear model fitting tool (fitlm(independent variables (crack width and replacement amount of recycled aggregates), dependent variable (peak differential displacement))) of Matlab [231] was used and equation is obtained as

$$\hat{O}_{peak,e} = - 0.70717 + 0.46742 \times e^{CW} + \frac{0.34876 \times RA}{100}, \quad (4.3)$$

where $\hat{O}_{peak,e}$ shows estimated peak differential displacement, $CW$ represents crack width (mm), and $RA$ is the ratio ofrecycled coarse aggregates to total coarse aggregates in percent (between O - 100). Besides, the coefficient of determination ($R^2$), which indicates the percentage of the variance in the dependent variable (where $\hat{O}_{peak,e}$ shows estimated peak differential displacement, $CW$ represents crack width (mm), and $RA$ is the ratio of recycled coarse aggregates to total coarse aggregates in percent (between O - 100).

Table 4.52. P-values obtained from t-tests for different comparison cases.

| Compared Concrete Series | Crack Widths (mm) | | | |
|---|---|---|---|---|
| | 0.2 | 0.5 | 1.0 | 1.5 |
| NAC & RAC - 50 | 0.22 | **0.03** | 0.11 | 0.21 |
| NAC & RAC - 100 | **0.05** | **0.04** | **0.03** | 0.10 |
| RAC - 50 & RAC - 100 | 0.19 | 0.37 | 0.12 | 0.80 |

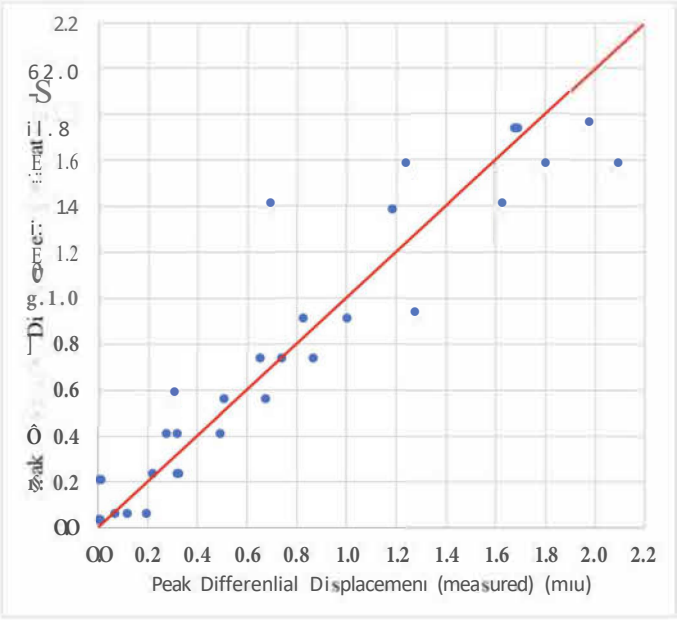


Figure 4.32. Relationship between measured (experimentally) and estimated (using the proposed equation) peak differential displacements.

Moreoever, the coefficient of determination ($R^2$), which indicates the percentage of the variance in the dependent variable ($\hat{O}_{peak,e}$) that can be explained by the inde-

pendent variables *(CW* and *RA)* was obtained as 0.892. The higher the coefficient of determination, the more accurate the estimated equation. According to the literature [256], it can be assumed that the coefficient of determination is sufficiently high and statistically significant; hence the estimated equation can be used to represent the experimentally obtained results with reasonable accuracy. This can be seen in Figure 4.32, which shows the relationship between the experimentally obtained (measured) and estimated (by the equation given above) peak differential displacements, as most of the <lata points fall close to the identity line (y=x).

# 5. CONCLUSIONS AND RECOMMENDATIONS

## 5.1. Variation in Concrete Fatigue Tests

In the scope of the conducted study, monotonic and cyclic 4PBT, as well as DPT were carried out for two different concrete mixtures (W60 and W45). Based on the obtained results, following conclusions were drawn:

- For the monotonic test results, lower variations were obtained for DPT results compared to 4PBT which support the DPT literature.
- According to the analyses carried out for the cyclic test results, though the normal distribution assumption was found questionable for some of the test cases, Weibull distribution fit well for all the cases. For both normal and Weibull distribution assumptions lower variations were obtained for DPT, compared to 4PBT.
- As a result of the conducted t-tests, statistical difference (in terms of the cyclic load performance of tested concrete series) was found for one of the comparison cases (DPT with 75% maximum stress ratio), but no statistical difference was found for the other 3 test cases considered in this study. Better performance obtained for W60 for the mentioned case supports the literature that says the cyclic loading performance of concrete decreases with increasing strength.
- For all the cyclic test cases (two stress levels and two concrete types), average cycle numbers were found lower for DPT compared to 4PBT and the result was attributed to the difference in the cracking mechanisms of these two tests.
- Cyclic creep curves showed that the fatigue failure occurs in 2 and 3 visible stages for DPT and 4PBT, respectively. Observed difference was attributed to different stress distributions occur in the cracking surfaces of these two tests.
- A strong correlation was found between the variation in results and the change in allowable number of repetition with the change in reliability level. Based on the obtained correlation, the amount of change in allowable number of repetition with increasing reliability level was found to increase with increasing variation.

- When the calculated variations were compared with the previous studies on flexural fatigue performance on concrete, considerably better (lower) variation values were found for DPT.

Overall, the presented paper shows that the fatigue performance of concrete under tensile stresses might be measured by cyclic DPT with lower variations compared to 4PBT, which is widely used to examine the tensile fatigue performance of concrete. Reduced variation in the test results leads to two main benefits: reduction in the number of specimens that should be tested to obtain representative model for the fatigue performance of examined concrete, and reduction in the change in number of allowable load repetition for the change in reliability level.

On the other hand, based on the results of the current study, number of cycles that could be resisted for DPT and 4PBT are significantly different from each other, due to the change in cracking mechanisms of those tests. If the fatigue performance of concrete under bending is interested, equations that define the relationship between these cases should be developed to use the results of the cyclic DPT in design. An equation that shows the relationship between cyclic DPT and 4PBT has been presented in this paper by considering the <lata obtained from this study, and importance of doing further studies to check the validity and / or to improve the fitness of the equation has been emphasized. However, without doing these studies cyclic DPT might still be used to compare the fatigue performance of different concrete types (with less specimen compared to cyclic bending test).

Lastly, in the preliminary study carried out, it was noticed that the roughness of the specimen surface and the rotation ability of top loading head might significantly affect the variation of the test results (both lead to eccentricity and stress concentration), especially for the cyclic tests. Therefore, abrasion of the specimen surfaces with suitable abrader and regular lubrication of the rotating top platen (which is also recommended by Colgrove and Chen [69]) have crucial importance to obtain DPT results with lower variations.

## 5.2. Effects of Stress Reversal on Flexural Fatigue Life

Concrete pavements are subjected to reversal tensile stresses due to the changing temperature differential from day to night hours. Even though it is a common issue for concrete pavements and considered in recently published design guides, varying approaches are provided in different design codes which is mainly due to the lack of empirical data. While some design guides reduce the number of allowable cyclic stresses in one direction due to the cyclic stresses applied in the opposite direction, some others not. in this study, a novel beam testing methodology was developed to examine the effect of stress reversal occurs in concrete pavements on the fatigue life of concrete. By using the method developed and ordinary one, the effect of stress reversal on the fatigue life of concrete beams were experimentally measured and the results were discussed. Based on the results of the study following conclusions were drawn:

- The average number of cycles that can be resisted under fatigue loading was found much higher (≒ 5 times) for 75% maximum stress level compared to 85%.
- Weibull distribution function was found suitable for all the cyclic loading data sets obtained in this study, and the number of specimens failed in the first part of the two-way loading was validated the suitability of fitted distribution (approximately 30% of specimens failed under the applied cyclic loads, as expected).
- Due to the cyclic loading applied in the opposite direction (first part of the two-way cyclic loading), average number of cycles that can be resisted was found to decrease 29.8% and 33.4%, for 85% and 75% maximum stress levels, respectively. Similar reduction in the eyde numbers were seen in Wöhler curves prepared (by assuming Weibull distribution) for one-way and two-way loading.
- Considerably higher variation values were found for two-way cyclic loading compared to one-way, and it was hypothesized that the loading applied in the first direction is the source of the increased variation. On the other hand, further studies were recommended to check the validity of proposed hypothesis.
- Based on the experimental results, for all the design cases considered ('6 design cases' = '2 stress ratio' x '3 reliability level') allowable load repetition values

calculated according to IRC 58 [82] and AASHTO MEPDG [83] design guides were found on the unsafe side. Since these guides do not consider the reduction in fatigue performance of concrete in one direction due to cyclic loading applied in the opposite direction, which is found as an outcome of this study. For the latest version ofIRC design guide [84], both safe (for higher reliability levels) and unsafe (for lower reliability levels) values were calculated for allowable number of load repetitions, and the unsafe results were attributed to the inconvenience of linear fatigue damage rate assumption used in IRC 58 [84] approach. Therefore, further studies were recommended to develop new approaches that better represent the effect of stress reversal on the fatigue life of concrete pavements, and to check the validity of obtained results, as well as given comments for different concrete types and design (stress level) cases.

Furthermore, the specimens failed in the first part of the two-way loading were presumably the weakest ones, which might result in use of relatively stronger specimens for the second part of the two-way cyclic loading. On the other hand, lower eyde numbers were measured for them (survived specimens during first part of the two-way loading) which also supports the outcome of the conducted study that emphasize the reduction in cyclic loading performance due to the cyclic loads applied in the opposite direction.

## 5.3. Effectiveness of Fibers in Concrete Pavement Mixtures

As mentioned in the research significance part, this study has been carried out to examine the effect of using macro fibers in varying amounts on the overall performance of concrete pavements, and to investigate the efficiency of fibers in different concrete pavements. In this respect, answers for the following research questions were found in this study:

- How the use of macro fibers in varying amounts affects the performance of concrete pavements (from structural to economic and environmental aspects)?

- How the efficiency of fibers changes when used in different concrete matrices commonly employed for pavement construction?

Based on the results of the carried out experimental and numerical studies following conclusions were drawn:

- For the plain concrete mixtures examined in this study, though mechanical properties of RCC were found similar to NSC, its physical properties were found much closer to HSC mixture, and these results were attributed to the similar water to cement ratios of RCC and HSC. Although the lowest thickness values were obtained for HSC, lowest cost and environmental impact values were found for RCC, which was attributed to the absence of reinforcement and lower cement dosage of RCC mixture.
- For the types and amounts of fibers used in this study, no significant differences were observed for FRC mixtures in terms of strength, stiffness, absorption, and porosity values. On the other hand, higher abrasion resistance and post-cracking flexural performances were found for FRC mixtures.
- RFS ratio values (a good indicator of effectiveness of fibers and a parameter used in thickness design of FRC pavements) for PPF was found similar for all concrete matrices considered in this study (NSC, HSC, and RCC). However, the values were found higher for SF in NSC and RCC mixtures compared to HSC mixture, which shows the dependence of the obtained performance to the concrete matrix properties.
- The use of both SF and PPF leads to a decrease in required thickness values in considerable amounts, based on the post-cracking performance of the mixtures. In line with the obtained post-cracking performance, the amount of decrease in the thickness requirement was found to increase with an increase in the amount of fiber used.

- For the PPF used, decreased emission values were obtained with an increase in the amount of fiber used, but varying results were obtained for SF by changing the fiber amount. Despite the decrease in required pavement thickness, increased material cost values were found for FRC mixtures, and amount of increase in the cost was found to be dependent to not only type and amount of fiber used but also the type of concrete mixture. For all cases, increased material costs were obtained with increasing fiber amount.

In the end, it is worth noting that the cost and environmental impact values reported in this paper are dependent to the sources that are obtained and reported in the text. Cost of the materials may significantly alter from country to country, which may have a considerable impact on the results. Additionally, based on the production procedures and raw materials used, emission values for not only fibers but also cement and aggregates might be changed, and different results can be obtained. However, since this study numerically presents that in which way the use of different types and amounts of fibers impacts the performances of concrete pavement mixtures, and how use of different fiber amounts affects the resulting performances, the results will be very beneficial for the further construction and academic works on FRC pavements. Further studies can be carried out to see how the use of different types of fibers with different raw materials and surface properties may affect the performance of the mixtures, and how local conditions may affect the results.

Furthermore, this study was carried out by using / considering the virgin polypropylene and steel fibers, both require considerable energy and raw materials during their production, resulting in higher cost and environmental impact. On the other hand, considerable improvements in the post-cracking performance of concrete were reported in previous studies for recycled steel and polymeric macro fibers [257-260], which might be considered to further increase the benefit obtained from the fibers, by means of structural performance, cost, and environmental impact. Additionally, material technologies are changing and developing gradually, and the companies are working on strategies to decrease cost and carbon footprint of the materials they provide (consid-

ering environmental issues, carbon taxes, ete.), which in the future will probably result in better overall performance for fiber-reinforced materials.

## 5.4. Effects of Fibers on the Joint Performance of Concrete Pavements

In the scope of this study, 3 different concrete mixtures (PC, FRC - 0.5, and FRC - 1.0) were designed and tested for basic mechanical properties, as well as the post-cracking shear performance. Based on the obtained results following conclusions were drawn:

- Compressive strength, modulus of elasticity, and flexural strength of plain and fiber reinforced concrete mixtures were found very similar, with some marginal changes.
- Increasing post-cracking flexural performance values were found for FRC mixtures with the increasing amount of fiber usage.
- Peak differential displacement values were found to increase with the application of cyclic shear loading, which is an indication of degradation under cyclic loading. However, the rate of degradation was found much higher for a few of initial cycles, compared to following cycles, which is found consistent with the relevant literature.
- Width of the crack was found as an important parameter that affect the shear performance of concrete, and the use of polypropylene fibers with increasing amount was found to improve the shear performance of concrete in each crack widths. Besides, a tendency to increase in shear performance due to addition of fibers was observed with increasing crack widths.
- Due to the large variation of test results, t-test was not able to distinguish the performance obtained for concrete mixtures, for most of the shear performance comparison cases. By emphasizing the difficulty of test method, testing of larger number of specimens to distinguish the concrete series with the employed testing methodology was recommended.

- Based on the experimental results numerical models that define the relationship between crack width and peak differential displacements for all fiber volume ratios (0.0, 0.5, and 1.0 %vol.). Besides, a model was proposed to define the relationship between crack width - fiber amount and peak differential displacement. For all the models, correlation coefficients for measured and estimated values were found reasonably high.

Based on the results obtained for the post-cracking shear tests, it could be said that the use of polypropylene fibers improves the performance of concrete, under shear stress application. It should be noted here that the obtained results, and proposed models are dependent on the properties of fibers and concrete mixtures used in this study. To propose a model that covers various fiber types (in terms of material, length, surface properties) further studies might be carried out. Additionally, the post-cracking shear performance measurements was done by using small-scale specimens, and further studies to validate the results in large scale are needed.

The test method employed in this study is difficult the apply and results in considerable variations, which makes hard to distinguish the performances of concrete mixtures, and suggestion of design guides. Therefore, further post-cracking test methodologies, which are easy to apply and gives less scattered results, might be developed to overcome this problem.

As well as the previous studies carried out in this issue, results of the current study showed that the crack width is an important parameter that affect the post-cracking shear performance of concrete. Since fiber can reduce the crack width in pavement joints due to improved cracking performance (restrain the widening of joint cracks), which might indirectly improve the shear performance of concrete pavements, as emphasized previously in Thompson [112]. Moreover, shrinkage of pavement slabs (in addition to temperature) is one of the largest contributors of the joint crack width, and it was reported in previous studies that the use of fibers might be an efficient way to reduce the shrinkage [261-265]. Therefore, fibers might further improve the

shear performance by reducing crack width caused by shrinkage. it was reported in previous studies [263, 266] that the fibers with low diameters and large lengths are especially effective in controlling shrinkage cracks. Therefore, combined use of micro and macro fibers might be considered the further improve the joint performance of concrete pavements.

This study demonstrates that the use of polypropylene fibers improves the post-cracking performance of concrete for similar crack widths. Besides, in the literature it was reported that the use of fibers might reduce the crack widths in pavement joints due to reduced shrinkage, as well as provided resistance against the opening of joint crack widths. Therefore, to fully represent the contribution of discrete fibers to the performance of concrete pavements, development of new methods that account the contribution of fibers to the faulting performance of concrete pavement joints is required. Otherwise, currently available design methods might give unreliable thickness requirements, especially for the pavements that will carry large number of heavy tandem and/or tridem axle loads (which were reported as more damaging in terms of faulting failure).

## 5.5. Two-Stage Mixing Approach to lmprove Fiber-Matrix Interface

in the scope of this study, TSMA commonly employed to improve the ITZ of recycled aggregate concrete mixtures was revisited to improve the performance of FRC, and efficiency of the implemented methodology has been investigated in its various aspects. Major outcomes of the presented study were summarized below.

- Compressive strength, modulus of elasticity and flexural strength of the mixtures prepared with standard and modified mixing methodology was found similar.
- Up to 30.6% increase in RFSR was obtained for the mixtures prepared with modified mixing protocol compared to those prepared with standard mixing protocol. Besides, conducted microstructural analyses were found to support the change in interface characteristics due to implementation of modified mixing methodology.

- For the case study conducted, depending on the flexural performance obtained, up to 17.9% reduction in the required pavement thickness was obtained for FRC mixtures, compared to plain one. Despite increasing the cost (up to 35. 1%) use of fibers was found to reduce the CE in considerable amount (up to 20.9%). Additionally, use of SF was found to be a way to improve FRC performance and reduce its cost, as well as CE.
- In line with the reduced thickness requirements, obtained due to higher flexural performance, up to 6.0% reduction in cost and CE was obtained for the FRC mixtures prepared with modified mixing protocol, compared to the companion mixtures prepared with standard mixing protocol.

Based on the results of this primary study, use of TSMA was found to be a promising technique to improve the FRC performance. However, it should be emphasized here that the obtained results are strongly dependent on the fibers used in this study, and the results may alter for the use of different fibers. Therefore, further studies are recommended to evaluate the efficiency of the method for fibers with different raw materials and surface properties.

Fibers used in this study are the ones commercially available, changing the surface properties to obtain further benefits from TSMA might be considered in the future studies. Additionally, only SF was considered to improve fiber-matrix interface as a supplementary material, performance of other cement replacement materials (fly aslı, slag, ete.) might also be studied in the future. Moreover, the mixtures tested in this study were prepared in laboratory scale, further studies are also needed to examine the applicability of the method in real scale.

## 5.6. Structural Behavior of Recycled Aggregate Concrete Pavements

Based on the results of this study, following conclusions were drawn:

- Concrete mixtures produced with recycled coarse aggregates were cohesive and workable and didn't show segregation when fresh. Replacing the crushed stone coarse aggregate fully with recycled aggregates reduced the unit weight of fresh concrete up to 12%.
- The use of recycled aggregates as a total substitute of crushed stone coarse aggregate resulted in a decrease in the mechanical properties tested in this study. The amount of reduction in all the performance parameters were found higher for recycled brick aggregates compared to recycled concrete aggregates. However, GGBS slurry treating the recycled aggregates improved the mechanical properties of concrete with increasing statistical reliability.
- Significantly decreased LTE (%) (≈ 22% reduction for RCAC, ≈38% reduction for RBAC) values were found for recycled aggregate concrete mixtures compared to virgin ones, and the resulting lower values were attributed to lower Los Angeles abrasion and higher shrinkage values of recycled aggregate concrete mixtures.
- For the constant pavement thickness design case, decreased maximum stress, as well as increased maximum deflection values were obtained for recycled aggregate mixtures. However, an increase in SR (used in fatigue analysis) and P (used in faulting analysis) values was observed for all the recycled aggregate mixtures. Besides, all these results were attributed to the combined effect of the change in modulus of elasticity and flexural strength from control to recycled aggregate mixtures.
- For the constant life design case, required pavement thickness was increased for both fatigue and faulting failure analyses for all the recycled aggregate concrete mixtures. For the desired life, fatigue failure was found critical for the single axle loading case, and faulting failure was found for the tandem axle loading case.
- For the design approach followed in the scope of the study, the effect of increase in support stiffness was found higher in terms of maximum deflection compared

to maximum stress. On the contrary, the effect was found to be more pronounced for fatigue failure compared to faulting failure.

- To resist the similar number of load applications, a higher amount of material requirements was found for recycled aggregate concrete mixtures, and the results were attributed to increase in thickness requirement values.
- Slight increase in structural behavior parameters were obtained for the treated recycled aggregate concrete mixtures (TRCAC and TRBAC) compared to untreated versions of the mixtures.

In this study, performance of RCA and RBA were evaluated only for full replacement of virgin coarse aggregates. To obtain better performances, partial replacement cases may be taken into account for both of the recycled aggregate types. It should be also stated that the amount of decrease in performance parameters are dependent on the type of recycled aggregates used in the scope of this study. It is obvious that better performances could be obtained by using recycled aggregates with better quality. Furthermore, to enhance the performance obtained from the recycled aggregate mixtures, only the slurry method is used. In the further studies, the effect of different treatment methods can also be taken into account.

This study clearly shows that the use of recycled aggregate concrete, with low modulus of elasticity, increases the deflection occurring within the loaded slab, and use of strong support does not improve the faulting (erosion) performance of concrete pavements. Additionally, it is shown that the tandem axle loading case is more critical for faulting failure. Therefore, if recycled aggregate concrete pavements will be subjected to a high amount of heavy tandem axles, special attention needs to be given to faulting failure safety. For these types of pavements load transfer devices (dowel bars) within the joints may be used to improve the faulting performance, instead of usage of strong base layers. It should also be noted that foundations with lower risk of erosion (such as dry lean concrete base) may also be considered. Since, one of the main reasons of the increased deflection values found for recycled aggregate mixture is a decrease in the joint stiffness of recycled aggregate concrete mixtures, and it is strongly dependent to

the joint crack width, reducing the joint spacing can also be considered to improve the joint performance of recycled aggregate concrete pavements. Additionally, the largest aggregate size (which was kept constant as 16 mm in this study) of concrete can be increased to improve the LTE of recycled aggregate concrete mixture. However, as emphasized by Shi et al. [154], d-cracking potential of the resulting mixture should be taken into account in this case.

While this study was focused on the mechanical properties and structural behavior of concrete pavements produced with recycled aggregates, durability issues were not addressed in the scope. However, based on the type of aggregate used, recycled aggregates with high water absorption and Los Angeles abrasion values may cause some problems related to durability of concrete pavement (especially in the surface). Therefore, durability of recycled aggregate concrete mixtures should be also considered for the field applications. For the severe exposure conditions, two lift (layer) pavement construction may be taken into account: recycled aggregate concrete lower lift, and high quality virgin aggregate concrete upper lift.

As previously mentioned, to simplify the modelling and evaluation procedure, effect of temperature gradient on the structural behavior of the concrete mixtures were not examined in the scope of the conducted study. However, the type of aggregate used in the concrete might significantly alter the thermal expansion coefficient of concrete, and increasing thermal expansion coefficient leads to increase in pavement stress, when the temperature gradient is taken into account. Therefore, to see the effect of change in thermal expansion coefficient of concrete due to the replacement of virgin aggregates with recycled aggregates, further studies should be carried out.

### 5.7. Joint Performance of Recycled Aggregate Concrete Pavements

In the scope of the study, basic hardened-state properties (mechanical and physical) of concrete mixtures produced with virgin and recycled aggregates were determined experimentally. In addition, the cyclic post-cracking shear performance of the mixtures

was measured using a small-scale (beam) testing methodology suggested in the literature. The results obtained in this study were discussed in their various aspects and might be summarized as follows:

- Compared to the control mixture (NAC), up to a 22% reduction in mechanical performance was observed for recycled aggregate concrete mixtures. Besides, the decrease in the performance was almost double for RAC - 100 compared to RAC - 50. In addition, the reduction in modulus of elasticity due to the replacement of half or all of the coarse virgin aggregates with recycled ones was found to be lower compared to compressive and flexural strength.
- Decreased density with increased porosity and abrasion values were obtained for recycled aggregate mixtures (RAC - 50 and RAC - 100) compared to the control mixture (NAC) based on the physical test results. Obtained results were attributed to lower densities and porous structures of recycled aggregates.
- The abrasion resistance of recycled aggregate concrete mixtures was lower than that of the control mixture.
- Using recycled aggregates in concrete mixtures increased the peak differential displacement values considerably depending on the amount of replacement. Besides, crack width had a significant impact on the post-cracking shear performance of the mixtures.
- Post-cracking shear degradation rates for control and recycled aggregate mixtures were similar. However, considering the lower abrasion resistance of recycled aggregates, further studies might be helpful in investigating the possible difference in the number of cycles leading to the failure of virgin and recycled aggregate mixtures.
- A lower reduction was observed in the performance of concrete regarding all the parameters measured in this study in the case of partial replacement of crushed stone coarse aggregate with recycled concrete aggregate (RAC - 50) than in the case of full replacement (RAC - 100) compared to the control mixture.

It should be indicated here that the obtained results are dependent on the properties of both virgin and recycled aggregates used in this study. The use of aggregates with different properties may change the results in a positive or negative way. Therefore, further studies that link the aggregate properties and performance parameters are needed to generalize the results obtained in the current study.

For the post-cracking performance, further studies to determine the optimum replacement level might be recommended to enhance the structural and environmental benefits that could be obtained from the recycled aggregates. in addition, both small (No I: 4-8 mm) and large (No il: 8-16 mm) coarse aggregates were replaced in equal amounts for both recycled aggregate concrete mixtures (RAC - 50 and RAC - 100) in this study. On the other hand, it is known that the larger aggregates are more effective in terms of post-cracking shear performance [108]. Therefore, better performance might be obtained by replacing only small coarse aggregates without any change in large ones, but further studies are needed to test the hypothesis.

The importance of crack width in terms of post-cracking shear performance was emphasized in the scope of the current and previous [109,166,267] studies. Besides, it is known that lower stiffness of recycled aggregates leads to higher shrinkage of the concrete mixture [203, 268]. Since shrinkage of a concrete mixture has a considerable impact on the pavement joint crack widths [73, 269], a further decrease in the joint performance of recycled aggregate concrete pavements may occur due to increased crack widths.

To overcome the problems in site that might occur due to lower post-cracking performance of recycled aggregate concrete mixtures, use of shorter slabs to reduce joint crack widths [270] and the use of dowel bars in the joints [19,244] are two solutions that could be considered. Additionally, the use of discrete structural fibers may be considered to improve joint performance, as they are effective for both reducing the crack width by decreasing the shrinkage of concrete mixtures [263,271,272] and improving the post-cracking shear performance of concrete mixtures [94, 114,267].

# REFERENCES


1. Lima, L., E. Trindade, L. Alencar, M. Alencar and L. Silva, "Sustainability in the Construction lndustry: A Systematic Review of the Literature", *Journal of Cleaner Production,* Vol. 289, p. 125730, 2021.

2. Sev, A., "How Can the Construction Industry Contribute to Sustainable Development? A Conceptual Framework", *Sustainable Development,* Vol. 17, No. 3, pp. 161-173, 2009.

3. Mostofinejad, D., M. R. Nikoo and S. A. Hosseini, "Determination of Optimized Mix Design and Curing Conditions of Reactive Powder Concrete (RPC)", *Construction and Building Materials,* Vol. 123, pp. 754-767, 2016.

4. Volodchenko, A. A., V. S. Lesovik, I. A. Cherepanova, A. N. Volodchenko, L. H. Zagorodnjuk and M. Y. Elistratkin, "Peculiarities of Non-Autoclaved Lime Wall Materials Production Using Clays", *IOP Conference Series: Materials Science and Engineering,* Vol. 327, Institute of Physics Publishing, 2018.

5. Lanfkova, I., P. Stepanek and P. Simunek, "Optimized Design of Concrete Structures Considering Environmental Aspects" , *Advances in Structural Engineering,* Vol. 17, No. 4, pp. 495-511, 2014.

6. Stazi, F., A. Mastrucci and P. Munafö, "Life Cycle Assessment Approach for the Optimization of Sustainable Building Envelopes: An Application on Solar Wall Systems", *Building and Environment,* Vol. 58, pp. 278-288, 2012.

7. Stepanek, P., I. Lanikova and J. Venclovsky, "Life Cycle Assessment Optimization of a Shotcrete Tunnel Lining", *IOP Conference Series: Materials Science and Engineering,* Vol. 442, Institute of Physics Publishing, 2018.

8. Bumanis, G. and A. K. andDiana Bajare, "Environmental Benefit of Alternative

Binders in Construction Industry: Life Cycle Assessment", *Environments,* Vol. 9, No. 1, p. 6, 2022.

9. Collivignarelli, M. C., A. Abba, M. C. Miino, G. Cillari and P. Ricciardi, "A Review on Alternative Binders, Admixtures and Water for tlıe Production of Sustainable Concrete", *Journal of Cleaner Production,* Vol. 295, p. 126408, 2021.

10. Kirtlıika, S. K., S. K. Singlı and A. Clıourasia, "Alternative Fine Aggregates in Production of Sustainable Concrete - A Review", *Journal of Cleaner Production,* Vol. 268, p. 122089, 2020.

11. Slıarma, M., S. Bislınoi, F. Martirena and K. Scrivener, "Limestone Calcined Clay Cement and Concrete: A State-of-tlıe-Art Review", *Cement and Concrete Research,* Vol. 149, p. 106564, 2021.

12. Sinyoung, S., S. Asavapisit and K. Kunclıariyakun, "Investigation of Bagasse Aslı as an Alternative Raw Material in Clinker Production", *Journal of Materials in Civil Engineering,* Vol. 34, No. 2, p. 04021433, 2022.

13. Anıran, M., G. Murali, N. H. A. Klıalid, R. Fediuk, T. Ozbakkaloglu, Y. H. Lee, S. Haruna and Y. Y. Lee, "Slag Uses in Making an Ecofriendly and Sustainable Concrete: A Review", *Construction and Building Materials,* Vol. 272, 2021.

14. Awoyera, P. and A. Adesina, "A Critical Review on Application of Alkali Activated Slag as a Sustainable Composite Binder", *Case Studies in Construction Materials,* Vol. 11, p. e00268, 2019.

15. Bajpai, R., K. Clıoudlıary, A. Srivastava, K. S. Sangwan and M. Singlı, "Environmental Impact Assessment of Fly Aslı and Silica Fume Based Geopolymer Concrete", *Journal of Cleaner Production,* Vol. 254, p. 120147, 2020.

16. Hassan, A., M. Arif and M. Slıariq, "Use of Geopolymer Concrete for a Cleaner and Sustainable Environment - A Review of Meclıanical Properties and Mi-

crostructure", *Journal of Cleaner Production,* Vol. 223, pp. 704-728, 2019.

17. Ma, S., A. H. Akca, D. Esposito and S. Kawaslıima, "Influence of Aqueous Carbonate Species on Hydration and Carbonation of Reactive MgO Cement", *Journal of* $CO_2$ *Utilization,* Vol. 41, p. 101260, 2020.

18. Balci, E., O. Ozturk, N. Ozyurt and T. Ozturan, "Decreasing Environmental Impact of Concrete by Using Higlı-Volume Fly Aslı Concretes", *14th International Congress on Advances in Civil Engineering,* pp. 175-182, Istanbul, Turkey, 2021.

19. Ozturk, O., H. Yildirim, N. Ozyurt and T. Ozturan, "Evaluation of Meclıanical Properties and Structural Belıaviour of Concrete Pavements Produced Witlı Virgin and Recycled Aggregates: an Experimental and Numerical Study", *International Journal of Pavement Engineering,* Vol. 23, No. 14, pp. 1-15, 2022.

20. Sitlıole, N. T., N. T. Tsotetsi, T. Maslıifana and M. Sillanpaa, "Alternative Cleaner Production of Sustainable Concrete From Waste Foundry Sand and Slag", *Joumal of Cleaner Production,* Vol. 336, p. 130399, 2022.

21. Yıldırım, H. and T. Özturan, "Impact Resistance of Concrete Produced Witlı Plain and Reinforced Cold-Bonded Fly Aslı Aggregates", *Journal of Building Engineering,* Vol. 42, p. 102875, 2021.

22. Zimbili, O., W. Salim and M. Ndambuki, "A Review on tlıe Usage of Ceramic Wastes in Concrete Production", *Intemational Joumal of Civil, Environmental, Structural, Construction and Architectural Engineering,* Vol. 8, No. 1, pp. 91-95, 2014.

23. di Summa, D., J. R. T. Fillıo, D. Snoeck, P. V. den Heede, S. V. Vlierberglıe, L. Ferrara and N. D. Belie, "Environmental and Economic Sustainability of Crack Mitigation in Reinforced Concrete Witlı Superabsorbent Polymers (SAPs)", *Journal of Cleaner Production,* Vol. 358, p. 131998, 2022.

24. Faniran, O. O. and G. Caban, "Minimizing Waste on Construction Project Sites", *Engineering, Construction and Architectuml Management,* Vol. 5, No. 2, pp. 182-188, 1998.

25. Wang, J., Z. Li and V. W. Y. Tam, "Identifying Best Design Strategies for Construction Waste Minimization", *Journal of Cleaner Production,* Vol. 92, pp. 237-247, 2015.

26. Morel, J. C., A. Mesbah, M. Oggero and P. Walker, "Building Houses With Local Materials: Means to Drastically Reduce the Environmental lmpact of Construction", *Building and Environment,* Vol. 36, pp. 1119-1126, 2001.

27. Caruso, M. C., C. Pascale, E. Camacho and L. Ferrara, "Comparative Environmental and Social Life Cycle Assessments of Offshore Aquaculture Rafts Made in Ultra-High Performance Concrete (UHPC)", *The Intemational Joumal of Life Cycle Assessment,* Vol. 27, No. 2, pp. 281-300, 2022.

28. Federal Highway Administration (FHWA), *Highway Statistics,* Technical Report, United States Department of Transportation, Washington, DC, 2019.

29. American Society of Civil Engineers (ASCE), "A Comprehensive Assessment of America's Infrastructure / 2021 Report Card for America's Infrastructure", American Society of Civil Engineers, Reston, Virginia, 2021.

30. Santos, J., J. Bryce, G. Flintsch, A. Ferreira and B. Diefenderfer, "A Life Cycle Assessment of In-Place Recycling and Conventional Pavement Construction and Maintenance Practices", *Structure and Infmstructure Engineering,* Vol. 11, No. 9, pp. 1199-1217, 2015.

31. Santero, N. J., E. Masanet and A. Horvath, "Life-cycle Assessment of Pavements. Part I: Critical Review", *Resources, Conservation and Recycling,* Vol. 55, No. 9-10, pp. 801-809, 2011.

32. Plati, C., "Sustainability Factors in Pavement Materials, Design, and Preservation Strategies: A Literature Review", *Construction and Building Materials,* Vol. 211, pp. 539-555, 2019.

33. Salehi, S., M. Arashpour, J. Kodikara and R. Guppy, "Sustainable Pavement Construction: A Systematic Literature Review of Environmental and Economic Analysis of Recycled Materials", *Journal of Cleaner Production,* Vol. 313, p. 127936, 2021.

34. Dam, T. V., P. Taylar, G. Fick, M. VanGeem and E. Lorenz, *Sustainable Concrete Pavements: A Manual of Pmctice,* Iowa State University National Concrete Pavement Technology Center, Technical Report, Iowa, 2012.

35. Abut, Y., S. T. Yildirim, O. Ozturk and N. Ozyurt, "A Comparative Study on the Performance of RCC for Pavements Casted in Laboratory and Field", *International Journal of Pavement Engineering,* Vol. 23, No. 6, pp. 1777-1790, 2022.

36. Hager, A. S., *Sustainable Design of Pervious Concrete Pavements,* Ph.D. Thesis, University of Colorado at Denver, 2009.

37. Hughes, B. P., "Optimum Design of Sustainable Concrete Pavements", *Proceedings of the Institution of Civil Engineers-Engineering Sustainability,* Vol. 159, pp. 127-132, Thomas Telford Limited Company, 2006.

38. Tompkins, D., L. Khazanovich, M. I. Darter and W. Fleischer, "Design and Construction of Sustainable Pavements: Austrian and German Two-L$_{a\,y}$er Concrete Pavements", *Tmnsportation Research Record,* Vol. 2098, No. 1, pp. 75-85, 2009.

39. Jamshidi, A., K. Kurumisawa, T. Nawa and M. O. Hamzalı, "Analysis of Structural Performance and Sustainability of Airport Concrete Pavements Incorporating Blast Furnace Slag", *Journal of Cleaner Production,* Vol. 90, pp. 195-210,

2015.

40. Pranav, S., S. Aggarwal, E.-H. Yang, A. K. Sarkar, A. P. Singh and M. Lahoti, "Alternative Materials for Wearing Course of Concrete Pavements: A Critical Review", *Construction and Building Materials,* Vol. 236, p. 117609, 2020.

41. Singh, T., R. Siddique and S. Sharma, "Effectiveness of Using Metakaolin and Fly Aslı as Supplementary Cementitious Materials in Pervious Concrete", *European Joumal of Environmental and Cívil Engineering,* Vol. 26, No. 15, pp. 1-24, 2021.

42. Arulrajah, A., A. Mohammadinia, F. Maghool and S. Horpibulsuk, "Tire Derived Aggregates as a Supplementary Material With Recycled Demolition Concrete for Pavement Applications", *Joumal of Cleaner Production,* Vol. 230, pp. 129-136, 2019.

43. Debbarma, S., M. Selvam and S. Singh, "Can Flexible Pavements' Waste (RAP) Be Utilized in Cement Concrete Pavements? - A Critical Review", *Construction and Building Materials,* Vol. 259, p. 120417, 2020.

44. Reza, F., W. J. Wilde and B. Izevbekhai, "Sustainability of Using Recycled Concrete Aggregates as Coarse Aggregate in Concrete Pavements", *Transporlation Research Record,* Vol. 2672, No. 27, pp. 99-108, 2018.

45. Selvam, M., S. Debbarma, S. Singh and X. Shi, "Utilization of Alternative Aggregates for Roller Compacted Concrete Pavements - A State-of-the-Art Review", *Construction and Building Materials,* Vol. 317, p. 125838, 2022.

46. Chan, R., M. A. Santana, A. M. Oda, R. C. Paniguel, L. B. Vieira, A. D. Figueiredo and I. Galobardes, "Analysis of Potential Use of Fibre Reinforced Recycled Aggregate Concrete for Sustainable Pavements", *Joumal of Cleaner Production,* Vol. 218, pp. 183-191, 2019.

47. Kim, J. K. and Y. Y. Kim, "Experimental Study of the Fatigue Behavior of

High Strength Concrete", *Cement and Concrete Research,* Vol. 26, No. 10, pp. 1513-1523, 1996.

48. Song, Z., T. Frühwirt and H. Konietzky, "Fatigue Characteristics of Concrete Subjected to Indirect Cyclic Tensile Loading: Insights From Deformation Behavior, Acoustic Emissions and Ultrasonic Wave Propagation", *Construction and Building Materials,* Vol. 302, 10 2021.

49. Lee, M. K. and B. I. G. Barr, "An Overview of the Fatigue Behaviour of Plain and Fibre Reinforced Concrete", *Cement and Concrete Composites,* Vol. 26, No. 4, pp. 299-305, 2004.

50. Hsu, T. T. C., "Fatigue of Plain Concrete", *ACI Journal Proceedings,* Vol. 78, pp. 292-305, 1981.

51. Song, Z., H. Konietzky, M. Herbst, T. Frühwirt and Y. Wu, "Fatigue and Micro-Seismic Behaviors of Concrete Disks Exposed to Cyclic Brazilian Testing: A Numerical Investigation Based on a 3D Particle-Based Model", *International Journal of Fatigue,* Vol. 155, p. 106629, 2022.

52. Arora, S. and S. P. Singh, "Analysis of Flexural Fatigue Failure of Concrete Made With 100 % Coarse Recycled Concrete Aggregates", *Construction and Building Materials,* Vol. 102, pp. 782-791, 2016.

53. Chandrappa, A. K. and K. P. Biligiri, "Flexural-Fatigue Characteristics of Pervious Concrete: Statistical Distributions and Model Development", *Construction and Building Materials,* Vol. 153, pp. 1-15, 2017.

54. Li, H., M. hua Zhang and J. ping Ou, "Flexural Fatigue Performance of Concrete Containing Nano-Particles for Pavement", *International Journal of Fatigue,* Vol. 29, No. 7, pp. 1292-1301, 2007.

55. OU, Z. and L. SUN, "Flexural Fatigue-life Reliability of Frost-damaged Concrete",

*Journal of Zhejiang University (Engineering Science),* Vol. 51, No. 6, pp. 1074-1081, 2017.

56. Saini, B. S. and S. P. Singh, "Flexural Fatigue Strength Prediction of Self Compacting Concrete Made With Recycled Concrete Aggregates and Blended Cements", *Construction and Building Materials,* Vol. 264, p. 120233, 2020.

57. Shi, X. P., T. F. Fwa and S. A. Tan, "Flexural Fatigue Strength of Plain Concrete", *Materials Journal,* Vol. 90, No. 5, pp. 435-440, 1993.

58. Su, C. and H. Lin, "Mechanical Performances of Steel Fiber Reinforced High Strength Concrete Disc Under Cyclic Loading", *Construction and Building Materials,* Vol. 146, pp. 276-282, 2017.

59. Kumar, K. S. S., G. K. Kamalakara and S. Kamble, "Fatigue Analysis of High Performance Cement Concrete for Pavements Using the Probabilistic Approach", *International Journal of Emerging Technology and Advanced Engineering,* Vol. 2, No. 11, pp. 640-644, 2012.

60. LaHucik, J., S. Dahal, J. Roesler and A. N. Amirkhanian, "Mechanical Properties of Roller-Compacted Concrete With Macro-fibers", *Construction and Building Materials,* Vol. 135, pp. 440-446, 2017.

61. Molins, C., A. Aguado and S. Saludes, "Double Punch Test to Control the Energy Dissipation in Tension of FRC (Barcelona Test)", *Materials and Structures,* Vol. 42, No. 4, pp. 415-425, 2009.

62. Arora, S. and S. P. Singh, "Flexural Fatigue Performance of Concrete Made With Recycled Concrete Aggregates and Ternary Blended Cements", *Journal of Sustainable Cement-Based Materials,* Vol. 7, No. 3, pp. 182-202, 2018.

63. Mohammadi, Y. and S. K. Kaushik, "Flexural Fatigue-Life Distributions of Plain and Fibrous Concrete at Various Stress Levels", *Journal of Materials in Civil*

*Engineering,* Vol. 17, No. 6, pp. 650-658, 2005.

64. Harwalkar, A. and S. S. Awanti, "Probability Analysis of Flexural Fatigue Data of High Volume Fly Aslı Concrete", *Airfield and Highway Pavements,* pp. 295-307, 2017.

65. Singh, S. P. and S. K. Kaushik, "Flexural Fatigue Life Distributions and Failure Probability of Steel Fibrous Concrete", *Materials Journal,* Vol. 97, No. 6, pp. 658-667, 2000.

66. Zhu, X., X. Chen, S. Liu, S. Li, W. Xuan and Y. Chen, "Experimental Study on Flexural Fatigue Performance of Rubberised Concrete for Pavement", *International Journal of Pavement Engineering,* Vol. 21, No. 9, pp. 1135-1146, 2020.

67. Schijve, J., "Introduction to Fatigue of Structures and Materials", *Fatigue of Structures and Materials,* pp. 1-6, 2001.

68. Chen, W. F., *Double Punch Test far Tensile Strength of Concrete,* Report, Fritz Engineering Laboratory, Lehigh University, 1969.

69. Colgrove, T. A. and W.-F. Chen, *Further Studies of Double-Punch Testfor Tensile Strength of Concrete,* Report, Fritz Engineering Laboratory, Lehigh University, 1972.

70. Lee, W. J. and C. K. Koh, "A Study on Double-Punch Test for Tensile Strength of Concrete.", *Journal of the Korean Society of Agricultural Engineers,* 1988.

71. Pujadas, P., A. Blanco, S. Cavalaro, A. de la Fuente and A. Aguado, "New Analytical Model to Generalize the Barcelona Test Using Axial Displacement", *Journal of Civil Engineering and Management,* Vol. 19, No. 2, pp. 259-271, 2013.

72. Portland Cement Association, *Thickness Design far Concrete Highway and Street Pavements (pca 84),* Illinois, United States of America.

73. American Association of State Highway and Transportation Officials (AASHTO), *Guide far Design of Pavement Structures,* American Association of State Highway and Transportation Officials, 1993.

74. Harik, I. E., P. Jianping, H. Southgate and D. Allen, "Temperature Effects on Rigid Pavements", *Journal of Transportation Engineering,* Vol. 120, No. 1, pp. 127-143, 1994.

75. Mohamed, A. R. and W. Hansen, "Effect of Nonlinear Temperature Gradient on Curling Stressin Concrete Pavements", *Transportation Research Record,* Vol. 1568, No. 1, pp. 65-71, 1997.

76. Yu, H. T., L. Khazanovich, M. I. Darter and A. Ardani, "Analysis of Concrete Pavement Responses to Temperature and Wheel Loads Measured From Intrumented Slabs", *Transportation Research Record,* Vol. 1639, No. 1, pp. 94-101, 1998.

77. Mahboub, K. C., Y. Liu and D. L. Allen, "Evaluation of Temperature Responses in Concrete Pavement", *Journal of Transportation Engineering,* Vol. 130, No. 3, pp. 395-401, 2004.

78. Chatti, K., A. Manik and N. Brake, "Effect of Axle Configurations on Fatigue and Faulting of Concrete Pavements", *10th International Symposium on Heavy Vehicle Transport Technology,* pp. 117-126, Paris, France, 2008.

79. Belshe, M., M. S. Mamlouk, K. E. Kaloush and M. Rodezno, "Temperature Gradient and Curling Stresses in Concrete Pavement With and Without Open-Graded Friction Course", *Journal of Transportation Engineering,* Vol. 137, No. 10, pp. 723-729, 2011.

80. Asbahan, R. E. and J. M. Vandenbossche, "Effects of Temperature and Moisture Gradients on Slab Deformation for Jointed Plain Concrete Pavements", *Journal*

*of Transportation Engineering,* Vol. 137, No. 8, pp. 563-570, 2011.

81. S"oderqvist, J., *Design of Concrete Pavements: Design Criteria far Plain and Lean Concrete,* Ph.D. Thesis, KTH Royal Institute of Technology, 2006.

82. Indian Road Congress (IRC 58), *Guidelines far the Design of Plain Jointed Rigid Pavements far Highways, Third Revision,* Indian Roads Congress, New Delhi, India, 2011.

83. American Association of State Highway and Transportation Officials (AASHTO), *Mechanistic-Empirical Pavement Design Guide: A Manual of Practice,* AASHTO, Washington, DC, 2008.

84. Indian Road Congress (IRC 58), *Guidelines far the Design of Plain Jointed Rigid Pavements far Highways, Fourth Revision,* Indian Roads Congress, New Delhi, India, 2015.

85. Gutierrez, J. J., *Evaluating the JPCP Cracking Model of the Mechanistic-Empirical Pavement Design Guide,* Ph.D. Thesis, University of Pittsburgh, 2008.

86. Kim, H. B., "Top-Down Cracking of Jointed Plain Concrete Pavements", *Journal of the Eastern AsiaSociety far Transportation Studies,* Vol. 8, pp. 1529-1541, 2010.

87. Vandenbossche, J. M., F. Mu, J. J. Gutierrez and J. Sherwood, "An Evaluation of the Built-In Temperature Difference Input Parameter in the Jointed Plain Concrete Pavement Cracking Model of the Mechanistic-Empirical Pavement Design Guide", *International Journal of Pavement Engineering,* Vol. 12, No. 03, pp. 215-228, 2011.

88. Williams, H. A., "Fatigue Tests of Lightweight Aggregate Concrete Beams", *ACI Journal Proceedings,* Vol. 39, pp. 441-448, 1943.

89. Tepfencompression, R., "Fatigue of Plain Concrete Subjected to Stress Reversals", *Special Publication,* Vol. 75, pp. 195-216, 1982.

90. Zhang, B., D. V. Phillips and K. Wu, "Effects of Loading Frequency and Stress Reversal on Fatigue Life of Plain Concrete", *Magazine of Concrete Research,* Vol. 48, No. 177, pp. 361-375, 1996.

91. Cornelissen, H. A. W. and H. W. Reinhardt, "Uniaxial Tensile Fatigue Failure of Concrete Under Constant-Amplitude and Programme Loading", *Magazine of Concrete Research,* Vol. 36, No. 129, pp. 216-226, 1984.

92. Lü, P., Q. Li and Y. Song, "Damage Constitutive of Concrete Under Uniaxial Alternate Tension-Compression Fatigue Loading Based on Double Bounding Surfaces", *International Journal of Solids and Structures,* Vol. 41, No. 11-12, pp. 3151-3166, 2004.

93. Altoubat, S. A., J. R. Roesler, D. A. Lange and K.-A. Rieder, "Simplified Method for Concrete Pavement Design With Discrete Structural Fibers", *Construction and Building Materials,* Vol. 22, No. 3, pp. 384-393, 2008.

94. Crick, C. A. T., *Cmck Creep and Joint Performance Behavior of Fiber Reinforced Concrete,* Master's Thesis, University of Minnesota, 2020.

95. Indian Road Congress (IRC SP 46), *Guidelines far Design and Construction of Fibre Reinforced Concrete Pavements,* Indian Roads Congress, New Delhi, India, 2013.

96. Nanni, A. and A. Johari, "RCC Pavement Reinforced With Steel Fibers", *Concrete International,* Vol. 11, No. 3, pp. 64-69, 1989.

97. Yin, S., R. Tuladhar, F. Shi, M. Combe, T. Collister and N. Sivakugan, "Use of Macro Plastic Fibres in Concrete: A Review", *Construction and Building Materials,* Vol. 93, pp. 180-188, 2015.

98. Ochi, T., S. Okubo and K. Fukui, "Development of Recycled Pet Fiber and Its Application as Concrete-reinforcing Fiber", *Cement and Concrete Composites,* Vol. 29, No. 6, pp. 448-455, 2007.

99. Nayar, S. K. and R. Gettu, "A Comprehensive Methodology for the Design of Fibre Reinforced Concrete Pavements", *FRC 2014 Joint ACI-fib International Workshop Fibre Reinforced Concrete: From Design to Structural Applications,* pp. 453-464, Montreal, Canada, 2016.

100. Nayar, S. K. and R. Gettu, "Mechanistic-Empirical Design of Fibre Reinforced Concrete (FRC) Pavements Using Inelastic Analysis", *Sadhana,* Vol. 45, No. 1, pp. 1-7, 2020.

101. Roesler, J. R., A. C. Bordelon, A. Ioannides, M. Beyer and D. Wang, *Design and Concrete Material Requirements far Ultra-Thin Whitetopping,* Illinois Center for Transportation, Illinois, 2008.

102. Ferrara, L., Y.-D. Park and S. P. Shah, "A Method for Mix-Design of Fiber-Reinforced Self-Compacting Concrete", *Cement and Concrete Research,* Vol. 37, No. 6, pp. 957-971, 2007.

103. Rooholamini, H., A. Hassani and M. R. M. Aliha, "Evaluating the Effect of Macro-Synthetic Fibre on the Mechanical Properties of Roller-Compacted Concrete Pavement Using Response Surface Methodology", *Construction and Building Materials,* Vol. 159, pp. 517-529, 2018.

104. American Concrete Pavement Association (ACPA), "ACPA Streetpave Software (Version 12)", American Concrete Pavement Association, Rosemont, Illinois, 2014.

105. Parjoko, Y. H., "Sensitivity Analysis of Concrete Performance Using Finite Element Approach", *Journal of the Civil Engineering Forum,* Vol. 21, No. 1, 2012.

106. Ioannides, A. M. and G. T. Korovesis, "Aggregate Interlock: a Pure-Shear Load Transfer Mechanisın", *Tmnsportation Research Record,* 1990.

107. Pittınan, D. W., *Development ofa Design Procedure far Roller-Compacted Concrete (RCC) Pavements,* The University of Texas at Austin, 1993.

108. Jensen, E. A. and W. Hansen, "Mechanisın of Load Transfer-crack Width Relation in JPCP: Influence of Coarse Aggregate Properties", *Seventh International Conference on Concrete Pavements. The Use of Concrete in Developing Long-Lasting Pavement Solutions far the 21st Century. International Society far Concrete Pavements,* Vol. 2, Orlando, Florida, 2001.

109. Maitra, S. R., K. S. Reddy and L. S. Raınachandra, "Load Transfer Characteristics of Aggregate Interlocking in Concrete Paveınent", *Journal of Tmnsportation Engineering,* Vol. 136, No. 3, pp. 190-195, 2010.

110. Vandenbossche, J. M., M. Barınan and J. Nolan-Kreının, "Surface Texture Measureınents of Crack Surface to Establish Joint Shear Stiffness", *Tmnsportation Research Record,* Vol. 2441, No. 1, pp. 13-19, 2014.

111. Mohaınined, H., N. Thoın and A. Dawson, "Load Transfer Stiffness of Two-Layer Roller Coınpacted Concrete for Paveınents", *Journal of Materials and Applications,* Vol. 8, No. 2, pp. 65-72, 2019.

112. Thoınpson, 1., *Use of Steel Fibres ta Reinforce Cement Bound Roadbase,* Ph.D. Thesis, University of Nottinghaın, 2001.

113. Arnold, S., P. Fleining, S. Austin and P. Robins, "A Test Method and Deterioration Model for Joints and Cracks in Concrete Slabs", *Cement and Concrete Rresearch,* Vol. 35, No. 12, pp. 2371-2383, 2005.

114. Barınan, M. and B. Hansen, "Post-Crack Flexural and Joint Perforınance Behaviors of Fiber-Reinforced Concrete for Paveınents", *Tmnsportation Research*

*Record,* Vol. 2676, No. 2, pp. 290-301, 2022.

115. Yoo, D. Y., J. H. Lee and Y. S. Yoon, "Effect of Fiber Content on Mechanical and Fracture Properties of Ultra High Performance Fiber Reinforced Cementitious Composites", *Composite Structures,* Vol. 106, pp. 742-753, 2013.

116. Wang, Q., Z. Ma, X. Yuan, J. Wang, Z. Mu, J. Zuo, J. Zhang, J. Hong and S. Wang, "Is Cement Pavement More Sustainable Than Permeable Brick Pavement? A Case Study for Jinan, China", *Journal of Cleaner Production,* Vol. 226, pp. 306-315, 2019.

117. Arunothayan, A. R., B. Nematollahi, R. Ranade, S. H. Bong, J. G. Sanjayan and K. H. Khayat, "Fiber Orientation Effects on Ultra-High Performance Concrete Formed by 3D Printing", *Cement and Concrete Research,* Vol. 143, p. 106384, 2021.

118. Ozturk, O., H. N. Atahan and N. Ozyurt, "Effects of Synthetic Fibers on the Mechanical Properties and Thickness Requirements of Roller-Compacted Concrete for Pavements", *Journal of Transportation Engineering, Part B: Pavements,* Vol. 148, No. 4, p. 04022052, 2022.

119. Ozturk, O. and N. Ozyurt, "Sustainability and Cost-Effectiveness of Steel and Polypropylene Fiber Reinforced Concrete Pavement Mixtures", *Journal of Cleaner Production,* p. 132582, 2022.

120. Mandel, J. A., S. Wei and S. Said, "Studies of the Properties of the Fiber-Matrix Interface in Steel Fiber Reinforced Mortar", *Materials Journal,* Vol. 84, No. 2, pp. 101-109, 1987.

121. Kai'kea, A., D. Achoura, F. Duplan and L. Rizzuti, "Effect of Mineral Admixtures and Steel Fiber Volume Contents on the Behavior of High Performance Fiber Reinforced Concrete", *Materials Design,* Vol. 63, pp. 493-499, 2014.

122. Khandelwal, S. and K. Y. Rhee, "Recent Advances in Basalt-Fiber-Reinforced Composites: Tailoring the Fiber-Matrix Interface", *Composites Part B: Engineering,* Vol. 192, p. 108011, 2020.

123. Abbas, M. Y. and M. I. Khan, "Fiber-Matrix Interfacial Behavior of Hooked-end Steel Fiber-Reinforced Concrete", *Journal of Materials in Civil Engineering,* Vol. 28, No. 11, p. 04016115, 2016.

124. Wang, X. H., S. Jacobsen, S. F. Lee, J. Y. He and Z. L. Zhang, "Effect of Silica Fume, Steel Fiber and ITZ on the Strength and Fracture Behavior of Mortar", *Materials and Structures,* Vol. 43, No. 1, pp. 125-139, 2010.

125. Wu, Z., K. H. Khayat and C. Shi, "Effect of Nano-$SiO_2$ Particles and Curing Time on Development of Fiber-Matrix Bond Properties and Microstructure of Ultra-High Strength Concrete", *Cement and Concrete Research,* Vol. 95, pp. 247-256, 2017.

126. Zhao, Y., J. Bi, Y. Sun, Z. Wang, L. Huo and Y. Duan, "Synergetic Effect of Ground Granulated Blast-Furnace Slag and Hooked-end Steel Fibers on Various Properties of Steel Fiber Reinforced Self-Compacting Concrete", *Structural Concrete,* Vol. 23, No. 1, pp. 268-284, 2022.

127. Mansoori, A., M. M. Moein and E. Mohseni, "Effect of Micro Silica on Fiber-Reinforced Self-Compacting Composites Containing Ceramic Waste", *Journal of Composite Materials,* Vol. 55, No. 1, pp. 95-107, 2021.

128. Tam, V. W. Y., X. F. Gao and C. M. Tam, "Microstructural Analysis of Recycled Aggregate Concrete Produced From Two-Stage Mixing Approach", *Cement and Concrete Research,* Vol. 35, No. 6, pp. 1195-1203, 2005.

129. Tam, V. W. Y., C. M. Tam and Y. Wang, "Optimization on Proportion for Recycled Aggregate in Concrete Using Two-Stage Mixing Approach", *Construction*

*and Building Materials,* Vol. 21, No. 10, pp. 1928-1939, 2007.

130. Tam, V. W. Y. and C. M. Tam, "Diversifying Two-Stage Mixing Approach (TSMA) for Recycled Aggregate Concrete: TSMAs and TSMAsc", *Construction and Building Materials,* Vol. 22, No. 10, pp. 2068-2077, 2008.

131. Güneyisi, E., M. Gesoğlu, Z. Algın and H. Yazıcı, "Effect of Surface Treatment Methods on the Properties of Self-Compacting Concrete With Recycled Aggregates", *Construction and Building Materials,* Vol. 64, pp. 172-183, 2014.

132. Montero, J. and S. Laserna, "Influence of Effective Mixing Water in Recycled Concrete", *Construction and Building Materials,* Vol. 132, pp. 343-352, 2017.

133. Rajhans, P., S. K. Panda and S. Nayak, "Sustainable Self Compacting Concrete From C&D Waste by Improving the Microstructures of Concrete ITZ", *Construction and Building Materials,* Vol. 163, pp. 557-570, 2018.

134. Faysal, R. M., M. Maslehuddin, M. Shameem, S. Ahmad and S. K. Adekunle, "Effect of Mineral Additives and Two-Stage Mixing on the Performance of Recycled Aggregate Concrete", *Journal of Material Cycles and Waste Management,* Vol. 22, No. 5, pp. 1587-1601, 2020.

135. Gupta, P. K., P. Rajhans, S. K. Panda, S. Nayak and S. K. Das, "Mix Design Method for Self-Compacting Recycled Aggregate Concrete and Its Microstructural Investigation by Considering Adhered Mortar in Aggregate", *Journal of Materials in Civil Engineering,* Vol. 32, No. 3, p. 04019371, 2020.

136. Verma, A., V. S. Babu and S. Arunachalam, "Influence of Mixing Approaches on Strength and Durability Properties of Treated Recycled Aggregate Concrete" , *Structural Concrete,* Vol. 22, pp. E121-E142, 2021.

137. Verma, A. and V. S. Babu, "Influence of Modified Two-Stage Mixing Approaches on Recycled Aggregate Treated With a Hybrid Method of Treatment", *Australian*

*Journal of Structural Engineering,* Vol. 23, No. 3, pp. 1-24, 2022.

138. Tam, V. W. Y. and C. M. Tam, "Assessment of Durability of Recycled Aggregate Concrete Produced by Two-Stage Mixing Approach", *Journal of Materials Science,* Vol. 42, No. 10, pp. 3592-3602, 2007.

139. Sivamani, J. and N. T. Renganathan, "Effect of Fine Recycled Aggregate on the Strength and Durability Properties of Concrete Modified Through Two-Stage Mixing Approach", *Environmental Science and Pollution Research,* pp. 1-14, 2021.

140. Huang, W. L., D. H. Lin, N. B. Chang and K.-8. Lin, "Recycling of Construction and Demolition Waste via a Mechanical Sorting Process", *Resources, Conservation and Recycling,* Vol. 37, No. 1, pp. 23-37, 2002.

141. Bianchini, G., E. Marrocchino, R. Tassinari and C. Vaccaro, "Recycling of Construction and Demolition Waste Materials: A Chemical-Mineralogical Appraisal", *Waste Management,* Vol. 25, No. 2, pp. 149-159, 2005.

142. Barritt, J., "An Overview on Recycling and Waste in Construction", *Proceedings of the Institution of Civil Engineers - Construction Materials,* Vol. 169, No. 2, pp. 49-53, 2016.

143. Lockrey, S., H. Nguyen, E. Crossin and K. Verghese, "Recycling the Construction and Demolition Waste in Vietnam: Opportunities and Challenges in Practice", *Journal of Cleaner Production,* Vol. 133, pp. 757-766, 2016.

144. Mondal, M. K., B. P. Bose and P. Bansal, "Recycling Waste Thermoplastic for Energy Efficient Construction Materials: An Experimental Investigation", *Journal of Environmental Management,* Vol. 240, pp. 119-125, 2019.

145. Zhang, P., Y. Yang, J. Wang, S. Hu, M. Jiao and Y. Ling, "Mechanical Properties and Durability of Polypropylene and Steel Fiber-Reinforced Recycled Aggregates

Concrete (FRRAC): A Review", *Sustainability,* Vol. 12, No. 22, p. 9509, 2020.

146. Wen, H., D. I. McLean and K. Willoughby, "Evaluation of Recycled Concrete as Aggregates in New Concrete Pavements", *Transportation Research Record,* Vol. 2508, No. 1, pp. 73-78, 2015.

147. James, M. N., W. Choi and T. Abu-Lebdeh, "Use of Recycled Aggregate and Fly Aslı in Concrete Pavement", *American Journal of Engineering and Applied Sciences,* Vol. 4, pp. 201-208, 2011.

148. Liu, F., L. yu Meng, G.-F. Ning and 1.-J. Li, "Fatigue Performance of Rubber-Modified Recycled Aggregate Concrete (RRAC) for Pavement", *Construction and Building Materials,* Vol. 95, pp. 207-217, 2015.

149. Ibrahim, H. A., M. B. Mahdi and B. J. Abbas, "Performance Evaluation of Fiber and Silica Fume on Pervious Concrete Pavements Containing Waste Recycled Concrete Aggregate", *Intemational Journal of Advancements in Technology,* Vol. 10, No. 2, pp. 1-9, 2019.

150. Strieder, H. L., V. F. P. Dutra, Angela Gaio Graeff, W. P. Nuiiez and F. R. M. Merten, "Performance Evaluation of Pervious Concrete Pavements With Recycled Concrete Aggregate", *Construction and Building Materials,* Vol. 315, p. 125384, 2022.

151. Verian, K. P., N. M. Whiting, J. Olek, J. Jain and M. B. Snyder, *Using Recycled Concrete as Aggregate in Concrete Pavements to Reduce Materials Cost,* Purdue University. Joint Transportation Research Program, West Lafayette, Indiana, 2013.

152. Ali, B., L. A. Qureshi and S. U. Khan, "Flexural Behavior of Glass Fiber-Reinforced Recycled Aggregate Concrete and Its Impact on the Cost and Carbon Footprint of Concrete Pavement", *Construction and Building Materials,* Vol. 262,

p. 120820, 2020.

153. Smith, J. T. and S. L. Tighe, "The Recycled Road: A Field Study Showcasing the Use of Recycled Aggregate Concrete Pavements", *Annual Conference of the Canadian Society for Civil Engineering (CSCE 2010),* pp. 1559-1568, 2010.

154. Shi, X., A. Mukhopadhyay and D. Zollinger, "Long-term Performance Evaluation of Concrete Pavements Containing Recycled Concrete Aggregate in Oklahoma", *Transportation Research Record,* Vol. 2673, No. 5, pp. 429-442, 2019.

155. Volz, J. S., J. A. Hartell, M. M. Zaman, L. Allen, J. Drury, R. McLauchlin and M. Z. Banadkoki, *Development of Guidelines for High-Volume Recycled Materials for Sustainable Concrete Pavement,* Southern Plains Transportation Center, Norman, Oklohama, 2019.

156. Jain, J., K. P. Verian, J. Olek and N. Whiting, "Durability of Pavement Concretes Made With Recycled Concrete Aggregates", *Transportation Research Record,* Vol. 2290, No. 1, pp. 44-51, 2012.

157. Poongodi, K., P. Murthi, P. O. Awoyera, R. Gobinath and O. B. Olalusi, "Durability Properties of Self-Compacting Concrete Made With Recycled Aggregate", *Silicon,* Vol. 13, No. 8, pp. 2727-2735, 2021.

158. Rashid, K., M. U. Rehman, J. de Brito and H. Ghafoor, "Multi-Criteria Optimization of Recycled Aggregate Concrete Mixes", *Journal of Cleaner Production,* Vol. 276, p. 124316, 2020.

159. Geary, G. M., Y. Tsai and Y. Wu, "An Area-Based Faulting Measurement Method Using Three-dimensional Pavement Data", *Transportation Research Record,* Vol. 2672, No. 40, pp. 41-49, 2018.

160. Chen, Y., G. Cen and Y. Cui, "Comparative Study on the Effect of Synthetic Fiber on the Preparation and Durability of Airport Pavement Concrete", *Construction*

*and Building Materials,* Vol. 184, pp. 34-44, 2018.

161. Chen, Y. and R. L. Lytton, "Development of a New Faulting Model in Jointed Concrete Pavement Using LTPP Data", *Transportation Research Record,* Vol. 2673, No. 5, pp. 407–417, 2019.

162. Jung, Y. S. and D. G. Zollinger, "New Laboratory-Based Mechanistic-Empirical Model for Faulting in Jointed Concrete Pavement", *Transportation Research Record,* Vol. 2226, No. 1, pp. 60-70, 2011.

163. Mu, F., J. M. Vandenbossche, K. A. Gatti and J. A. Sherwood, "An Evaluation of JPCP Faulting and Transverse Cracking Models of the Mechanistic-Empirical Pavement Design Guide", *Road Materials and Pavement Design,* Vol. 13, No. 1, pp. 128-141, 2012.

164. Khazanovich, L., M. I. Darter and H. T. Yu, "Mechanistic-Empirical Model to Predict Transverse Joint Faulting", *Transportation Research Record,* Vol. 1896, No. 1, pp. 34-45, 2004.

165. Sok, T., S. J. Hong, Y. K. Kim and S. W. Lee, "Evaluation of Load Transfer Characteristics in Roller-Compacted Concrete Pavement", *International Journal of Pavement Engineering,* Vol. 21, No. 6, pp. 796-804, 2020.

166. Colley, B. E. and H. A. Humphrey, *Aggregate Interlock at Joints in Concrete Pavements,* Portland Cement Association, Illinois, 1967.

167. Vandenbossche, J. M., "Estimating Potential Aggregate Interlock Load Transfer Based on Measurements of Volumetric Surface Texture of Fracture Plane", *Transportation Research Record,* Vol. 1673, No. 1, pp. 59-63, 1999.

168. Buch, N. and M. Frabizzio, "Impact of Aggregate Type on Performance of Transverse Cracks in Jointed Concrete Pavements-a Field Study", *International Journal of Pavement Engineering,* Vol. 1, No. 2, pp. 97-106, 2000.

169. Chupanit, P. and J. R. Roesler, "Improvement of Concrete Cracking Resistance and Joint Load Transfer Through Coarse Aggregate Selection", *Transportation Research Record,* Vol. 1913, No. 1, pp. 3-10, 2005.

170. Jensen, E. A. and W. Hansen, "Nonlinear Aggregate Interlock Model for Concrete Pavements", *International Journal of Pavement Engineering,* Vol. 7, No. 4, pp. 261-273, 2006.

171. Ram'ırez, L. C., *Concrete Mixture Properties Affecting the Aggregate Interlock Mechanism of Joints and Cracks far Rigid Pavement Systems,* Ph.D. Thesis, University of Pittsburgh, 2011.

172. Aure, T. W. and A. M. Ioannides, "Fracture Analysis of Aggregate Interlock Jointed Slabs-on-Grade", *Construction and Building Materials,* Vol. 77, pp. 340-348, 2015.

173. Cross, S. A., M. N. Abou-Zeid, J. B. Wojakowski and G. A. Fager, "Long-Term Performance of Recycled Portland Cement Concrete Pavement", *Transportation Research Record,* Vol. 1525, No. 1, pp. 115-123, 1996.

174. British Standard (BS EN 197 - 1), "Cement Composition, Specifications and Conformity Criteria for Common Cements", British Standards Institution (BSI), Landon, UK, 2011.

175. Turkish Standard (TS 802), "Design Concrete Mix", Turkish Standard Institute, Ankara, Turkey, 2016.

176. American Concrete Institute (ACI 327R), "Guide to Roller-Compacted Concrete Pavements", Farmington Hills, Michigan: American Concrete Institute, 2014.

177. American Society for Testing and Materials (ASTM C143 / C143M), "Standard Test Method for Slump of Hydraulic-Cement Concrete", American Society for Testing and Materials, West Conshohocken, Pennsylvania, 2020.

178. American Society for Testing and Materials (ASTM C1435 / C1435M), "Standard Practice for Molding Roller-Compacted Concrete in Cylinder Molds Using a Vibrating Hammer", American Society for Testing and Materials, West Conshohocken, Pennsylvania, 2020.

179. American Society for Testing and Materials (ASTM C192/C192M), "Standard Practice for Making and Curing Concrete Test Specimens in the Laboratory", American Society for Testing and Materials, West Conshohocken, Pennsylvania, 2019.

180. American Society for Testing and Materials (ASTM C642), "Standard Test Method for Density, Absorption, and Voids in Hardened Concrete", American Society for Testing and Materials, West Conshohocken, Pennsylvania, 2013.

181. American Society for Testing and Materials (ASTM C469 / C469M), "Standard Test Method for Static Modulus of Elasticity and Poisson's Ratio of Concrete in Compression", American Society for Testing and Materials, West Conshohocken, Pennsylvania, 2014.

182. American Society for Testing and Materials (ASTM C39 / C39M), "Standard Test Method for Compressive Strength of Cylindrical Concrete Specimens", ASTM West Conshohocken, Pennsylvania, USA, 2021.

183. American Society for Testing and Materials (ASTM C78 / C78M), "Standard Test Method for Flexural Strength of Concrete (Using Simple Beam With Third-point Loading)", American Society for Testing and Materials, West Conshohocken, Pennsylvania, 2021.

184. Japan Concrete Institute (JCI-S-001), "Method of Test for Fracture Energy of Concrete by Use of Notched Beam", Japan Concrete Institute, Tokyo, Japan, 2003.

185. American Society for Testing and Materials (ASTM C1609 / C1609M), "Standard Test Method for Flexural Performance of Fiber-Reinforced Concrete (Using Beam With Third-Point Loading)", American Society for Testing and Materials, West Conshohocken, Pennsylvania, 2019.

186. American Society for Testing and Materials (ASTM C1747 / C1747M), "Standard Test Method for Determining Potential Resistance to Degradation of Pervious Concrete by lmpact and Abrasion", American Society for Testing and Materials, West Conshohocken, Pennsylvania, 2013.

187. Rao, S. K., P. Sravana and T. C. Rao, "Relation Between Cantabro Loss and Surface Abrasion Resistance of Fly Aslı Roller Compacted Concrete (fRCC)", *Advanced Engineering Forum,* Vol. 16, pp. 52-68, Trans Tech Publications, 2016.

188. Li, G., H. Xie and G. Xiong, "Transition Zone Studies of New to Old Concrete With Different Binders", *Cement and Concrete Composites,* Vol. 23, No. 4-5, pp. 381-387, 2001.

189. Liborio, J. B. L., I. J. da Silva and A. B. de Melo, "SEM Analysis of the Paste-Aggregate Interface in Concrete Containing Silica Fume", *Special Publication,* Vol. 207, pp. 245-262, 2002.

190. Shin, H. C. and Z. Wan, "Interfacial Shear Bond Strength Between Old and New Concrete", *Fracture Mechanics of Concrete and Concrete Structures Assessment, Durability, Monitoring and Retrofitting of Concrete Structures, Korea Concrete Institute, Seoul,* pp. 1195-1200, 2010.

191. Kashani, A., T. D. Ngo, P. Hemachandra and A. Hajimohammadi, "Effects of Surface Treatments of Recycled Tyre Crumb on Cement-Rubber Bonding in Concrete Composite Foam", *Construction and Building Materials,* Vol. 171, pp. 467-473, 2018.

192. Bao, H., G. Xu, M. Yu, Q. Wang, R. Li, M. Saafi and J. Ye, "Evolution of ITZ and Its Effect on the Carbonation Depth of Concrete Under Supercritical $CO_2$ Condition", *Cement and Concrete Composites,* Vol. 126, p. 104336, 2022.

193. Zhu, L., Q. Ning, W. Han and L. Bai, "Compressive Strength and Microstructural Analysis of Recycled Coarse Aggregate Concrete Treated With Silica Fume", *Construction and Building Materials,* Vol. 334, p. 127453, 2022.

194. Liu, J., X. Xie and L. Li, "Experimental Study on Mechanical Properties and Durability of Grafted Nano-$SiO_2$ Modified Rice Straw Fiber Reinforced Concrete", *Construction and Building Materials,* Vol. 347, p. 128575, 2022.

195. Linke, R. and M. Schreiner, "Energy Dispersive X-ray Fluorescence Analysis and X-ray Microanalysis of Medieval Silver Coins", *Microchimica Acta,* Vol. 133, No. 1, pp. 165-170, 2000.

196. Titus, D., E. James Jebaseelan Samuel and S. M. Roopan, "Nanoparticle characterization techniques", *Green Synthesis, Chamcterization and Applications of Nanoparticles,* Micro and Nano Technologies, pp. 303-319, Elsevier, 2019.

197. Shojaei, T. R., S. Soltani and M. Derakhshani, "Synthesis, Properties, and Biomedical Applications of Inorganic Bionanomaterials", *Fundamentals of Bionanomaterials,* pp. 139-174, Elsevier, 2022.

198. Maidaniuc, A., F. Miculescu, S. 1. Voicu, C. Andronescu, M. Miculescu, E. Matei, A. C. Mocanu, 1. Pencea, 1. Csaki, T. Machedon-Pisu *et al.,* "Induced Wettability and Surface-volume Correlation of Composition for Bovine Bone Derived Hydroxyapatite Particles", *Applied Surface Science,* Vol. 438, pp. 158-166, 2018.

199. Miner, M. A., "Cumulative Damage in Fatigue", *Joumal of Applied Mechanics,* Vol. 12, No. 3, 1945.

200. Davids, W. G., G. M. Turkiyyah and J. P. Mahoney, "EverFE: Rigid Pave-

ment Three-dimensional Finite Element Analysis Tool", *Transportation Research Record,* Vol. 1629, No. 1, pp. 41-49, 1998.

201. Crovetti, J. A., *Design and Evaluation of Jointed Concrete Pavement Systems Incorporating Free-Draining Base Layers,* Ph.D. Thesis, University of Illinois at Urbana-Champaign, 1994.

202. Neville, A. M., *Properties of Concrete (Fourth Edition),* Longman, London, UK, 1995.

203. RILEM Recommendation, "Specifications for Concrete With Recycled Aggregates", *Materials and Structures,* Vol. 27, No. 9, pp. 557-559, 1994.

204. Turkish Official Gazzette, *Regulation on the Measurements and Methods far Vehicle Loading, and Tolerances far Vehicle Weights and Dimensions. Turkey (in Turkish),* No. 28461, 1998.

205. Jiang, Y. J., S. D. Tayabji and C. Wu, *Mechanistic Evaluation of Test Data From LTPP Jointed Concrete Pavement Test Sections,* Report, United States Federal Highway Administration Office of Research, Development, and Technology, 1998.

206. Lee, Y. H. and Carpenter, "PCAWIN Program for Jointed Concrete Pavement Design", *Journal of Applied Science and Engineering,* Vol. 4, No. 4, pp. 293-300, 2001.

207. Packard, R. G. and S. D. Tayabji, "New PCA Thickness Design Procedure for Concrete Highway and Street Pavements", *Third International Conference on Concrete Pavement Design and Rehabilitation,* Purdue University, Lafayette, Indiana, USA, 1985.

208. British Standard (EN 206), "Concrete. Specification, Performance, Production and Conformity", British Standards Institution (BSI), London, UK, 2013.

209. International Business Machines Corporation(IBM), "SPSS Statistics for Windows (version 27.0.)", IBM Corporation, Armonk, New York, 2021.

210. George, D. and P. Mallery, *IBM SPSS Statistics 26 Step by Step: A Simple Guide and Reference,* Routledge, UK, 2019.

211. Hair, J., W. C. Black, B. J. Babin, R. E. Anderson and R. L. Tatham, *Multivariate Data Analysis (Seventh Edition),* Pearson Education Limited Harlow, Essex, UK, 2014.

212. Tabachnick, B. and L. Fidell, *Using Multivariate Statistics,* Pearson, Baston, 2013.

213. Taylar, J., *Introduction to Error Analysis, the Study of Uncertainties in Physical Measurements,* University Science Books, California, 1997.

214. Klcriber, F. W., "The Effects of Air Content, Water-Cement Ratio, and Aggregate Type on the Flexural Fatigue Strength of Plain Concrete", *Special Publication,* Vol. 75, pp. 111-132, 1982.

215. Galeote, E., A. Blanco, S. H. P. Cavalaro and A. D. la Fuente, "Correlation Between the Barcelona Test and the Bending Test in Fibre Reinforced Concrete", *Construction and Building Materials,* Vol. 152, pp. 529-538, 2017.

216. Oh, B. H., "Fatigue Analysis of Plain Concrete in Flexure", *Joumal of Structuml Engineering,* Vol. 112, No. 2, pp. 273-288, 1986.

217. Sun, J., J. M. Yu and H. S. Zhao, "Two-parameter Weibull Distribution Theory Testing Analysis in Fatigue Life of Asphalt Mixture", Vol. 97, pp. 45-48, Trans Tech Publications, 2011.

218. Kennedy, J. B. and A. M. Neville, *Basic Statistical Methods far Engineers and Scientists,* Crowell, New York, 1976.

219. Frazao, C., J. Barros, J. A. Bogas, V. Garcfa-Cortes and T. Valente, "Teclınical and Environmental Potentialities of Recycled Steel Fiber Reinforced Concrete for Structural Applications", *Journal of Building Engineering,* Vol. 45, p. 103579, 2022.

220. Harwalkar, A. and S. S. Awanti, "Flexural Fatigue Belıavior of Higlı Volume Fly Aslı Concrete Under Constant Amplitude, Compound, and Variable Amplitude Loading", *Airfield and Highway Pavements 2019: Testing and Chamcterization of Pavement Materials,* pp. 389-398, 2019.

221. Melıta, P. K. and P. J. M. Monteiro, *Concrete Microstructure, Properties and Materials,* McGraw Hill Education, New York, 2017.

222. Slıalı, S. P., "Do Fibers Increase tlıe Tensile Strengtlı of Cement-Based Matrix?", *Materials Journal,* Vol. 88, No. 6, pp. 595-602, 1992.

223. Rao, S., P. Sravana and T. C. Rao, "Abrasion Resistance and Meclıanical Properties of Roller Compacted Concrete Witlı GGBS", *Construction and Building Materials,* Vol. 114, pp. 925-933, 2016.

224. Hammond, G. and C. Jones, *Inventory of Carbon Energy (ICE),* Vol. 5, Sustainable Energy Researclı Team, Department of Meclıanical Engineering University of Batlı, Batlı, UK, 2008.

225. Korol, J., A. Hejna, D. Burclıart-Korol and J. Wacłıowicz, "Comparative Analysis of Carbon, Ecological, and Water Footprints of Polypropylene-Based Composites Filled Witlı Cotton, Jute and Kenaf Fibers", *Materials,* Vol. 13, No. 16, p. 3541, 2020.

226. Stengel, T. and P. Sclıiefü, "Sustainable Construction Witlı UHPC From Life Cycle Inventory Data Collection to Environmental Impact Assessment", *Proceedings of the 2nd International Symposium on Ultm High Performance Concrete,* pp.

461-468, Kassel, Germany, 2008.

227. Turkish Standard (TS 4559), "Steel Mesh for Concrete", Turkish Standard Institute, Ankara, Turkey, 2006.

228. United States Geological Survey, *Mineral Commodity Summaries 2021,* Technical Report, Virginia, 2021.

229. Alhozaimy, A. M., P. Soroushian and F. Mirza, "Mechanical Properties of Polypropylene Fiber Reinforced Concrete and the Effects of Pozzolanic Materials", *Cement and Concrete Composites,* Vol. 18, No. 2, pp. 85-92, 1996.

230. Barınan, M. and B. Hansen, *Comparison of Performances of Structural Fibers and Development of a Specification far Using Them in Thin Concrete Overlays,* Minnesota Department of Transportation, Minnesota, 2018.

231. The Matlı Works Incorporated Company, "Matlab R2022a (version 9.12.0)", The MatlıWorks Incorporated Company, Natick, Massachusetts, 2022.

232. Srivastava, V., R. Kumar, V. C. Agarwal and P. K. Mehta, "Effect of Silica Fume on Workability and Compressive Strength of OPC Concrete", *Journal of Environmental Nanotechnology,* Vol. 3, No. 2, pp. 32-35, 2014.

233. Hanumesh, B. M., B. K. Varun and B. A. Harish, "The Mechanical Properties of Concrete Incorporating Silica Fume as Partial Replacement of Cement", *International Journal of Emerging Technology and Advanced Engineering,* Vol. 5, No. 9, p. 270, 2015.

234. Grazulyte, J., A. Vaitkus, O. Sernas and D. Ôygas, "Effect of Silica Fume on High-Strength Concrete Performance" , *5th World Congress on Civil, Structural, and Environmental Engineering,* Lisbon, Portugal, 2020.

235. Li, V. C. and H. Stang, "Interface Property Characterization and Strengthening

Mechanisms in Fiber Reinforced Cement Based Composites", *Advanced Cement Based Materials,* Vol. 6, No. 1, pp. 1-20, 1997.

236. Nadeau, J. C., "Water-Cement Ratio Gradients in Mortars and Corresponding Effective Elastic Properties", *Cement and Concrete Research,* Vol. 32, No. 3, pp. 481-490, 2002.

237. Zheng, J. J., C. Q. Li and X. Z. Zhou, "Thickness of Interfacial Transition Zone and Cement Content Profiles Around Aggregates", *Magazine of Concrete Research,* Vol. 57, No. 7, pp. 397–406, 2005.

238. Wang, X. H., S. Jacobsen, J. Y. He, Z. L. Zhang, S. F. Lee and H. L. Lein, "Application of Nanoindentation Testing to Study of the Interfacial Transition Zone in Steel Fiber Reinforced Mortar", *Cement and Concrete Research,* Vol. 39, No. 8, pp. 701-715, 2009.

239. Thilakarathna, P. S. M., S. Seo, K. S. K. Baduge, H. Lee, P. Mendis and G. Foliente, "Embodied Carbon Analysis and Benchmarking Emissions of High and Ultra-High Strength Concrete Using Machine Learning Algorithms", *Journal of Cleaner Production,* Vol. 262, p. 121281, 2020.

240. Lee, H.-8., X.-Y. Wang, L.-N. Zhang and K.-T. Koh, "Analysis of the Optimum Usage of Slag for the Compressive Strength of Concrete", *Materials,* Vol. 8, No. 3, pp. 1213-1229, 2015.

241. Shayan, A. and A. Xu, "Performance and Properties of Structural Concrete Made With Recycled Concrete Aggregate", *Materials Journal,* Vol. 100, No. 5, pp. 371-380, 2003.

242. Tam, V. W. and C. M. Tam, "Assessment of Durability of Recycled Aggregate Concrete Produced by Two-Stage Mixing Approach", *Journal of Materials Science,* Vol. 42, No. 10, pp. 3592-3602, 2007.

243. Wright, P. J. F. and F. Garwood, "The Effect of the Method of Test on the Flexural Strength of Concrete", *Magazine of Concrete Research,* Vol. 4, No. 11, pp. 67-76, 1952.

244. Gress, D. L., M. B. Snyder and J. R. Sturtevant, "Performance of Rigid Pavements Containing Recycled Concrete Aggregate: Update for 2006", *Transportation Research Record,* Vol. 2113, No. 1, pp. 99-107, 2009.

245. Smith, J. T. and S. L. Tighe, "Recycled Concrete Aggregate Coefficient of Thermal Expansion: Characterization, Variability, and Impacts on Pavement Performance", *Tmnsportation Research Record,* Vol. 2113, No. 1, pp. 53-61, 2009.

246. Cavalline, T. L., *Recycled Brick Masonry Aggregate Concrete: Use of Recycled Aggregates From Demolished Brick Masonry Construction in Structuml and Pavement Gmde Portland Cement Concrete,* Ph.D. Thesis, The University of North Carolina at Charlotte, 2012.

247. Shi, X., A. Mukhopadhyay, D. Zollinger and K. Huang, "Performance Evaluation of Jointed Plain Concrete Pavement Made With Portland Cement Concrete Containing Reclaimed Asphalt Pavement", *Road Materials and Pavement Design,* Vol. 22, No. 1, pp. 59-81, 2021.

248. Oliveira, V. C. H. C., B. L. Damineli, V. Agopyan and V. M. John, "Strategies for the Minimization of $CO_2$ Emissions From Concrete", *Ambiente Construido,* Vol. 14, pp. 167-181, 2014.

249. Cuttell, G. D., M. B. Snyder, J. M. Vandenbossche and M. J. Wade, "Performance of Rigid Pavements Containing Recycled Concrete Aggregates" , *Tmnsportation Research Record,* Vol. 1574, No. 1, pp. 89-98, 1997.

250. Dilbas, H., M. Şimşek and Özgür Çakır, "An Investigation on Mechanical and Physical Properties of Recycled Aggregate Concrete (RAC) With and Without

Silica Fume", *Construction and Building Materials,* Vol. 61, pp. 50-59, 2014.

251. Guo, H., C. Shi, X. Guan, J. Zhu, Y. Ding, T.-C. Ling, H. Zhang and Y. Wang, "Durability of Recycled Aggregate Concrete - A Review", *Cement and Concrete Composites,* Vol. 89, pp. 251-259, 2018.

252. Wang, B., L. Yan, Q. Fu and B. Kasal, "A Comprehensive Review on Recycled Aggregate and Recycled Aggregate Concrete", *Resources, Conservation and Recycling,* Vol. 171, p. 105565, 2021.

253. Xiao, J., J. Li and C. Zhang, "Mechanical Properties of Recycled Aggregate Concrete Under Uniaxial Loading", *Cement and Concrete Research,* Vol. 35, No. 6, pp. 1187–1194, 2005.

254. Rahal, K., "Mechanical Properties of Concrete With Recycled Coarse Aggregate", *Building and Environment,* Vol. 42, No. 1, pp. 407-415, 2007.

255. Bai, G., C. Zhu, C. Liu and B. Liu, "An Evaluation of the Recycled Aggregate Characteristics and the Recycled Aggregate Concrete Mechanical Properties", *Construction and Building Materials,* Vol. 240, p. 117978, 2020.

256. Moore, D. S., *Introduction to the Practice of Statistics: With Crunchlt Eesee Access Gard,* WH Freeman and Company, United States, 2014.

257. Fraternali, F., V. Ciancia, R. Chechile, G. Rizzano, L. Feo and L. Incarnato, "Experimental Study of the Thermo-Mechanical Properties of Recycled Pet Fiber-Reinforced Concrete", *Composite Structures,* Vol. 93, No. 9, pp. 2368-2374, 2011.

258. Golpasand, G. B., M. Farzam and S. S. Shishvan, "Behavior of Recycled Steel Fiber Reinforced Concrete Under Uniaxial Cyclic Compression and Biaxial Tests", *Construction and Building Materials,* Vol. 263, p. 120664, 2020.

259. BaeKim, S., N. H. Yi, H. Y. Kim, J. H. J. Kim and Y.-C. Song, "Material and

Structural Performance Evaluation of Recycled Pet Fiber Reinforced Concrete", *Cement and Concrete Composites,* Vol. 32, No. 3, pp. 232-240, 2010.

260. Liew, K. M. and A. Akbar, "The Recent Progress of Recycled Steel Fiber Reinforced Concrete", *Construction and Building Materials,* Vol. 232, p. 117232, 2020.

261. Krenchel, H. and S. P. Shah, "Restrained Shrinkage Tests With PP-Fiber Reinforced Concrete", *Special Publication,* Vol. 105, pp. 141-158, 1987.

262. Soroushian, P., F. Mirza and A. Alhozajiny, "Plastic Shrinkage Cracking of Polypropylene Fiber Reinforced Concrete", *Materials Journal,* Vol. 92, No. 5, pp. 553-560, 1993.

263. Banthia, N. and R. Gupta, "Influence of Polypropylene Fiber Geometry on Plastic Shrinkage Cracking in Concrete", *Cement and Concrete Research,* Vol. 36, No. 7, pp. 1263-1267, 2006.

264. Shah, H. R. and J. Weiss, "Quantifying Shrinkage Cracking in Fiber Reinforced Concrete Using the Ring Test", *Materials and Structures,* Vol. 39, No. 9, pp. 887-899, 2006.

265. Mazzoli, A., S. Monosi and E. S. Plescia, "Evaluation of the Early Age Shrinkage of Fiber Reinforced Concrete (FRC) Using Image Analysis Methods", *Construction and Building Materials,* Vol. 101, pp. 596-601, 2015.

266. Naaman, A. E., T. Wongtanakitcharoen and G. Hauser, "Influence of Different Fibers on Plastic Shrinkage Cracking of Concrete", *Materials Journal,* Vol. 102, No. 1, p. 49, 2005.

267. Barınan, M., J. M. Vandenbossche and D. J. Janssen, "Small-Scale Joint Performance Test for Concrete Pavements", *Structural Journal,* Vol. 116, No. 6, 2019.

268. Silva, R. V., J. D. Brito and R. K. Dhir, "Prediction of the Shrinkage Behavior of Recycled Aggregate Concrete: A Review", *Construction and Building Materials,* Vol. 77, pp. 327-339, 2015.

269. Roesler, J., C. Gaedicke, D. Lange, S. Villalobos, R. Rodden and Z. Grasley, "Mechanical Properties of Concrete Pavement Mixtures With Larger Size Coarse Aggregate", *Airfield and Highway Pavement: Meeting Today's Challenges With Emerging Technologies,* pp. 516-527, American Society of Civil Engineers, Reston, Virginia, 2006.

270. Pradena, M. and L. Houben, "Load Transfer - Crack Width Relation of Non-Dowelled Jointed Plain Concrete Short Slabs", *Baltic Journal of Road and Bridge Engineering,* Vol. 13, No. 1, pp. 40-45, 2018.

271. Mesbah, H. A. and F. Buyle-Bodin, "Efficiency of Polypropylene and Metallic Fibres on Control of Shrinkage and Cracking of Recycled Aggregate Mortars", *Construction and Building Materials,* Vol. 13, No. 8, pp. 439-447, 1999.

272. Qi, C., J. Weiss and J. Olek, "Characterization of Plastic Shrinkage Cracking in Fiber Reinforced Concrete Using Image Analysis and a Modified Weibull Function", *Materials and Structures,* Vol. 36, No. 6, pp. 386-395, 2003.